

**Sediment Transport on Arctic Shelves – Seasonal
Variations in Suspended Particulate Matter Dynamics
on the Laptev Sea Shelf (Siberian Arctic)**

**Sedimenttransport auf arktischen Schelfen –
Jahreszeitliche Schwankungen in der Schwebstoff-
dynamik auf dem Laptev-See-Schelf (sibirische Arktis)**

Carolyn Wegner

**Ber. Polarforsch. Meeresforsch. 455 (2003)
ISSN 1618 - 3193**

Carolyn Wegner

GEOMAR Forschungszentrum für marine Geowissenschaften

Wischhofstr. 1-3

D - 24148 Kiel

Die vorliegende Arbeit ist die inhaltlich unveränderte Fassung einer Dissertation, die 2002 der Mathematisch-Naturwissenschaftlichen Fakultät der Christian-Albrechts-Universität zu Kiel vorgelegt wurde.

Contents

ABSTRACT	I
ZUSAMMENFASSUNG.....	III
1 INTRODUCTION	1
1.1 MAIN OBJECTIVES	1
1.2 STUDY AREA	4
1.2.1 Physiography	4
1.2.2 Hydrography.....	5
1.2.3 Ice conditions.....	7
1.2.4 Modern depositional environment.....	8
1.3 INDIVIDUAL STUDIES	9
2 MATERIAL AND METHODS	11
2.1 WATER SAMPLES	11
2.2 TURBIDITY METER MEASUREMENTS	12
2.3 ADCP MEASUREMENTS	14
2.3.1 Current measurements	14
2.3.2 SPM concentration measurements	15
2.4 ESTIMATION OF THRESHOLD VELOCITY AND SETTLING VELOCITY	18
2.5 ESTIMATION OF HORIZONTAL SEDIMENT FLUXES	19
3 CHAPTER 3	
Suspended Particulate Matter on an Arctic Shelf: Field Comparison Between ADCP and Optical Backscatter Measurements	21
3.1 ABSTRACT	21
3.2 INTRODUCTION.....	22
3.3 MEASUREMENTS OF SUSPENDED MATTER CONCENTRATION.....	24
3.3.1 Optical backscatter measurements	24
3.3.2 Acoustic backscatter measurements	25
3.4 COMPARISON OF OPTICAL AND ACOUSTIC BACKSCATTER SENSORS.....	28
3.4.1 General comparison of all sites	29
3.4.2 Detailed profile comparison	30
3.5 SUMMARY AND CONCLUSIONS.....	32
4 CHAPTER 4	
Suspended Particulate Matter on the Laptev Sea Shelf (Siberian Arctic) During Ice-Free Conditions	33
4.1 ABSTRACT	33

4.2	INTRODUCTION.....	34
4.3	METHODS.....	36
4.4	RESULTS.....	38
4.4.1	Vertical distribution of SPM	38
4.4.2	Horizontal distribution of SPM	40
4.4.3	Bottom currents	43
4.5	DISCUSSION.....	44
4.5.1	The formation and spatial distribution of the nepheloid layers.....	44
4.5.2	The significance of the bottom nepheloid layer for the sediment transport.....	46
4.6	CONCLUSIONS	47
5	CHAPTER 5	
	Seasonal Variations in Sediment Dynamics on the Laptev Sea Shelf	
	(Siberian Arctic)	49
5.1	ABSTRACT	49
5.2	INTRODUCTION.....	50
5.3	METHODS.....	52
5.4	RESULTS.....	54
5.4.1	Currents and hydrography	54
5.4.2	SPM concentration	58
5.5	DISCUSSION.....	58
5.5.1	SPM dynamics during and after the river-ice breakup (June/early July).....	58
5.5.2	Ice-free period (mid-July to September)	60
5.5.3	Sediment transport during the freeze-up period (October).....	63
5.5.4	Period of ice coverage (November to June/July).....	63
5.5.5	Sediment dynamics beneath the polynya	64
5.6	SUMMARY	66
6	SUMMARY AND CONCLUSIONS.....	69
7	REFERENCES	73
	DANKSAGUNG	85
	LIST OF ABBREVIATIONS.....	87

Abstract

The main objective of the study was to investigate seasonal sediment dynamics on the Laptev Sea shelf. The Laptev Sea comprises one of the largest Siberian shelf areas and is characterized by seasonal ice coverage and thus, by a strong seasonality in sediment input. The pathways and the final fate of the sediments derived from the Siberian hinterland are central questions for understanding the complex land-shelf-ocean interactions and their seasonal variations. In order to characterize seasonal variations in suspended particulate matter (SPM) dynamics on the eastern Laptev Sea shelf, one-year Acoustic Doppler Current Profiler (ADCP) records and complementary optical backscatter profiles from the ice-free period were analyzed.

In order to use indirect measuring devices for the quantification of SPM concentration, optical (turbidity meter) and acoustic (ADCP) backscatter sensors were compared to assess their potential for the investigation of SPM dynamics on the Laptev Sea shelf. To estimate SPM concentrations from optical backscatter signals, these were converted using the linear relation between the backscatter signals and SPM concentrations derived from filtered water samples. Applying the theoretical interaction of sound in the water to SPM, the acoustic backscatter signals were transformed adapting a previously established approach. SPM concentrations estimated from the backscattered signals of both sensors showed a close similarity to SPM concentrations obtained from filtered water samples. In general both the ADCPs and the turbidity meters provided good estimations, with ADCPs underestimating and turbidity meters slightly overestimating SPM concentrations. Hence, both sensors can be used for the determination of SPM dynamics on the Laptev Sea shelf with its comparably low SPM concentrations. However, ADCPs are more convenient for investigation of sediment transport dynamics as they provide reasonable SPM concentration and current records for the entire water column simultaneously.

Combined turbidity meter, pigment, plankton, and current records were analyzed to describe the composition, transport dynamics, and short-term variability of SPM in the nepheloid layers (i.e., layers of increased SPM concentration in the water column) during the ice-free period. The combined measurements indicate that most of the sediment transport takes place in the bottom nepheloid layer on the eastern and the central Laptev Sea shelf. The bottom nepheloid layer comprises riverine material, resuspended bottom material, and decaying organic matter from the upper water column. The SPM concentration within the bottom nepheloid layer decreases from south to north and from east to west, respectively, mainly due to dispersion. On the inner shelf in the vicinity of the Lena Delta the SPM concentration in the surface nepheloid layer is strongly dependent on riverine discharge. On the mid-shelf the formation and dynamics of the surface layer are mainly related to changes in phytoplankton biomass and zooplankton migration. On the eastern Laptev Sea shelf paleo-river valleys act as transport conduits during the ice-free period, where bottom material is resuspended on the mid-shelf during and after storm events and transported onto the inner shelf. On the central Laptev Sea shelf resuspension events seem to be less common and SPM is mainly transported over the continental margin into the deep Arctic Ocean.

To investigate seasonal variations in SPM dynamics on the eastern Laptev Sea shelf, one-year records on currents and SPM concentrations were examined. The data indicated that during and shortly after the river-ice breakup (June to early July) sediment transport on the inner shelf is dominated by riverine input and transport onto the mid-shelf within the surface nepheloid layer. When ice-free conditions prevail (mid-July to September), SPM is mainly trapped on the eastern Laptev Sea shelf. SPM discharged by the Lena River is transported within the surface layer onto the mid-shelf, where it sinks through the water column into the bottom nepheloid layer. In the bottom layer it is transported back onto the inner shelf with additional bottom material, which was resuspended during and after storm events. On the inner shelf the material is partly conveyed back into the surface layer by turbid mixing and carried out onto the shelf again. During freeze-up (October) SPM in the surface layer on the inner shelf is rather incorporated into newly formed ice and partly transported with the ice over the continental margin into the deep Arctic Ocean. Beneath the ice cover (November to June/July) on the inner shelf SPM slowly sinks and sediment transport is of minor importance. However, beneath the polynya bottom material is still resuspended after storm events and transported onto the inner shelf where it temporarily settles. The data suggest a quasi-estuarine sediment circulation and a sediment export dominated by ice export rather than bottom transport on the eastern Laptev Sea shelf.

Since for the first time currents and SPM concentrations were recorded simultaneously for a one-year period, the unique dataset gave new insights into sediment dynamics on the Laptev Sea shelf and its complex land-shelf-ocean interactions. The data provided the basis for a conceptual model of sediment transport on the Laptev Sea shelf, which emphasizes the significance of sea ice export for the sediment budget of the Laptev Sea shelf and as a sediment source for the deep Arctic Ocean. The conceptual model can presumably be extended to other Siberian shelf seas.

Zusammenfassung

Das Hauptanliegen dieser Arbeit war die Untersuchung von jahreszeitlichen Schwankungen in der Sedimentdynamik auf dem Laptev-See-Schelf. Die Laptev-See umfasst eines der größten sibirischen Schelfmeere, das durch saisonale Eisbedeckung und eine damit einhergehende Saisonalität im Sedimenteintrag gekennzeichnet ist. Der Transport und der Verbleib des vom sibirischen Hinterland eingebrachten Materials sind wichtige Aspekte im Verständnis der vielseitigen Wechselbeziehungen zwischen Hinterland, Schelf und tiefem Arktischen Ozean und deren jahreszeitlich bedingten Schwankungen. Zur Beschreibung von jahreszeitlich bedingten Schwankungen in der Schwebstoffdynamik wurden Strömungs- und Schwebstoffmessungen für den Verlauf eines Jahres mit einem akustischen Strömungsmesser (ADCP; Acoustic Doppler Current Profiler) und ergänzend für die eisfreien Monate optische Trübungsmessungen erhoben und ausgewertet.

Zur Quantifizierung von Schwebstoffkonzentrationen auf dem Laptev-See-Schelf wurden optische Trübungsmesser mit akustischen (ADCP) Messmethoden verglichen, um deren Leistungsvermögen hinsichtlich der Untersuchung der Schwebstoffdynamik abzuschätzen. Die Messwerte des optischen Trübungsmessers wurden durch die lineare Abhängigkeit der optischen Signale von der Schwebstoffkonzentration umgerechnet. Zur Umwandlung der ADCP-Rückstreuungswerte wurde ein schon etablierter Ansatz, der sich die theoretische Wechselwirkung zwischen Schallausbreitung im Wasser und der Schwebstoffkonzentration zunutze macht, an die Bedingungen in der Laptev-See angeglichen. Die durch die Umrechnung der Signale beider Messgeräte ermittelten Schwebstoffkonzentrationen zeigen eine gute Übereinstimmung mit Konzentrationen, die durch die Filtration von Wasserproben bestimmt worden sind. Im Allgemeinen konnte sowohl mit den ADCPs als auch mit den optischen Trübungsmessern eine gute Abschätzung der Schwebstoffkonzentrationen erzielt werden, wobei die ADCPs zu einer Unterschätzung und die optischen Trübungsmesser zu einer geringfügigen Überschätzung der tatsächlichen Schwebstoffgehalte neigten. Zusammenfassend kann angenommen werden, dass beide Geräte zur Bestimmung von Schwebstoffkonzentrationen auf dem Laptev-See-Schelf eingesetzt werden können. Zur Untersuchung von Sedimenttransportereignissen sind ADCPs allerdings anwendungsfreundlicher, da Strömungsdaten und Daten zur Abschätzung von Schwebstoffkonzentrationen gleichzeitig für die gesamte Wassersäule erhoben werden können.

Zur Untersuchung der Zusammensetzung von Nepheloidlagen (Lagen erhöhter Schwebstoffkonzentration innerhalb der Wassersäule), deren Transportdynamik und der kurzfristigen Schwankungen des Schwebstofftransportes innerhalb der Lagen während der eisfreien Monate wurden optische Trübungsmessungen mit Pigment-, Plankton- und Strömungsmessungen kombiniert. Die Messungen deuten darauf hin, dass ein Großteil des Sedimenttransportes innerhalb der bodennahen Nepheloidlage stattfindet. Die Schwebstoffe innerhalb dieser bodennahen Nepheloidlage bestehen aus flusstransportiertem Material, resuspendiertem Schelfbodenmaterial und abgestorbener organischer Substanz aus der oberen Wassersäule. Die Schwebstoffkonzentration nahm jeweils von Süd nach Nord und von Ost nach

West ab. In der Nähe des Lena-Deltas auf dem inneren Schelf ist die Schwebstoffkonzentration innerhalb der oberflächennahen Nepheloidlage stark vom Flusseintrag abhängig. Auf dem mittleren Schelf dagegen sind die Bildung der oberflächennahen Lage und die Konzentrationsschwankungen darin hauptsächlich auf Veränderungen in der Phytoplanktonmasse und der Zooplankton-Migration zurückzuführen. Auf dem östlichen Laptev-See-Schelf dienen Paläo-Flusstäler während der eisfreien Monate als Transportrinnen, in denen Schelfbodenmaterial im mittleren Schelf resuspendiert und auf den inneren Schelf transportiert wird. Auf dem zentralen Schelf scheint es dagegen nur selten zur Resuspension von Schelfbodenmaterial zu kommen. Schwebstoffe werden dort hauptsächlich über den Kontinentalhang hinweg in den tiefen Arktischen Ozean transportiert.

Um jahreszeitlich bedingte Schwankungen der Schwebstoffdynamik auf dem östlichen Laptev-See-Schelf zu ermitteln, wurden Aufzeichnungen über Strömungen und Schwebstoffkonzentrationen eines ganzen Jahres untersucht. Die Aufzeichnungen deuten darauf hin, dass während und unmittelbar nach dem Flussaufbruch (Juni/Anfang Juli) auf dem inneren Schelf der Sedimenteintrag durch den Flusseintrag und den Weitertransport des eingebrachten Materials innerhalb der oberflächennahen Nepheloidlage bestimmt wird. Während der eisfreien Monate (Mitte Juli bis September) verbleiben die Schwebstoffe hauptsächlich auf dem östlichen Laptev-See-Schelf: Das durch die Lena eingetragene Material wird innerhalb der oberflächennahen Nepheloidlage auf den mittleren Schelf transportiert, wo es durch die Wassersäule in die bodennahe Nepheloidlage abseigert. Innerhalb der Bodenlage wird das abgeseigerte zusammen mit resuspendiertem Schelfbodenmaterial zurück auf den inneren Schelf transportiert. Hier wird das rücktransportierte Material durch turbulente Vermischung teilweise wieder in die oberflächennahe Nepheloidlage befördert, um von dort wieder auf den mittleren Schelf transportiert zu werden. Im Frühwinter, wenn die Neueisbildung beginnt (Oktober), wird das Material innerhalb der oberflächennahen Nepheloidlage eher in neu gebildetes Meereis eingearbeitet und teilweise mit dem Eis über den Kontinentalhang hinweg in den tiefen Arktischen Ozean transportiert. Wenn der Schelf eisbedeckt ist (November bis Juni/Juli), seigern die Schwebstoffe unterhalb der Festeisdecke langsam durch die Wassersäule ab, und der Transport in Bodennähe nimmt an Bedeutung ab. Unterhalb der Polynja wird allerdings noch immer Schelfbodenmaterial resuspendiert und auf den inneren Schelf transportiert, wo es sich zeitweise ablagert. Die Auswertung der Daten weisen auf einen quasi-ästuarinen Sedimentkreislauf auf dem östlichen Laptev-See-Schelf hin, der einen durch Eisexport dominierten Sedimenttransport zur Folge hat.

Durch die erstmalig gleichzeitige Erfassung von Strömungen und Schwebstoffkonzentrationen wurden neue Erkenntnisse über die Sedimentdynamik auf dem Laptev-See-Schelf gewonnen. Dadurch konnte ein deskriptives Modell über den Sedimenttransport auf dem Laptev-See-Schelf erstellt werden, das die Bedeutung des Sedimentexportes durch Meereis für die Erstellung eines Sedimentbudgets für die Laptev-See und für den Sedimenteintrag in den tiefen Arktischen Ozean hervorhebt. Dieses Modell über die Sedimentdynamik kann wahrscheinlich auch auf andere sibirische Schelfmeere ausgeweitet werden.

1 INTRODUCTION

1.1 Main objectives

The present study is focused on the characterization of seasonal variations in sediment dynamics on the Laptev Sea shelf and their implications for present and past sedimentary processes using optical and acoustic backscatter sensors.

The quantification of suspended particulate matter (SPM) concentration and the characterization of sediment transport are of major importance for the understanding of land-shelf-ocean interactions. During the past decades, studies on sediment dynamics have focused on the actual processes that control the sediment transport on continental shelves and the final fate of most particulate matter derived from the continents. The Laptev Sea is one of the largest Siberian shelf seas and characterized by a high freshwater inflow and sediment input through riverine discharge and coastal erosion during the 3 months when ice-free conditions prevail (Ivanov & Piskun, 1999; Pivovarov et al., 1999; Rachold et al., 2000, 2002; Figure 1-1). Furthermore the Laptev Sea has been identified as a region of high sea-ice production and a potential source of sediment-laden ice (Dethleff, 1995; Harder, 1996; Kolatschek et al., 1996; Lindemann, 1998; Dethleff et al., 2000; Eicken et al., 2000). While some of the terrestrial sediments remain on the shelf (Kuptsov & Lisitsin, 1996), part of the sediments might be transported by bottom currents into the deep Arctic Ocean (Stein, 2000) or incorporated into sea ice (Dethleff, 1995; Eicken et al., 1997; Lindemann, 1998). Part of the sediment-laden ice is transported across the Arctic Ocean through the Fram Strait into the Greenland Sea via the Transpolar Drift (Bischof et al., 1990; Reimnitz et al., 1994; Eicken et al., 1997; Dethleff et al., 2000; Figure 1-1). As riverine input (Gordeev et al., 1996), coastal erosion (Are, 1999; Rachold et al. 2000, 2002), and sea ice export are important factors in the sediment budget of the Laptev Sea and presumably of the deep Arctic Ocean as well (Eicken et al., 1997), the Laptev Sea shelf is an important link between the Siberian hinterland and the deep Arctic Ocean in terms of sediment and ice export. However, insights into sediment dynamics on the Laptev Sea shelf are still

limited, and the pathways and the final fate of the SPM is partly unknown as studies on direct current and SPM measurements are rare.

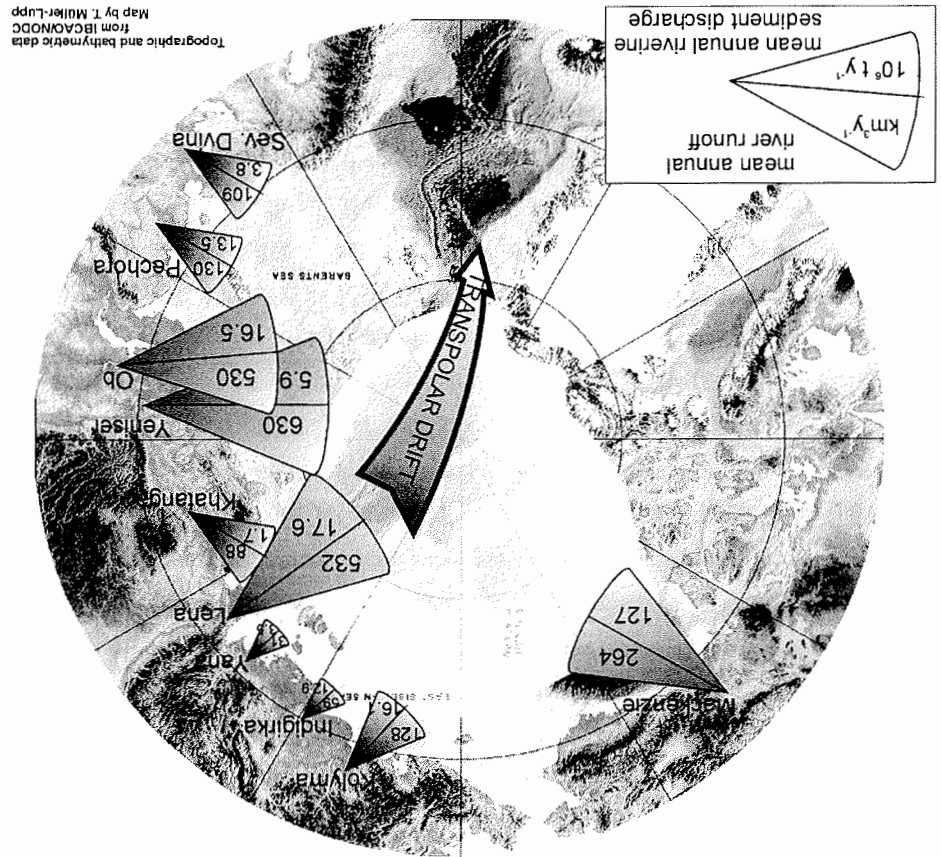


Figure 1-1: General map of the Arctic Ocean showing the mean summer ice coverage, mean annual circum-arctic river runoff according to Aagaard and Carmack (1989) and mean annual circum-arctic riverine sediment input according to Gordeev (2000). The Transpolar Drift has been modified from Reimnitz et al. (1992).

The evaluation of present-day sediment-transport processes is necessary to reconstruct former sedimentary environments and to forecast the impact of environmental changes on land-shelf-ocean interactions. Moreover, the distribution and dynamics of SPM influence the primary production in terms of the availability of nutrients (e.g., Marsh &

Tenore, 1990; Graf & Rosenberg, 1997) and of the absorption of light (e.g., Reid et al., 1990). Hence, to quantify sediment transport and to establish a complete sediment budget on the Laptev Sea shelf, the investigation of SPM dynamics is of particular interest.

While information on SPM is necessary, quantitative measurements of this highly variable parameter prove difficult (Gartner, 2002). SPM concentrations can be obtained from direct (water samples) and indirect (optical and acoustic backscatter sensors) measurements. However, the collection and analysis of water samples are extremely labor intensive and on Arctic shelves limited to a very short period as they are exceedingly difficult to reach during the 7 to 9 months of ice coverage. Therefore, optical (turbidity meter) and acoustic (Acoustic Doppler Current Profiler; ADCP) backscatter sensors are compared and their potential for the investigation of SPM dynamics on the Laptev Sea shelf is examined. Optical and acoustic backscatter signals can be used to estimate SPM concentrations when calibrated with water samples (e.g., Lynch & Agrawal, 1991; Bunt et al., 1999). ADCPs are conventionally used for the determination of the current system (e.g., Griffiths & Flatt, 1987; Gordon, 1996) but provide information on SPM in form of the backscattered ADCP signals as well (Lynch, 1985; Thorne et al., 1991). Thus, ADCPs have gained increasing acceptance for the measurement of SPM dynamics (e.g., Hay & Sheng, 1992; Griffiths & Roe, 1993; Deines, 1999; Holdaway et al., 1999).

In order to describe seasonal variations in SPM dynamics on the eastern Laptev Sea shelf, one-year ADCP records and complementary optical backscatter profiles for the ice-free period are investigated. The conversion of the optical and, in particular, of the ADCP backscatter data give new insights into sediment dynamics on the Laptev Sea shelf since currents and particle concentration were recorded simultaneously for the first time for a one-year period. This data is the basis for a conceptual model of sediment transport on the Laptev Sea shelf and its implications for sediment budget calculations.

1.2 Study area

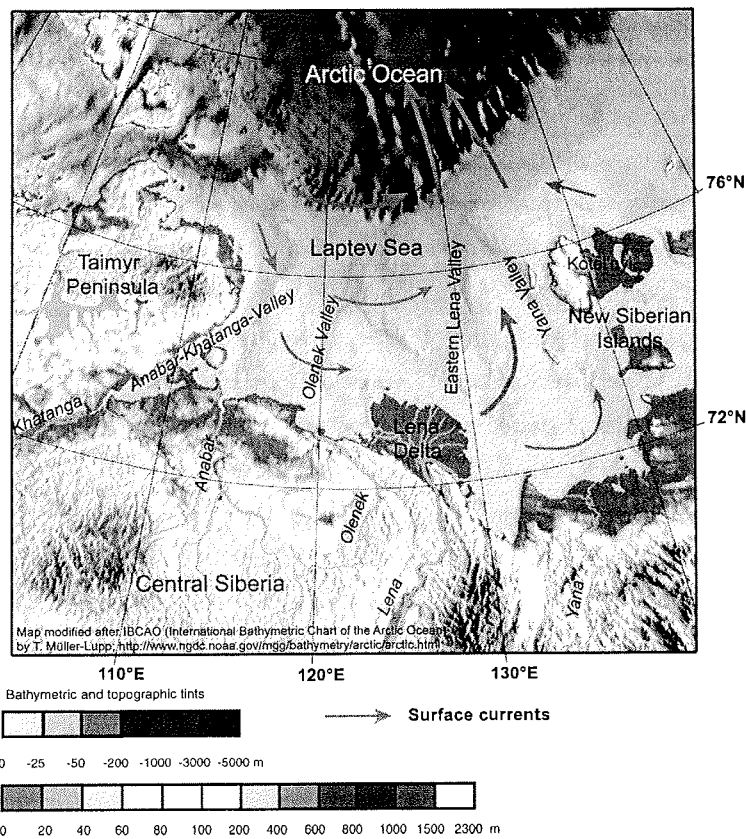


Figure 1-2: Shaded relief of the Laptev Sea shelf and the Siberian hinterland with surface currents according to Pavlov et al. (1996).

1.2.1 Physiography

The Laptev Sea is one of the epicontinental seas along the northern coast of Siberia and is located between the Kara and the East Siberian seas. With 460,000 km² the shelf area covers about 72% of the total surface area of the Laptev Sea (Holmes, 1967; Timokhov, 1994). It extends from Taymyr Peninsula and the Severnaya Zemlya archipelago in the west to the New Siberian Islands in the east (Figure 1-2). The shelf is rather shallow

with averaging water depths of less than 50 m. It dips gently northwards with a slope of only 0–5 m km⁻¹ and its northern boundary at about 200 m depth is marked by a steep continental slope (Holmes & Creager, 1974). Five submarine channels orientated in a northerly and northwesterly direction cut through the shelf (Figure 1-2). These channels represent Pleistocene river valleys that were eroded during times of the last glacial sea level drop and are named after these rivers (Holmes, 1967; Kleiber & Niessen, 1999). Some channels run along tectonic structures related to a rift zone extending from south to southeast from the shelf break to the mainland (Drachev et al., 1999).

1.2.2 Hydrography

The hydrography of the Laptev Sea shelf is characterized by a strong seasonality in freshwater discharge by several Siberian rivers in the south, an almost complete ice cover for about nine months a year and advection of Arctic water masses from the north (Pavlov et al., 1996). The rivers Anabar, Khatanga, Olenek, Lena, and Yana drain broad parts of the Siberian hinterland with a total catchment area of about 3.4 x 10⁶ km² (Treshnikov, 1985). The yearly freshwater discharge of the largest rivers is all in all about 714 km³ (Pivovarov et al., 1999). The discharge by the Lena River is proportionally highest with about 520 km³ per annum (Aagaard & Carmack, 1989; Figure 1-1). The freshwater inflow is highest during and shortly after the river ice breakup in June (Pivovarov et al., 1999; Figure 1-3). In the case of the Lena River about 40% of the mean annual discharge can be observed during the river-ice breakup (Ivanov & Piskun, 1999). The enormous freshwater inflow is of vital importance for the freshwater balance of the Laptev Sea as well as of the Arctic Ocean (e.g., Bareiss et al., 1999; Dmitrenko et al., 1999). It induces a strong thermohaline stratification of the water column on the Laptev Sea shelf with generally lowest salinities in the southeastern part and increasing salinities towards the shelf edge (e.g., Dmitrenko et al., 1999).

Wave parameters in the Laptev Sea are dependent on the extent of open water (Pavlov et al., 1996). The wind fetch ranges between 90 to 100 km in July and 550 to 650 km in September; maximal wind fetch can reach lengths of up to 850 to 1000 km

(Timokhov, 1994; Pavlov et al., 1996). Thus, waves with more than 3 m height are observed mainly during September, when the extent of open water is largest. In general waves of up to 1.5 m height are more common (Timokhov, 1994; Pavlov et al., 1996).

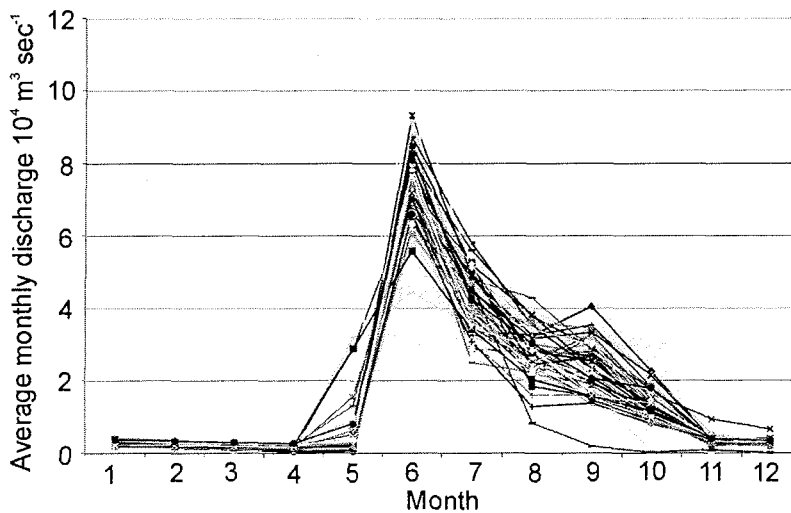


Figure 1-3: Average monthly freshwater discharge [$10^4 \text{ m}^3 \text{ sec}^{-1}$] of the Lena River at Kyusy from 1935-1994. Data source: Global Runoff Data Center (GRDC), Bundesanstalt für Gewässerkunde, Koblenz.

Non-periodic currents can be assumed to be mainly the sum of permanent and wind-driven currents in the Laptev Sea (Pavlov et al., 1996). The permanent currents are relatively stable in their spatial and temporal distribution as they are generally dependent on the position of the Icelandic Low and Arctic High and on the water exchange with the surrounding shelf seas and with the deep Arctic Ocean (Pavlov et al., 1996). The surface currents form a cyclonic circulation pattern with current velocities of less than 10 cm s^{-1} (Treshnikov, 1985; Pavlov et al., 1996; Figure 1-2). Reversal bottom currents caused by wind-induced deformation of the sea level measured in the Eastern Lena Valley show a strong seasonality. They can reach velocities of up to 59 cm s^{-1} during the ice-free period but are much weaker or even absent during the time of ice

coverage (Dmitrenko et al., 2001b). They seem to be a characteristic phenomenon for the Pleistocene river valleys on the Laptev Sea shelf (Dmitrenko et al., 2001b).

Semidiurnal tides prevail in the Laptev Sea (Timokhov, 1994). On the open shelf the tidal range reaches only 20 cm (Dmitrenko et al., 2001b) but exceeds 2 m in Khatanga Bay (Timokhov, 1994; Pavlov et al., 1996). Unfortunately direct sea level measurements are still rare.

1.2.3 Ice conditions

The Laptev Sea is one of the regions of the highest net-ice production rates in the Arctic Ocean with a mean annual production rate of about 374,000 km² (Rigor & Colony, 1997). One third of the produced ice is transported north with prevailing offshore winds. It is transported across the Arctic Ocean through the Fram Strait into the Greenland Sea via the Transpolar Drift (Kolatschek et al., 1996; Rigor & Colony, 1997; Figure 1-1). The Laptev Sea is ice-covered about nine months a year. Only during the summer months between July and September are broad parts of the Laptev Sea ice-free (Reimnitz et al., 1994; Kolatschek et al., 1996). The freeze-up starts at the end of September/beginning of October (Mysak & Manak, 1989; Eicken et al., 1997; Kassens et al., 1997). About three weeks later the entire Laptev Sea is covered with new ice (Eicken et al., 1997). During winter the ice coverage can be classified into fast ice, flaw polynya, and drift ice (from south to north). Fast ice, which is formed near the shore, reaches an average thickness of about 1.5 to 2 m and a north-south extension of up to 500 km (e.g., Barnett, 1991; Dethleff et al., 1993; Timokhov, 1994). In December a flaw polynya starts to develop. This is an area which remains either partially or totally ice-free at times and under climatological conditions where the water is expected to be ice-covered (Smith et al., 1990). The flaw polynya is relatively stable between the 20 to 30 m isobaths from mid-December (Reimnitz et al., 1994) with a maximum width of 100 km (Barnett, 1991) and a length of 1800 km (Dethleff et al., 1993). It is an area of intensive new-ice production (Reimnitz et al., 1994; Rigor & Colony, 1997). At the time of the river-ice breakup (early June) the ice in the vicinity of the Lena Delta (Barnett, 1991) and at the border of the fast ice starts to melt (Eicken et al., 1997;

Bareiss et al., 1999). In September the drift ice is generally found farthest north whereas the position of the ice edge varies from year to year (Timokhov, 1994; Eicken et al., 1997).

1.2.4 Modern depositional environment

Since the sea-level high stand on the Laptev Sea shelf was reached 5 ky BP (e.g., Bauch et al., 2001; Müller-Lupp, 2002), conditions in terms of sea level, current circulation, and sediment transport can be assumed to be similar to the modern environment. With a mean annual sediment input of about $24 \times 10^6 \text{ t yr}^{-1}$ the rivers discharging onto the Laptev Sea shelf are an important sediment source (Ivanov & Piskun, 1999; Rachold et al., 2000). The main contribution is made by the Lena River with a mean annual sediment discharge of $16.7 \times 10^6 \text{ t yr}^{-1}$ (Ivanov & Piskun, 1999; Figure 1-1). Other rivers like the Khatanga ($1.7 \times 10^6 \text{ t yr}^{-1}$), Anabar ($0.1 \times 10^6 \text{ t yr}^{-1}$), Olenek ($1.1 \times 10^6 \text{ t yr}^{-1}$), and Yana ($3.5 \times 10^6 \text{ t yr}^{-1}$) are of minor importance (Gordeev et al., 1996). The substantial load of SPM is assumed to either accumulate on the shelf (Kuptsov & Lisitsin, 1996), to be transported further into the deep Arctic Ocean (Stein, 2000), or to be incorporated into sea ice and transported via the Transpolar Drift (Bischof et al., 1990; Reimnitz et al., 1994; Eicken et al., 1997; Dethleff et al., 2000). Ice rafting represents an important component in the sediment budget of the Laptev Sea: roughly $4 \times 10^6 \text{ t}$ of sediments are exported annually, with maximum export estimates of more than $10 \times 10^6 \text{ t yr}^{-1}$ (Eicken et al., 1997). Like the freshwater discharge the riverine sediment input is highest during and shortly after the spring breakup (Pivovarov et al., 1999). For the Lena River 60% of the mean annual sediment discharge takes place during the spring breakup (Ivanov & Piskun, 1999). Other sediment sources are the erosion of the ice-bearing permafrost coast (Are, 1999; Rachold et al., 2000) and seafloor erosion (Burenkov et al., 1997). Rachold et al. (2000) calculated a mean annual sediment input by coastal erosion of $58.4 \times 10^6 \text{ t yr}^{-1}$. But up to now the percentage of the material kept within the nearshore area and of that actually transported onto the shelf is not yet known.

Generally three sedimentary provinces in the surface sediments can be distinguished on the Laptev Sea shelf (Lindemann, 1994): more sandy sediments on the western shelf and on the shoals, clayey silt (silt > 50 weight %) in the southeastern part, and dominantly sediments with a proportion of clay between 40 and 60 weight % in the Eastern Lena Valley, in the northern Yana Valley, and on the northern shelf. As a result of differences in the lithology of the catchment area of the rivers, the Laptev Sea shelf can be divided into three provinces in terms of heavy mineral and trace element distribution (Hölemann et al., 1999; Peregovich, 1999). Especially the rivers Lena and Khatanga control the mineralogical and geochemical composition of surface sediments in the eastern (Lena River) and western (Khatanga River) part of the Laptev Sea (Hölemann et al., 1999). The western and eastern provinces are therefore mainly related to the different geochemical composition of the rivers (Hölemann et al., 1999; Rachold, 1999). The central Laptev Sea shelf seems to combine characteristics of both provinces. Sedimentary organic carbon content (TOC) is highest near the river mouths and in the Pleistocene river valleys of the eastern and central Laptev Sea. The TOC deposited in the surface sediments shows a mainly terrigenous signal (Hölemann et al., 1999; Stein et al., 1999).

1.3 Individual studies

This thesis comprises three manuscripts (CHAPTER 3-5), which are accepted or are in the state of submission to peer-reviewed scientific journals. A short overview will be given in the following. All references are compiled into one reference list at the end of this volume.

CHAPTER 3

Suspended particulate matter on an Arctic shelf: field comparison between ADCP and optical backscatter measurements

The major task of this paper was to convert optical (turbidity meter) and, in particular, acoustic (ADCP) backscatter signals into SPM concentrations. Both sensors were

compared to examine their potential for the investigation of SPM dynamics on the Laptev Sea shelf. The study discussed an approach to convert acoustic backscatter signals of the ADCPs into SPM concentration, which could be applied to the examination of the one-year ADCP records as well.

CHAPTER 4

Suspended particulate matter on the Laptev Sea shelf (Siberian Arctic) during ice-free conditions

In order to describe the composition, transport dynamics, and short-term variability of SPM in the nepheloid layers on the Laptev Sea shelf during the ice-free period and the significance of the nepheloid layers for sediment transport, combined optical turbidity data, pigment, plankton, and current measurements were analyzed.

CHAPTER 5

Seasonal variations in sediment dynamics on the Laptev Sea shelf (Siberian Arctic)

For the first time one-year records on current, SPM and bottom-temperature were examined to investigate their seasonal variations and their implications for sediment transport and sediment budget calculations. Moreover, a conceptual model of sediment transport on the Laptev Sea shelf was discussed.

2 MATERIAL AND METHODS

To investigate the dynamics and seasonal variations of suspended particulate matter (SPM) on the Laptev Sea shelf, SPM concentrations were quantified by various approaches: direct measurements with filtered water samples and indirect estimations with optical and acoustic backscatter sensors. The various approaches will be outlined in the following. The current system was studied with an Acoustic Doppler Current Profiler (ADCP). Data obtained during various TRANSDRIFT expeditions (TD) were used for this purpose (Table 2-1).

Table 2-1: TRANSDRIFT-expeditions (TD) 1998 – 2000.

Expedition	Cruise	Research Platform	Month Year
TD V	PS51 XIV 1b ¹	RV Polarstern	August 1998
TD VI	TI1999 ²	land-based expedition, Tiksi	May 1999
TD VII	YS1999	RV Yakov Smirnitskiy	August 1999
TD VIII	YS2000	RV Yakov Smirnitskiy	September 2000

¹ Kassens & Dmitrenko (in press a)

² Kassens & Dmitrenko (in press b)

2.1 Water samples

In order to directly determine the SPM concentration and to calibrate the optical signals of the turbidity meter and the acoustic signals of the ADCP, water samples were collected (Table 2-2; Figure 2-1). During TD V–VII water samples of about two liters each were gathered from defined water depths. During TD VIII the sampling depth was chosen depending on the turbidity meter signals (see CHAPTER 4). The water samples were filtered through pre-weighed HVLP filters by MILLIPORE (0.45 microns). Filters were washed with distilled water, dried at about 60°C and weighed. Concentrations $\leq 0.3 \text{ mg l}^{-1}$ were set to 0.3 mg l^{-1} due to the elutable portion of the filters.

2.2 Turbidity meter measurements

During TD VII SPM concentrations were quantified with an optical backscatter sensor (turbidity meter). Turbidity measurements were carried out with a SEAPOINT TURBIDITY METER connected to a Conductivity Temperature Depth Meter (CTD; OTS, ME Marine Electronics, Germany) (Table 2-2; Figure 2-1a; see CHAPTER 4). The turbidity meter emits light of 880 nm wavelength with a constant output time of 0.1 sec. It detects light scattered by particles within the water column and generates an output voltage proportional to particle concentration. The output is given in Formazine Turbidity Unit (FTU), a calibration unit based on formazine as a reference suspension. The calibration procedure and the conversion of FTU into SPM concentration are explained in detail in CHAPTER 4.

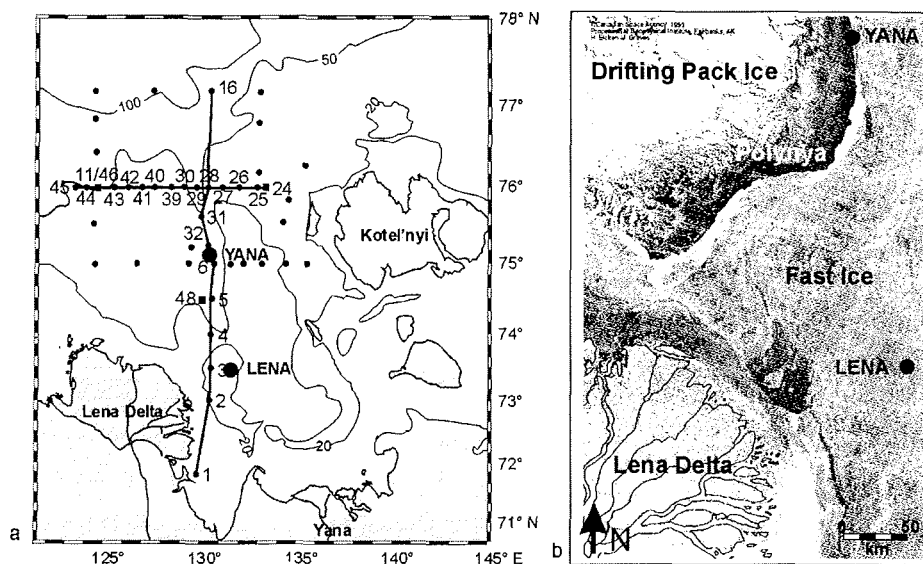


Figure 2-1: Station map of the investigated sites (a) with big solid circles indicating the one-year bottom-mooring stations and the respective stations for water sampling during TD V-VII (LENA: PS51-808-2, TI99-020, YS9908; YANA: PS51-138-2, TI99-024, YS9909), solid squares the bottom-mooring stations during TD VIII, and small solid circles indicating the stations of turbidity meter measurements. (b) shows the positions of the one-year bottom-mooring stations indicated with a solid circle on May 5, 1999, on a RADARSAT ScanSAR satellite image.

Table 2-2: Description of the monitoring stations; ADCP=Acoustic Doppler Current Profiler, CTD=Conductivity Temperature Depth meter, TM=Turbidity meter; WS=Water sampler.

Station	Device	Long. [°E]	Lat. [°N]	Water depth [m]	Deployment time mm/dd/yy	Expedition
LENA ¹ (PS51-086)	ADCP, CTD	131.4198	73.2737	22.00	08/02/98-08/29/99	TD V TD VII
YANA ¹ (PS51-138-14)	ADCP, CTD	130.4994	75.0901	44.00	08/13/98-08/30/99	TD V TD VII
PS51-080-2 ¹	CTD, WS	131.6393	73.4590	22.50	08/01/98	TD V
PS51-138-2 ¹	CTD, WS	130.8264	75.1509	43.00	08/13/98	TD V
TI99-020 ²	CTD, WS	131.6967	73.4573	22.30	05/03/99	TD VI
TI99-024 ²	CTD, WS	131.0340	75.0745	29.60	05/06/99	TD VI
YS9908	CTD, WS	131.7092	73.4592	22.80	08/29/99	TD VII
YS9909	CTD, WS	130.8338	75.1563	42.50	08/30/99	TD VII
YS0001	CTD, TM	128.5000	75.6490	7.00	09/03/00	TD VIII
YS0002	CTD, TM	130.5010	73.0170	21.00	09/06/00	TD VIII
YS0003	CTD, TM, WS	129.4840	73.5010	26.00	09/06/00	TD VIII
YS0004	CTD, TM	130.5000	74.0000	25.00	09/06/00	TD VIII
YS0005	CTD, TM	130.5000	74.5000	24.00	09/06/00	TD VIII
YS0006	CTD, TM	130.5020	75.0020	35.00	09/06/00	TD VIII
YS0009	CTD, TM, WS	124.5010	74.9980	44.00	09/07/00	TD VIII
YS0011	ADCP, CTD, TM, WS	124.5080	75.9970	50.00	09/07–09/15/00	TD VIII
YS0016	CTD, TM	130.404	77.2520	64.00	09/09/00	TD VIII
YS0020	CTD, TM	133.8260	76.0030	44.00	09/10/00	TD VIII
YS0021	CTD, TM, WS	135.4980	74.9980	31.00	09/10/00	TD VIII
YS0023	CTD, TM, WS	134.7380	75.7790	40.00	09/10/00	TD VIII
YS0024	ADCP, CTD, TM, WS	133.836	76.0000	44.00	09/11–09/15/00	TD VIII
YS0025	CTD, TM, WS	133.1220	76.0000	40.00	09/12/00	TD VIII
YS0026	CTD, TM	132.2020	75.9880	34.00	09/12/00	TD VIII
YS0027	CTD, TM	131.3940	76.0010	36.00	09/12/00	TD VIII
YS0028	CTD, TM, WS	130.3530	76.0010	49.00	09/12/00	TD VIII
YS0029	CTD, TM	129.8340	76.0010	50.00	09/12/00	TD VIII
YS0030	CTD, TM, WS	129.1980	76.0160	49.00	09/12/00	TD VIII
YS0031	CTD, TM	129.9990	75.6840	49.00	09/12/00	TD VIII
YS0032	CTD, TM, WS	130.3620	75.3390	44.00	09/13/00	TD VIII
YS0034	CTD, TM, WS	132.6680	75.0000	15.00	09/13/00	TD VIII
YS0036	CTD, TM, WS	134.6640	75.0010	23.00	09/13/00	TD VIII
YS0037	CTD, TM	134.6380	76.1220	25.00	09/13/00	TD VIII
YS0039	CTD, TM	128.5050	76.0030	45.00	09/14/00	TD VIII
YS0040	CTD, TM, WS	127.8290	76.0010	47.00	09/14/00	TD VIII
YS0041	CTD, TM	127.0780	76.0000	43.00	09/14/00	TD VIII
YS0042	CTD, TM, WS	126.3300	76.0010	46.00	09/14/00	TD VIII
YS0043	CTD, TM	125.4670	76.0010	51.00	09/14/00	TD VIII
YS0044	CTD, TM	123.9950	76.0020	55.00	09/14/00	TD VIII
YS0045	CTD, TM	123.5030	75.9840	50.00	09/14/00	TD VIII
YS0046	CTD, TM	124.4340	76.0010	55.00	09/15/00	TD VIII
YS0048	ADCP, CTD, TM, WS	129.9960	74.5190	33.00	09/15–09/16/00	TD VIII

¹ Kassens & Dmitrenko (in press a)² Kassens & Dmitrenko (in press b)

2.3 ADCP measurements

Two bottom-mooring stations, LENA and YANA, were deployed at key positions for sediment transport on the eastern Laptev Sea shelf for a one-year period (Table 2-2; Figure 2-1; see CHAPTER 5). In both one-year bottom-mooring stations an upwards-looking broadband ADCP (WH Sentinel 307.2 kHz, RD-Instruments) and a CTD (OTS, ME Marine Electronics, Germany) were installed. The bottom-mooring stations gathered data for one seasonal cycle on current, SPM, and bottom-temperature variations. Station LENA was positioned in the vicinity of important outlets of the Lena River (Bykovskaya and Trofimovskaya channels) at a water depth of 22 m (Table 2-2; Figure 2-1). During the time of ice coverage bottom-mooring station LENA was beneath the fast ice (Figure 2-1b). Station YANA was deployed at a water depth of 44 m on the slope of the Eastern Lena Valley in the region of the average position of the fast ice edge (Table 2-2; Figure 2-1b). ADCP measurements in the one-year bottom-mooring stations were carried out in intervals of 1 minute and averaged over 30 minutes. Station LENA had a depth-cell (bin) size of 1.5 m with the first bin measuring at 3.5 m above bottom (mab). Bin size of station YANA was 2 m with the first bin measuring at 4 mab (Figure 2-2).

During TD VIII three bottom-moored ADCPs (WH Sentinel 307.2 kHz, RD-Instruments; YS0011, YS0024, YS0048) were deployed for a monitoring period of at least 28 hours in the eastern and central Laptev Sea (Table 2-2; Figure 2-1; see CHAPTER 3). ADCP measurements were performed at YS0011 in intervals of 2 seconds and averaged over 5 minutes, at YS0024 and YS0048 in intervals of 1 second and averaged over 1 minute. Bin sizes were 1 m with the first bin measuring at 3 mab at all three stations.

2.3.1 Current measurements

Primarily, ADCPs are used for the investigation of current speeds by measuring the Doppler shift of the backscattered acoustic signal (e.g., Griffiths & Roe, 1993; Gordon, 1996). They transmit sound signals at a fixed frequency. The signal is scattered from particles moving with the same velocity as the surrounding water. The backscattered

sound signal returns with a frequency shift dependent on the particle speed (Doppler effect). Comparing the return frequency with the frequency of the initially emitted sound pulse the current speed can be computed in different depth cells (bins). All instruments used in the present study integrate the return signals of four simultaneous sound pulses emitted at constant intervals and orientated 20° from the vertical.

2.3.2 SPM concentration measurements

In addition to current data ADCPs provide information on particle concentration within the water column by recording echo intensity (e.g., Thorne et al., 1991; Hay & Sheng, 1992; Griffiths & Roe, 1993; Seibt-Winckler, 1996; Deines, 1999; Holdaway et al., 1999; Santamarina Cuneo & Flemming, 2000; Rose & Thorne, 2001). As the acoustic pulse propagates through the water column, particles in suspension backscatter part of the sound signal (Figure 2-2). The echo intensity of the backscattered sound can be used to estimate the SPM concentration ($SPM_{acoustic}$; e.g., Thorne et al., 1991; Hay & Sheng, 1992; Crawford & Hay, 1993; Deines, 1999; Holdaway et al., 1999; see CHAPTER 3). In general low echo intensities represent low SPM concentrations and high echo intensities represent high concentrations (Figure 2-2).

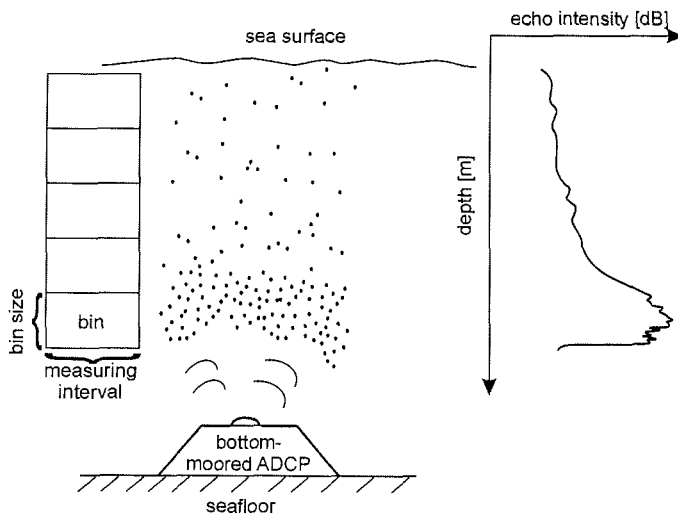


Figure 2-2: The echo intensity is a measure for SPM concentration within the water column: high echo intensity generally represents high SPM concentration and low echo intensity low concentration.

But acoustic backscatter sensors are sensitive to any change in the acoustic impedance and will, therefore, respond to fish, plankton, and gas bubbles as well (Libicki et al., 1989; Osborne et al., 1994; Seibt-Winckler, 1996). Hence, a calibration of the relationship between echo intensity and SPM concentration with *in situ* measurements is absolutely necessary (Gordon, 1996; Holdaway et al., 1999). The calibration and the conversion of echo intensity into SPM concentration will be discussed in detail in CHAPTER 3 focusing on data gathered during TD VII.

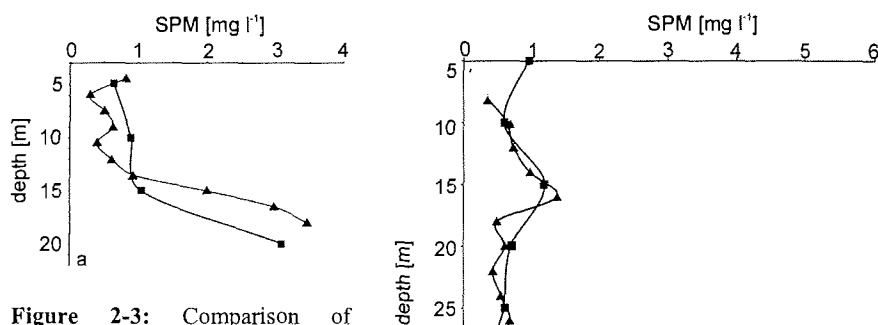


Figure 2-3: Comparison of $SPM_{acoustic}$ (solid triangles) at one-year bottom-mooring-station LENA on 08/29/99 at 8:00 am with SPM_{filter} (solid squares) at YS9908 (a) and at one-year bottom-mooring station YANA on 08/03/99 at 1:30 pm with YS9909 (b).

At bottom-mooring station LENA and YANA the conditions in terms of grain size, temperature and salinity variations, and in terms of echo intensity spectrum were similar compared to the conditions during TD VIII. Therefore, it can be assumed that the approach to convert echo intensity to SPM concentrations discussed in CHAPTER 3 can be applied to the echo intensity data of LENA and YANA as well. The spectrum of echo intensity recorded during TD VIII (43-186 dB) covered the spectrum of the one-year bottom-mooring stations (42-183 dB). Events with echo intensity > 190 dB were only recorded near the sea surface. They could be related to the presence of ice, which generates extremely high echo intensities. Conditions in terms of system parameters

were identical since during TD VIII the same devices were deployed as at stations LENA and YANA. To convert the echo intensity data, a parameter K is computed for one bin with known SPM concentrations (see CHAPTER 3). K describes the system response to SPM concentration. It was computed for the bottom-mooring stations LENA and YANA at various time and depth intervals using water samples of TD V-VIII respectively (Table 2-3).

Table 2-3: Parameter K describing the system response to SPM concentration at bottom-mooring stations LENA and YANA computed for various time and depth intervals.

Station	Time interval mm/(dd)/yy	Depth interval [m]	K [$\text{mg l}^{-1} \text{ dB}^{-3} \text{ m}^{-2}$]
LENA ¹	08/98–09/98	4.50	1.51E-05
		9.00-6.00	2.37E-06
		10.50-13.50	5.42E-07
		15.00-18.00	4.2E-07
	10/98–07/19/99	4.50-6.00	1.82E-06
		7.50-15.00	2.58E-07
		16.50-18.00	1.62E-07
	07/20/99 – 08/30/99	4.50	2.21E-06
		9.00-6.00	6.31E-07
		10.50-13.50	2.39E-07
		15.00-18.00	3.26E-07
	YANA ¹	08/98 – 04/99	7.50
9.50-13.50			4.18E-06
15.50-19.50			1.39E-06
21.50-27.50			7.79E-07
29.50-35.50			1.35E-07
37.50-39.50			1.32E-07
05/99		7.50	3.51E-05
		9.50-13.50	3.19E-06
		15.50-19.50	1.28E-06
		21.50-27.50	5.62E-07
		29.50-35.50	2.26E-07
		37.50-39.50	1.32E-07
06/99 – 08/99		7.50	2.87E-06
		9.50-13.50	4.29E-07
		15.50-19.50	3.12E-07
		21.50-23.50	9.58E-08
		25.50-29.50	5.19E-08
		31.50-35.50	2.88E-08
		37.50-39.50	1.00E-08

¹ Kassens & Dmitrenko (in press a)

Figure 2-3 shows the good correspondence between $SPM_{acoustic}$ and filtered water samples at the one-year bottom-mooring stations indicating the applicability of the

approach discussed in CHAPTER 3 to the echo intensity data of LENA and YANA. Hence, the echo intensity data can be used to estimate the $SPM_{acoustic}$ dynamics, especially in the lower water column even though there are some uncertainties, mainly during the time of ice coverage because there are no water samples of the time from October to April (Table 2-2). In order to obtain more accurate SPM estimations, water samples for each season (ice-free, freeze-up, ice-covered, polynya, river-ice breakup) would be desirable.

2.4 Estimation of threshold current velocity and settling velocity

To examine the implications of current and SPM dynamics for sediment transport, threshold current velocities for incipient motion and settling velocities have been estimated for the bottom-mooring stations respectively.

Table 2-4: Positions and grain-size characteristics for surface samples in the vicinity of the respective ADCP mooring-stations (Lindemann, 1994).

Surface sample	Position of surface samples		ADCP station	Median grain size [Phi]
	Long. [°E]	Lat. [°N]		
IK93 21-4 ¹	131.404	73.300	LENA ²	8
IK93 53-8 ¹	129.573	75.000	YANA ²	8
IK93 67-1 ¹	123.500	75.290	YS0011	3.5
IK93 73-3 ¹	131.482	75.230	YS0024	4.5
IK93 44-10 ¹	131.059	74.280	YS0048	3.5

¹ Kassens & Karpiy (1994)

² Kassens & Dmitrenko (in press a)

Sediment transport starts to take place when the current speed exceeds the threshold current velocity for incipient grain motion (u_{cr}).

$$u_{cr} = 7 \left(\frac{z}{d_{50}} \right)^{1/7} (g(s-1)d_{50}\theta_{cr})^{1/2} \quad (2.1)$$

with $s = \frac{\rho_s}{\rho_w}$

where z is the depth of flow, d_{50} the median grain diameter, g the acceleration due to gravity, ρ_s the grain density, ρ_w the water density, and θ_{cr} the threshold Shields

parameter by Soulsby and Whitehouse (1997). To estimate u_{cr} , grain-size characteristics of surface samples according to Lindemann (1994) were used (Table 2-4).

To convert u_{cr} into the respective threshold current velocity for the lowest bin of each ADCP ($u(z)$) at the flow depth z , the Karman-Prandtl equation was applied:

$$u(z) = \frac{u_{cr}}{\kappa} \ln\left(\frac{z}{z_0}\right) \quad (2.2)$$

where κ is the von Karman's constant ($\kappa = 0.4$), and z_0 is the bed roughness length, a parameter describing the roughness of the sea bed (Table 2-5).

Table 2-5: Bed roughness length z_0 , critical threshold velocity for incipient grain motion u_{cr} , and threshold current velocities at the lowest bin $u(z)$ for the bottom-mooring stations.

Parameters	LENA ¹	YANA ¹	YS0011	YS0024	YS0048
z_0 [cm] ^a	0.02	0.02	0.07	0.07	0.07
u_{cr} [cm s ⁻¹] ^b	1.10	1.21	2.53	2.59	2.42
$u(z)$ [cm s ⁻¹]	27 ^c	30 ^d	46 ^c	47 ^e	44 ^e

¹ Kassens & Dmitrenko (in press a)

^a from the compilation of Soulsby (1983), Table 5.4.

^b estimated following Soulsby and Whitehouse (1997)

^c $z=3.5$ mab; ^d $z=4$ mab; ^e $z=1$ mab

Settling velocities have been estimated by Stoke's Law with SPM grain-size parameters of Dethleff (1995), Burenkov et al. (1997), and Binder (2001). As the average SPM grain-size is $< 15.6 \mu\text{m}$, the settling velocity is mostly $< 0.001 \text{ cm s}^{-1}$ ($\approx < 1 \text{ m day}^{-1}$; e.g., McCave, 1975; Puls et al., 1995). Higher settling velocities ($> 0.001 \text{ cm s}^{-1}$) can be assumed for flocs or coarser material although comparatively little is known about the relationship between floc size and density (Dyer, 1994).

2.5 Estimation of horizontal sediment fluxes

In order to estimate the transport direction and the quantity of transported SPM, the horizontal flux was estimated from the respective current records. Assuming that the SPM moves with the same velocity as the surrounding water (Wright, 1995), the instantaneous horizontal SPM flux $q(t)$ can be computed following Puig et al. (2001) and Palanques et al. (2002):

$$q_u(t) = u(t)C(t) \quad (2.3)$$

$$q_v(t) = v(t)C(t) \quad (2.4)$$

where $u(t)$ is the eastward and $v(t)$ the northward instantaneous current component of the velocity field and $C(t)$ is the SPM concentrations at time t . Averaging instantaneous SPM fluxes over time produces along- ($\langle q(u) \rangle$) and across-shelf ($\langle q(v) \rangle$) SPM fluxes. The magnitude and direction of the horizontal SPM flux at one mooring station for a defined time period can be estimated from the resulting vector $\vec{q} = (\langle q_u \rangle, \langle q_v \rangle)$ of the along- and across-shelf SPM fluxes.

3 CHAPTER 3

Suspended Particulate Matter on an Arctic Shelf: Field Comparison Between ADCP and Optical Backscatter Measurements

3.1 Abstract

Colocated measurements of suspended particulate matter (SPM) concentrations were carried out with optical (turbidity meter) and acoustic (Acoustic Doppler Current Profiler; ADCP) backscatter sensors on the Laptev Sea shelf (Siberian Arctic) in the year 2000. Both sensors were compared to assess their potential for the investigation of SPM dynamics on the Laptev Sea shelf with its rather low SPM concentrations.

The turbidity meter signals were converted into SPM concentrations using the linear relationship between the optical backscatter signals and SPM concentrations derived from filtered water samples. The ADCP signals were transformed adapting a previously established approach on the theoretical interaction between sound in water and SPM. In general, the ADCPs and turbidity meters provided good SPM estimations. The estimated SPM concentrations showed a close similarity to concentrations derived from filtered water samples, with ADCPs underestimating and turbidity meter slightly overestimating SPM concentrations. Thus, both sensors can be used for investigations on SPM dynamics on the Laptev Sea shelf but ADCPs are more convenient as they provide reasonable SPM estimations and current records for the entire water column simultaneously.

3.2 Introduction

To describe sediment transport dynamics and to understand many land-shelf-ocean interaction processes the quantification of suspended particulate matter (SPM) and the investigation of its dynamics are of major importance. Shelves cover about 35% of the surface area of the Arctic Ocean (Grebmeier & Whitley, 1996) and some of the world's largest rivers discharge onto them. However, the fate of the large amount of riverine material is still partly unknown. Arctic shelves are ice-covered for seven to nine months a year and hence, studies on seasonal sediment dynamics on Arctic shelves are mostly restricted to the ice-free season. To quantify SPM dynamics, especially beneath the ice cover, indirect measuring devices which can be deployed on the seafloor are therefore especially suitable.

The most common devices for indirect measurements of SPM concentrations are optical and acoustic backscatter sensors (e.g., Hanes et al., 1988; Lynch et al., 1994; Osborne et al., 1994; Lynch et al., 1997; Wheatcroft & Butman, 1997; Bunt et al., 1999). Optical backscatter sensors have been used with success on Arctic shelves for the last ten years (e.g., Anoshkin et al., 1995; Burenkov et al., 1997; Johnson et al., 2000; Lisitsin et al., 2000; Wegner et al., in press). Yet they have the disadvantage that they are intrusive, susceptible to biological fouling, and that they provide data from only one single depth (e.g., Thorne et al., 1991; Gartner, 2002). For more than a decade Acoustic Doppler Current Profilers (ADCPs) have been conventionally used to determine current speeds through the entire water column (e.g., Griffiths & Flatt, 1987; Griffiths & Roe, 1993; Gordon, 1996). It has been recognized over this period that the backscattered ADCP signal provides information on the scatterers as well (e.g., Lynch, 1985; Thorne et al., 1991; Byrne & Patino, 2001; Gartner & Cheng, 2001). However, studies on the application of ADCPs for SPM concentration measurements on Arctic shelves do not yet exist.

During the TRANSRIFT VIII expedition 2000, bottom-moored ADCPs were deployed on the Laptev Sea shelf, one of the largest Siberian shelf seas, within the framework of the German-Russian project "Laptev Sea System 2000" for a monitoring period of at least 28 hours (Figure 3-1). Hourly optical backscatter profiles were carried out at each monitoring site respectively. Optical and acoustic sensors were calibrated with filtered

water samples and compared to assess their potential to measure SPM concentrations on the Laptev Sea shelf with comparatively low SPM concentrations (Hölemann et al., 1995). The calibration campaign provided sufficient data to examine the use of ADCPs on the Laptev Sea shelf and the differences in optical and acoustic backscatter sensors.

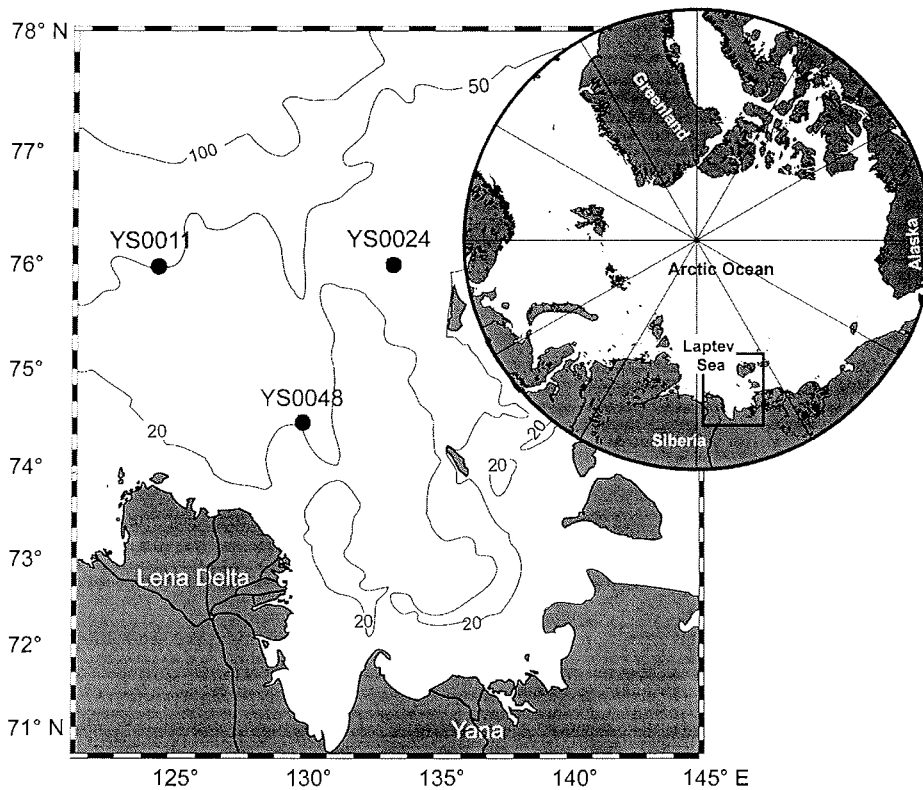


Figure 3-1: Bathymetric map of the eastern Laptev Sea shelf and locations of the measuring sites (YS0011: 75°99.70N 124°50.80E; YS0024: 76°N 133°83.60E; YS0048: 74°51.90N 129°99.60E).

3.3 Measurements of suspended matter concentration

SPM concentrations were quantified using optical (turbidity meter) and acoustic (ADCP) backscatter sensors at three sites on the eastern and central Laptev Sea shelf for a monitoring period of at least 28 hours (Figure 3-1). Both sensors were calibrated with filtered water samples in the working area to avoid the problem of simulating Arctic conditions in the laboratory. Every four hours water samples of two liters each were collected from different water depths and treated using the conventional filtering and weighing procedures to obtain the SPM concentrations (SPM_{filter}). Concentrations $< 0.3 \text{ mg l}^{-1}$ were set to 0.3 mg l^{-1} due to the elutable portion of the filters (MILLIPORE \varnothing 0.45 microns). Colocated supplementary Chlorophyll *a* and zooplankton measurements were carried out to quantify the algal and plankton portion of SPM (Abramova et al., 2002).

3.3.1 Optical backscatter measurements

Hourly profiles of optical backscatter measurements were obtained with a SEAPOINT TURBIDITY METER. The turbidity meter emits infrared light with a constant output time of 0.1 sec and detects light scattered by particles within the water column. It generates an output voltage proportional to particle concentration in front of the sensor face. The output is given in Formazine Turbidity Units (FTU), a calibration unit based on formazine as a reference suspension. The intensity of the backscattered infrared light is a function primarily of the SPM concentration and size in front of the sensor (Ludwig & Hanes, 1990; Lynch & Agrawal, 1991; Hatcher et al., 2000; Hatje et al., 2001). A strong correlation between concentrations derived from the filtered water samples and the optical backscatter was observed ($R^2=0.931$; $p=0.01$; $n=129$; (Wegner et al., in press)). Optical backscatter intensity (*OI*) can be converted into SPM concentrations (SPM_{optic}) by the linear regression: $SPM_{optic}=0.166+0.651 \text{ } OI$ (Wegner et al., in press). SPM concentrations derived from turbidity meter measurements coincided very well with SPM_{filter} (Figure 3-2a). The line of best linear fit matches almost with the 1:1 line. Thus, the turbidity meter provided very good results and overestimated SPM concentrations only slightly.

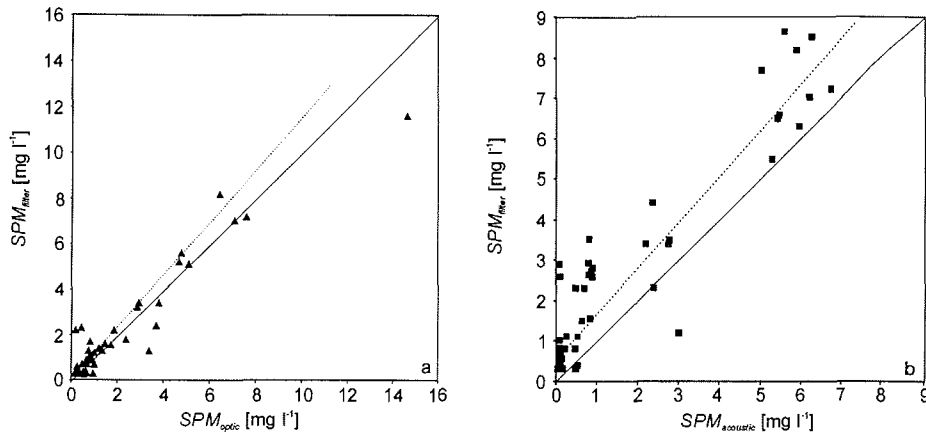


Figure 3-2: a) Scatter plot of SPM concentrations derived from optical backscatter signals (SPM_{optic}) and concentrations derived from filtered water samples (SPM_{filter}); b) scatter plot of SPM concentrations derived from acoustic backscatter signals ($SPM_{acoustic}$) and SPM_{filter} ; the continuous line indicates the 1:1 line and the dotted line indicates the line of least square fit respectively.

3.3.2 Acoustic backscatter measurements

Bottom-moored, upwards-looking broadband ADCPs (WH Sentinel 307.2 kHz, RD-Instruments) were deployed at each site for the entire monitoring period. ADCP measurements were carried out at station YS0011 in intervals of 2 sec and averaged over 5 minutes, at stations YS0024 and YS0048 in intervals of 1 sec and averaged over 1 minute in different depth cells (bins) respectively. Bin sizes were 1 m with the first bin measuring 3 m above seafloor.

As the intensity of the backscattered acoustic signal (echo intensity) provides information on particle concentrations, ADCPs have gained increasing acceptance by researchers for the measurement of SPM dynamics (Thorne et al., 1991; Hay & Sheng, 1992; Griffiths & Roe, 1993; Seibt-Winckler, 1996; Deines, 1999; Holdaway et al., 1999; Santamarina Cuneo & Flemming, 2000; Rose & Thorne, 2001). The theoretical interaction of sound with SPM is now well documented (Sheng & Hay, 1988; Thorne et al., 1991; Hay & Sheng, 1992; Thevenot & Kraus, 1993; Lynch et al., 1994; Thorne & Hardcastle, 1997; Thosteson & Hanes, 1998).

According to Crawford and Hay (1993), Thorne and Hardcastle (1997), and Holdaway et al. (1999), the SPM concentration $SPM_{acoustic}$ at a distance r from the transducer can be written as:

$$SPM_{acoustic}(r) = \left\{ \frac{EI}{K_s K_t} \right\}^2 r^2 e^{4r(\alpha_w + \alpha_s)} \quad (3.1)$$

with

$$K_s(r) = \frac{f_m(r)}{\sqrt{\rho_s \langle a_s(r) \rangle}}$$

$$K_t = s_g R_s p_0 r_0 \sqrt{\left\{ \frac{3\tau c}{16} \right\} \left\{ \frac{0.96}{ka_t} \right\}}$$

where EI is the recorded echo intensity, α_w is the attenuation coefficient due to water (computed following Fisher and Simmonis, 1977), and α_s is the attenuation due to scatterers in suspension. At low concentrations, α_s is low, resulting in an increase in echo intensity with increasing SPM concentrations (Thosteson & Hanes, 1998). K_s characterizes SPM properties with $f_m(r)$ describing scattering properties of SPM, ρ_s the sediment density, and $a_s(r)$ the mean particle radius. The angular brackets represent the average over all particle radii within the respective bin. Echo intensity is sensitive to SPM concentration as well as to SPM size. Hence, the SPM-size distribution should be constant to ensure that an increase in echo intensity can be related to an increase in SPM concentration (Libicki et al., 1989; Thorne et al., 1991; Gordon, 1996). Previous investigations of SPM grain-size on the Laptev Sea shelf showed that the size distribution can be assumed to be almost constant (Dethleff, 1995; Burenkov et al., 1997; Binder, 2001). However, some degree of uncertainty in SPM concentration estimates must be tolerated when the information on grain-size distribution is insufficient (Lynch et al., 1997). Assuming that $f_m(r)$, ρ_s , and $\langle a_s(r) \rangle$ remained constant for different depth intervals as suggested by Holdaway et al. (1999), K_s is a constant. K_t contains system parameters, where s_g is the system gain, R_s is the receive sensitivity of the transducer, p_0 is the pressure at r_0 (usually 1 m) when there are no scatterers in suspension, τ is the pulse duration, c is the speed of sound in water, k is the wave number and a_t is the transceiver radius. In the present study K_t can be assumed to be constant for each ADCP. Therefore equation (3.1) can be transformed to:

$$SPM_{acoustic}(r) = K_{st} (EI(r))^2 r^2 e^{4r(\alpha_w + \alpha_s)} \quad (3.2)$$

$$\text{with } K_{st} = (K_s K_t)^{-2}$$

being constant.

Acoustic backscatter sensors are sensitive to any change in the acoustic impedance and respond therefore to fish, plankton, and gas bubbles as well (e.g., Libicki et al., 1989; Osborne et al., 1994; Seibt-Winckler, 1996). Hence, to apply equation (3.2) calibrations with water samples are absolutely necessary (e.g., Gordon, 1996; Holdaway et al., 1999).

The echo intensity from a certain bin at the height r_s was calibrated against filtered water samples of the concentration SPM_{filter} at the same depth. Substituting $SPM_{acoustic}$ with SPM_{filter} equation (3.2) can be reformulated as (Holdaway et al., 1999):

$$K(r_s) = \left\langle \frac{SPM_{filter}(r_s)}{(EI(r_s))^2 r_s^2 e^{4r_s \alpha_w}} \right\rangle$$

$$K(r_s) = K_{st} e^{4r_s \langle \alpha_s(r_s) \rangle}$$

$$\langle \alpha_s(r_s) \rangle = \frac{\zeta}{r_s} \int_0^{r_s} \langle SPM_{acoustic} \rangle dr \quad (3.3)$$

K describes the system response to SPM concentration. The angular brackets represent the average over all measurements during the time when the water samples were obtained. $\langle \alpha_s(r_s) \rangle$ describes the mean attenuation of the acoustic signal due to sediments up to r_s where ζ is the sediment attenuation constant. $\langle \alpha_s(r_s) \rangle$ can be determined by an iterative approach (Thorne et al., 1991). For frequencies below 1 MHz the attenuation due to sediment is dominated by the viscous absorption (Seibt-Winckler, 1996; Holdaway et al., 1999). These frequencies are less sensitive to the attenuation due to sediments in suspension (Crawford & Hay, 1993). The viscous absorption coefficient (estimated following Urlick, 1948) is in the range of $10^{-4} \text{ m}^{-1} \text{ mg}^{-1}$ for the frequency of 300 kHz. SPM concentrations on the Laptev Sea shelf are comparatively small. Consequently this estimation for the viscous absorption coefficient is assumed to be

sufficient for the present study. $\langle \alpha_s(r_s) \rangle$ and K_{st} are included within the constant K by the calibration procedure. K was computed for each site for various depth intervals (Table 3-1).

Table 3-1: Parameter K describing the system response to SPM concentration at stations YS0011, YS0024, and YS0048 for various depth intervals.

Station	Depth interval [m]	K [$\text{mg l}^{-1} \text{ dB}^{-3} \text{ m}^{-2}$]
YS0011	2.50–5.50	1.06E-06
	6.50–15.50	1.30E-07
	16.50–25.50	3.39E-08
	26.50–35.50	1.15E-08
	36.50–46.50	1.13E-08
YS0024	2.50–15.50	1.82E-07
	16.50–25.50	1.57E-08
	26.50–35.50	5.13E-08
	36.50–40.50	8.14E-08
YS0048	1.50–15.50	1.08E-06
	16.50–20.50	3.87E-07
	21.50–29.50	2.17E-07

K can be used for the estimation of $SPM_{acoustic}$ (Holdaway et al., 1999). By combining equation (3.2) with equation (3.3) SPM concentration can be estimated:

$$SPM_{acoustic}(r) = K(r)(EI(r))^2 r^2 e^{4r\alpha_w} \quad (3.4)$$

SPM_{filter} and $SPM_{acoustic}$ showed a high correlation ($R^2=0.886$; $n=75$; $p=0.01$; Figure 3-2b) indicating that the conversion adapted from Holdaway et al. (1999) is a good approximation for the working area. The line of best linear fit is within the sector of higher estimations derived from filtered water samples indicating that the ADCPs tend to underestimate SPM concentrations.

3.4 Comparison of optical and acoustic backscatter sensors

For a comparison of optical and acoustic backscatter sensors SPM concentrations obtained from the turbidity meter (SPM_{optic}) were depth-averaged over 1 m to the same spatial resolution of the ADCP. $SPM_{acoustic}$ data were time-averaged over the sampling period of the respective SPM_{optic} profiles to the same temporal resolution of the turbidity meter.

3.4.1 General comparison of all sites

The correlation of SPM_{optic} and $SPM_{acoustic}$ is reasonably good ($R^2=0.787$; $n=704$; $p=0.01$; Figure 3-4) in accordance with other authors (Osborne et al., 1994; Seibt-Winckler, 1996; Thorne & Hardcastle, 1997; Holdaway et al., 1999; Rose & Thorne, 2001; Fugate & Friedrichs, 2002). Figure 3-3 shows the line of best linear fit as well as the line $SPM_{acoustic}=SPM_{optic}$. Acoustic backscatter sensors respond to the particle volume compared to optical backscatter, which is directly governed by the cross-sectional area of the suspended particles (Ishimaru, 1978; Lynch et al., 1997; Fugate & Friedrichs, 2002). Acoustic backscatter sensors are therefore generally more sensitive to particle size than are optical sensors (Gartner, 2002). The average SPM grain-size in the Laptev Sea is smaller than 6 Phi (15.6 μm ; Dethleff, 1995; Burenkov et al., 1997; Binder, 2001). Thus, the SPM concentration may be underestimated by acoustic backscatter sensors, which show better correlations with suspended sand fractions (Thorne et al., 1991; Lynch et al., 1997; Santamarina Cuneo & Flemming, 2000; Gartner, 2002). Deviations from the 1:1 line into the sector of higher estimations by the turbidity meter can probably be associated with the differences of both sensors in sensitivity to particle size. As the line of best linear fit is within the sector of higher SPM estimations by the turbidity meter, it can be assumed that in general SPM concentrations on the Laptev Sea shelf estimated from ADCP echo intensities are lower than estimations derived from turbidity meter measurements.

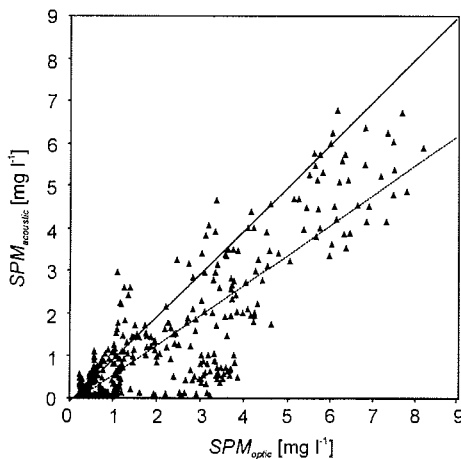


Figure 3-3: Comparison of SPM concentrations derived from acoustic backscatter signals ($SPM_{acoustic}$) with concentrations derived from optical backscatter signals (SPM_{optic}) with the continuous line indicating the 1:1 line and the dotted line indicating the line of least square fit.

3.4.2 Detailed profile comparison

To assess the concentration profiles obtained at each site using the ADCP and the turbidity meter, $SPM_{acoustic}$ and SPM_{optic} were compared with SPM_{filter} profiles as an absolute reference (Figure 3-4 to 3-6).

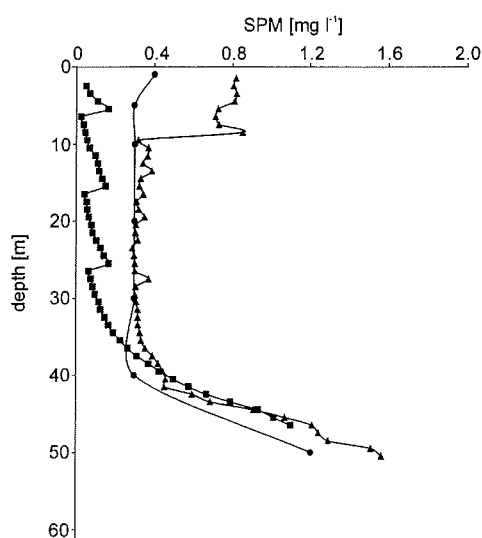


Figure 3-4: Vertical SPM distribution at station YS0011 with the solid squares indicating SPM concentrations derived from acoustic backscatter signals ($SPM_{acoustic}$), solid triangles concentrations from optical backscatter signals (SPM_{optic}), and solid circles indicating concentrations obtained from filtered water samples (SPM_{filter}). The $SPM_{acoustic}$ profile shows small artificial peaks when changing the parameter K .

At stations YS0011 and YS0048 a close similarity of both sensors with the SPM_{filter} profiles was recognized. SPM concentrations at station YS0011 were generally low (Figure 3-4). In the upper water column they were in the range of the elutable portion of the filters and thus SPM_{filter} was arguable. Differences in $SPM_{acoustic}$ and SPM_{optic} were small and not significant. At station YS0048 the general trend was similar for both $SPM_{acoustic}$ and SPM_{optic} , compared to SPM_{filter} : lowest concentrations in the upper water layer, an intermediate layer of increased SPM concentrations and highest concentrations near the bottom (Figure 3-6). At both sites SPM_{optic} and $SPM_{acoustic}$ coincided well with SPM_{filter} . In general SPM_{optic} was higher and $SPM_{acoustic}$ was lower than SPM_{filter} . The SPM_{optic} and SPM_{filter} profiles at station YS0024 at different time steps exhibited a higher variability in SPM dynamics (Figure 3-5a-c).

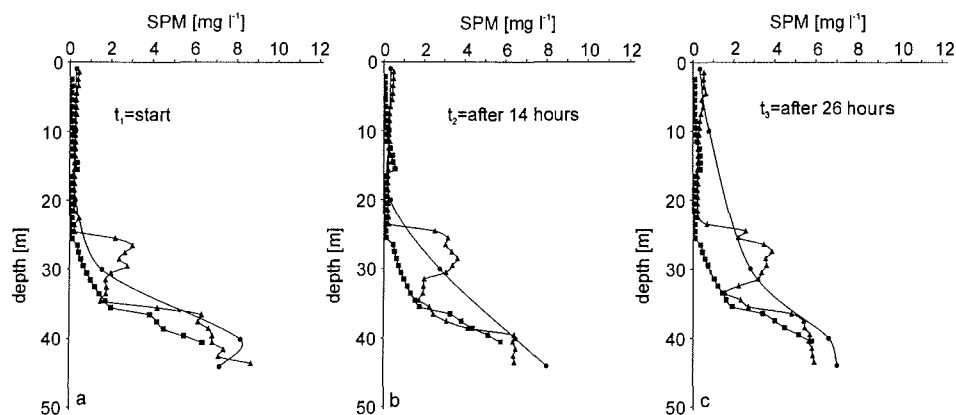


Figure 3-5: SPM profiles for a time period of 26 hours at station YS0024 (a-c). The solid squares indicate SPM concentrations derived from acoustic backscatter signals ($SPM_{acoustic}$), solid triangles concentrations from optical backscatter signals (SPM_{optic}), and solid circles indicate concentrations obtained from filtered water samples (SPM_{filter}).

At a water depth between 25 and 35 m, a dynamic layer with increased SPM concentrations was recognized, which was not revealed within the $SPM_{acoustic}$ profiles. The increased SPM concentrations were related to lateral transport events of probably fine material (Wegner et al., in press). Hence, the ADCP, more sensitive to the fine sand fraction, did not detect the inter-layer of increased SPM concentration and its dynamics. But the SPM estimations in the bottom layer of the optical and acoustic backscatter sensors were very close to the SPM_{filter} profile. Since most of the sediment transport is assumed to take place within the bottom layer (Wegner et al., in press), it can be sufficiently described by both ADCP and turbidity meter measurements.

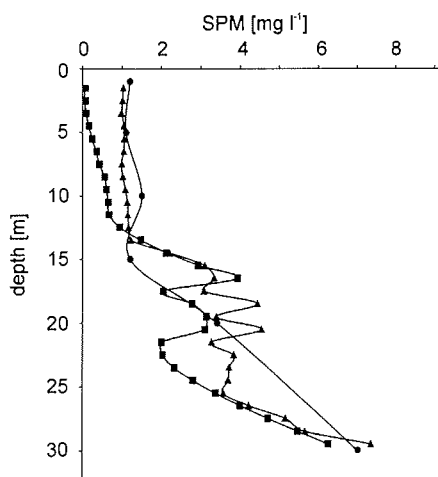


Figure 3-6: Vertical SPM distribution at station YS0048 with the solid squares indicating SPM concentrations derived from acoustic backscatter signals ($SPM_{acoustic}$), solid triangles concentrations from optical backscatter signals (SPM_{optic}), and solid circles indicating concentrations obtained from filtered water samples (SPM_{filter}).

3.5 Summary and conclusions

During the TRANSDRIFT VIII expedition 2000, SPM concentrations were quantified on the Laptev Sea shelf with optical (turbidity meter) and acoustic (ADCP) backscatter sensors and calibrated with filtered water samples. With comparatively small effort in terms of water sampling a conversion of both the turbidity meter and ADCP signals into SPM concentrations was possible. In general SPM concentrations estimated from backscattered signals of both sensors coincided well with SPM concentrations derived from filtered water samples even though one sensor might miss one event recorded by the other depending on the SPM grain-size. ADCPs tend to underestimate and turbidity meters tend to slightly overestimate SPM concentrations. For the investigation of sediment transport dynamics on the Laptev Sea shelf ADCPs are more convenient as they provide reasonably good SPM concentrations as well as current records for the entire water column. Turbidity meters are suggested as a completion to improve the SPM measurements.

4 CHAPTER 4

Suspended Particulate Matter on the Laptev Sea Shelf (Siberian Arctic) During Ice-Free Conditions

4.1 Abstract

Optical turbidity surveys combined with pigment, plankton, and current measurements were used to investigate the vertical and horizontal dynamics of suspended particulate matter (SPM) in the Laptev Sea, one of the largest Siberian shelf seas, during the ice-free period. Optical measuring devices provide an excellent tool to measure SPM distribution in real time. SPM concentrations were quantified due to the high correlation of water samples and optical backscatter signals. Thus the formation and distribution of the bottom nepheloid layer, a layer of increased SPM concentration, and its significance for the sediment transport on the Laptev Sea shelf can be described.

Two nepheloid layers exist in the eastern and central Laptev Sea. Formation and concentration of the surface layer are mainly related to phytoplankton and zooplankton abundance. However, in the vicinity of the Lena Delta the concentration is strongly dependent on riverine discharge. The bottom nepheloid layer is suggested to develop during and briefly after the river-ice breakup when about 60% of the mean annual sediment input is discharged onto the shelf. SPM spreads over the shelf and is kept in suspension within the bottom layer. Especially during the ice-free period almost no sedimentation takes place. Bottom material is resuspended due to wind-induced increased bottom currents, mainly in Pleistocene river valleys and on shoals. Valleys act as transport conduits in the ice-free period and SPM is shifted within them. An intermediate layer near Stolbovoy Bank is probably caused by the displacement of the bottom layer from the topographic highs into the valleys. The combined turbidity and current measurements indicate that most of the sediment transport on the Laptev Sea shelf takes place in the bottom nepheloid layer.

4.2 Introduction

The Laptev Sea is characterized by one of the largest Siberian shelf areas (Figure 4-1). The shelf is rather shallow (mainly <50 m) and dips gently northwards. It is cut by five submarine channels orientated in a northerly and northwesterly direction, which represent Pleistocene river valleys (Holmes & Creager, 1974; Kleiber & Niessen, 1999). Several rivers discharge onto the shelf with a yearly freshwater input of about $714 \text{ km}^3 \text{ yr}^{-1}$ (Pivovarov et al., 1999), of which the input by the Lena River into the eastern Laptev Sea is highest with about $520 \text{ km}^3 \text{ yr}^{-1}$ (Aagaard & Carmack, 1989). The rivers as well as coastal and seafloor erosion (Burenkov et al., 1997; Are, 1999; Rachold et al., 2000), are an important sediment source for the Laptev Sea. The riverine influence reveals a strong seasonality, as the Laptev Sea is almost entirely ice-covered for about nine months a year. The freshwater discharge and riverine sediment input are highest during and briefly after the river-ice breakup (Pivovarov et al., 1999). At the Lena River, about 40% of the mean annual discharge and nearly 60% of the mean annual sediment input can be observed during the river-ice breakup (Ivanov & Piskun, 1999).

In general, suspension transport is the dominant transport mode on many continental shelves (Cacchione & Drake, 1990). Most SPM transport is assumed to take place in benthic or/and in intermediate nepheloid layers, i.e., layers of increased SPM concentration in the water column (e.g., Drake et al., 1972; McCave, 1975). However, with respect to the Arctic shelves little is known on the formation of the bottom nepheloid layer, its dynamics and its significance for the paleo-sediment record. The investigation of SPM dynamics is therefore of particular interest for the quantification of sediment transport and for a complete sediment budget of Arctic shelves.

Up to now the SPM distribution as well as its horizontal and vertical dynamics on the Laptev Sea shelf have been poorly documented. Within the German-Russian project "Laptev Sea System" the dynamic system of the Laptev Sea has been studied for several years based on data gained during eight expeditions (TRANSDRIFT (TD) expeditions). Studies of SPM distribution during the river-ice breakup off the Lena Delta were carried out by Pivovarov et al. (1999). During and briefly after the river-ice breakup SPM concentrations $>70 \text{ mg l}^{-1}$ were measured within the freshwater layer. Most of the

discharged material is transported onto the SE Laptev Sea shelf. Below the pycnocline SPM concentration changed only slightly during and after the river-ice breakup.

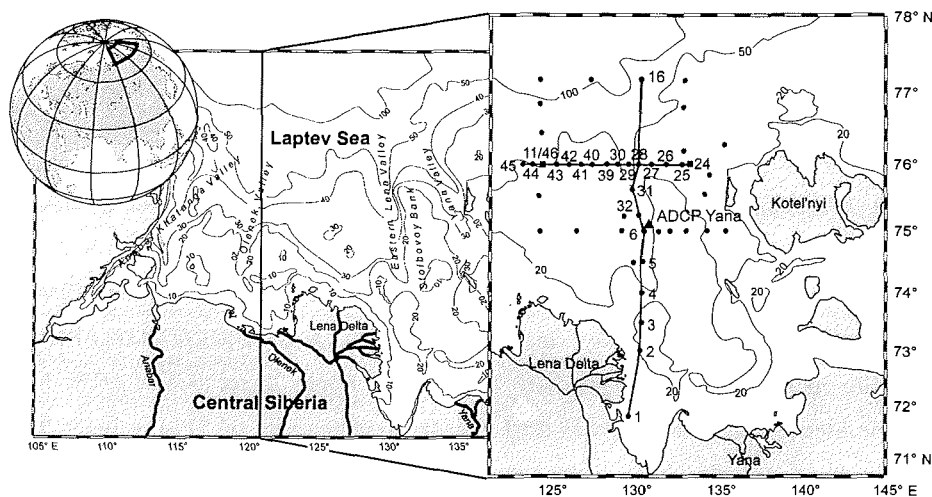


Figure 4-1: Bathymetric map of the Laptev Sea shelf and the locations of presented profiles and bottom-mooring stations (YS00.). Solid circles indicate short-term, solid squares long-term stations during the TD VIII expedition. The solid triangle represents the one-year bottom-mooring station YANA in 1998/99.

Anoshkin et al. (1995) and Antonow et al. (1997) used hydro-optical measuring devices, which produced only relative values of SPM concentration on the Laptev Sea shelf, as an *in situ* calibration of the hydro-optical data was not available. These authors and others (Hölemann et al., 1995; Burenkov et al., 1997; Lisitsin et al., 2000) described a maximum of SPM near the bottom on the shelf during the ice-free period, representing the bottom nepheloid layer. A second maximum of SPM concentration was observed in the upper part of the water column in the vicinity of the Lena Delta and is thought to be due to riverine input (Burenkov et al., 1997; Kuptsov et al., 1999). The major conclusions of these previous works with regard to SPM distribution and dynamics were that a bottom nepheloid layer was permanently present during the ice-free period on the Laptev Sea shelf with decreasing concentrations from south to north, probably fed by riverine input, coastal and seafloor erosion. Zones of river water on the shelf

could be clearly distinguished in terms of SPM concentration and fluorescence intensity. The present paper tackles such unsolved questions as short-term variability, transport dynamics, and composition of SPM in the nepheloid layer as it combines SPM, current, pigment, and plankton measurements.

4.3 Methods

To investigate the vertical and horizontal distributions of SPM as well as their dynamics on the Laptev Sea shelf, turbidity and current measurements along a grid of 48 short- and long-term stations on the eastern and central shelf were carried out during TD VIII aboard RV “Yakov Smirnitskiy” in September 2000. A SEAPOINT TURBIDITY METER connected to a Conductivity Temperature Depth Meter (CTD; OTS, ME Marine Electronics, Germany) was used in order to obtain data on SPM, salinity, and temperature distribution in the water column. The turbidity meter emits light of 880 nm wavelength with a constant output time of 0.1 sec. It detects light scattered by particles within the water column and generates an output voltage proportional to particle concentration. The output is given in Formazine Turbidity Unit (FTU), a calibration unit based on formazine as a reference suspension. The turbidity meter and the CTD were mounted on a frame during all measurements. At each station the frame was lowered until it touched the seafloor. Measurements showed that the turbidity meter signal increased significantly when the cage touched the ground. Consequently, neither have these data been taken into account for the evaluation nor have data above 1.50 m below water surface to avoid any disturbances caused by air bubbles (Johnson et al., 2000).

To describe the vertical dynamics of SPM within the water column, the turbidity meter and CTD measurements were carried out hourly at long-term stations (station YS0011 and YS0024) for a period of at least 28 hours each (Figure 4-1). Every four hours water samples of two liters each were collected from different water depths to obtain the SPM concentrations by using the traditional filtering and weighing procedures and to calibrate the optical backscatter signals. All SPM concentrations obtained from water samples ($SPM_{filter} \leq 0.3 \text{ mg l}^{-1}$) were set to 0.3 mg l^{-1} , as the elutable portion of the used filters (MILLIPORE \varnothing 0.45 microns) is $<0.3 \text{ mg l}^{-1}$. All turbidity measurements were

correlated with corresponding filtered water samples to obtain accuracy by taking the effects of different mineralogy, varying particle darkness, and salinity of ambient water on the response of the turbidity meter into account (Maa et al., 1992; Sutherland et al., 2000). A strong correlation was observed (Figure 4-2).

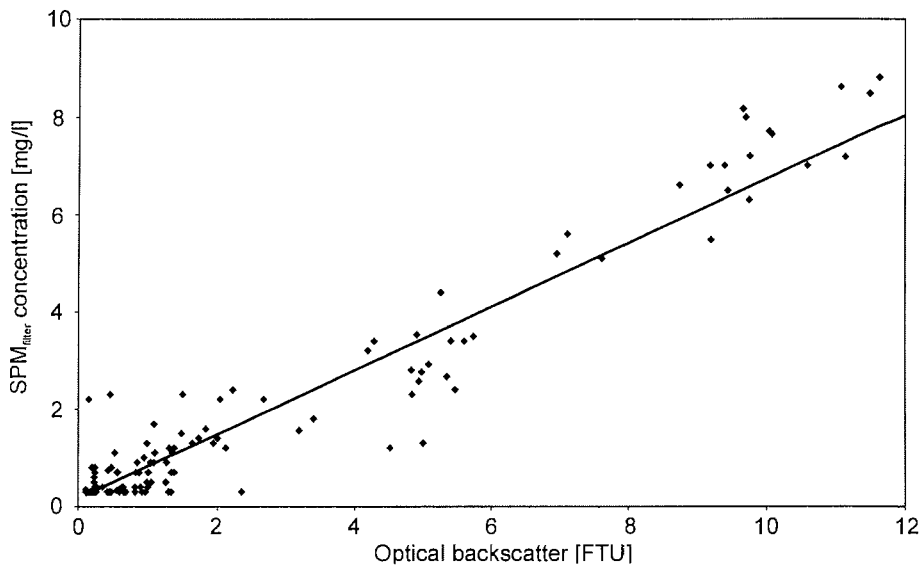


Figure 4-2: Linear relation between concentrations derived from filtered water samples (SPM_{filter}) and optical backscatter in Formazine Turbidity Units (FTU; $R^2=0.931$; $p=0.01$; $n=129$).

The linear relation between SPM concentration (SPM_{optic}) and optical backscatter intensity (OI) can be expressed as: $SPM_{optic} = 0.166 + 0.651 OI$. The correlation of SPM_{filter} concentrations and optical backscatter signals is strongest in the lower part of the water column (mostly below the pycnocline). This is probably due to the high portion of phytoplankton in the upper 5 m of the water column. The presence of phytoplankton in suspension generates slightly increased optical backscatter signals but cannot be recognized on SPM filters. This may lead to a poor instrument calibration (Bunt et al., 1999). At each short-term station turbidity and CTD profiles were carried out. Partly water samples were obtained.

In order to specify the algal portion of SPM, water samples of one liter each were obtained at defined depths every four hours, filtered through WHATMAN GF/F glasfiber filters and then treated according to the method of Arar & Collins (1992). Chl *a* and Phaeo *a* concentrations were analyzed, with Chl *a* as a measure for the biomass of phytoplankton, and Phaeo *a* indicating the portion of decaying algae. In order to get a better determination of the portion of living and dead organisms, zooplankton samples were obtained (Abramova et al., 2001).

At each long-term station a bottom-moored broadband Acoustic Doppler Current Profiler (ADCP; WH Sentinel 307.2 kHz, RD-Instruments) was deployed in order to better understand resuspension and transport processes of SPM. Supplementary current data of the one-year bottom-mooring station, deployed during TRANSDRIFT V (1998), were analyzed for the general trend of current magnitudes and directions in the Eastern Lena Valley in September. Threshold current velocities for incipient motion for each station were estimated according to Soulsby & Whitehouse (1997) from seabed characteristics of Lindemann (1994). The conversion of current data to critical velocities for erosion or resuspension is used as a first estimation even though it does not replace long-term SPM data completely.

4.4 Results

4.4.1 Vertical distribution of SPM

Turbidity measurements at station YS0024 near Stolbovoy Bank (Figure 4-1) during the monitoring period of 28 hours in September 2000 clearly reflect the vertical dynamics of SPM within the water column close to slopes. Three nepheloid layers were distinguished (Figure 4-3a) with the intermediate and bottom layer showing noticeable changes in concentration and thickness. SPM_{optic} concentration in the intermediate nepheloid layer ranged between 2 to 4 mg l⁻¹ at water depths between 25 to 35 m (Figure 4-3a). The bottom layer had a thickness of 7 to 12 m with SPM_{optic} concentrations ranging between 5 to 8 mg l⁻¹. Pigment measurements showed a distinct maximum in the Chl *a* concentration with a small portion of Phaeo *a* in the upper 5 m of

the water column (Figure 4-3b) indicating a high portion of living phytoplankton. Near the seafloor the algal portion of SPM is mostly due to decaying material, indicated by a high portion of Phaeo *a* (Figure 4-3b). The temperature and salinity profiles (Figure 4-3c) exhibited a bottom mixed layer of about 10 m thickness that roughly corresponded with the thickness of the bottom nepheloid layer. An increase in temperature was identified in 12 to 22 m water depth.

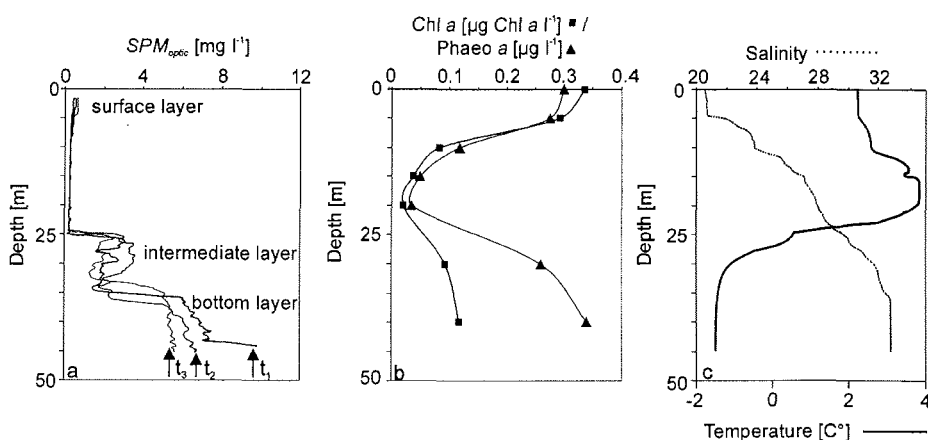


Figure 4-3: (a) Vertical SPM_{optic} distribution for different time steps (t_1 =time 1; $t_2=t_1+14$ hours; $t_3=t_1+26$ hours), (b) typical Chlorophyll *a* (Chl *a*) and Phaeopigment *a* (Phaeo *a*) concentrations, (c) temperature and salinity profiles at station YS0024.

During the monitoring period of 33 hours at station YS0011 no distinct changes in the distribution of SPM in the water column were observed. The thickness of the bottom nepheloid layer ranged between 7 and 10 m (Figure 4-4a). The SPM_{optic} concentration with up to 1.8 mg l⁻¹ was significantly lower compared to the bottom concentration at station YS0024. The upper boundary of the bottom nepheloid layer was less distinct than in the northern Yana Valley (station YS0024). Chl *a* concentration near the water surface was generally more than twice as high as at station YS0024 (Figure 4-4b). The salinity and temperature profiles (Figure 4-4c) showed a well-mixed bottom layer with a thickness of about 20 m. Thus, the thickness of the well-mixed bottom layer did not

correspond with the thickness of the bottom nepheloid layer. An intermediate nepheloid layer, comparable to the situation observed at station YS0024, was absent.

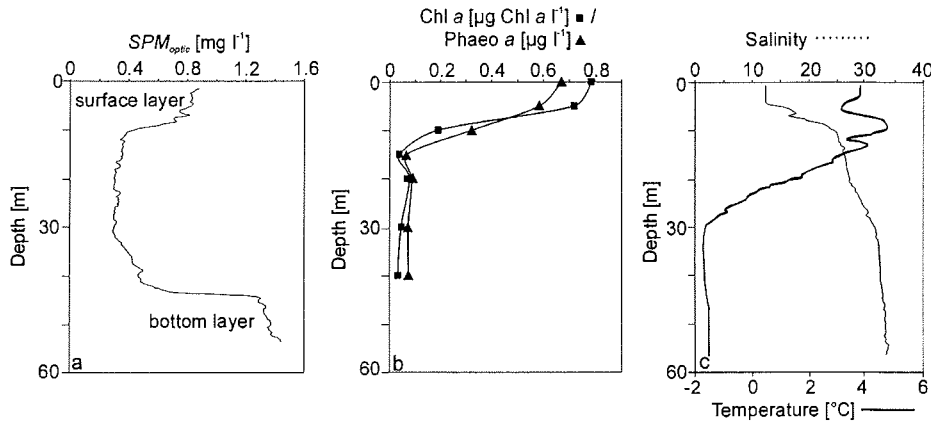


Figure 4-4: (a) Typical SPM_{optics} , (b) Chlorophyll *a* (Chl *a*) and Phaeopigment *a* (Phaeo *a*) concentrations, (c) temperature and salinity profiles at station YS0011 in the central Laptev Sea.

4.4.2 Horizontal distribution of SPM

EW- and NS-orientated transects were studied in order to investigate the horizontal distribution of SPM and the bottom transport on the Laptev Sea shelf. The EW-profile along 76°N showed a bottom nepheloid layer with concentrations decreasing from east to west (Figure 4-5a). The bottom nepheloid layer in the eastern Laptev Sea was distinct and showed a sharp upper boundary with highest SPM_{optics} concentrations of up to 6 mg l⁻¹ in the Yana Valley and a second maximum with concentrations of up to 4 mg l⁻¹ on Stolbovoy Bank. Towards the west the bottom nepheloid layer was less distinct with SPM_{optics} concentrations of only up to 1.8 mg l⁻¹. Neither the temperature nor the salinity profiles showed distinct changes (Figure 4-5b and 4-5c).

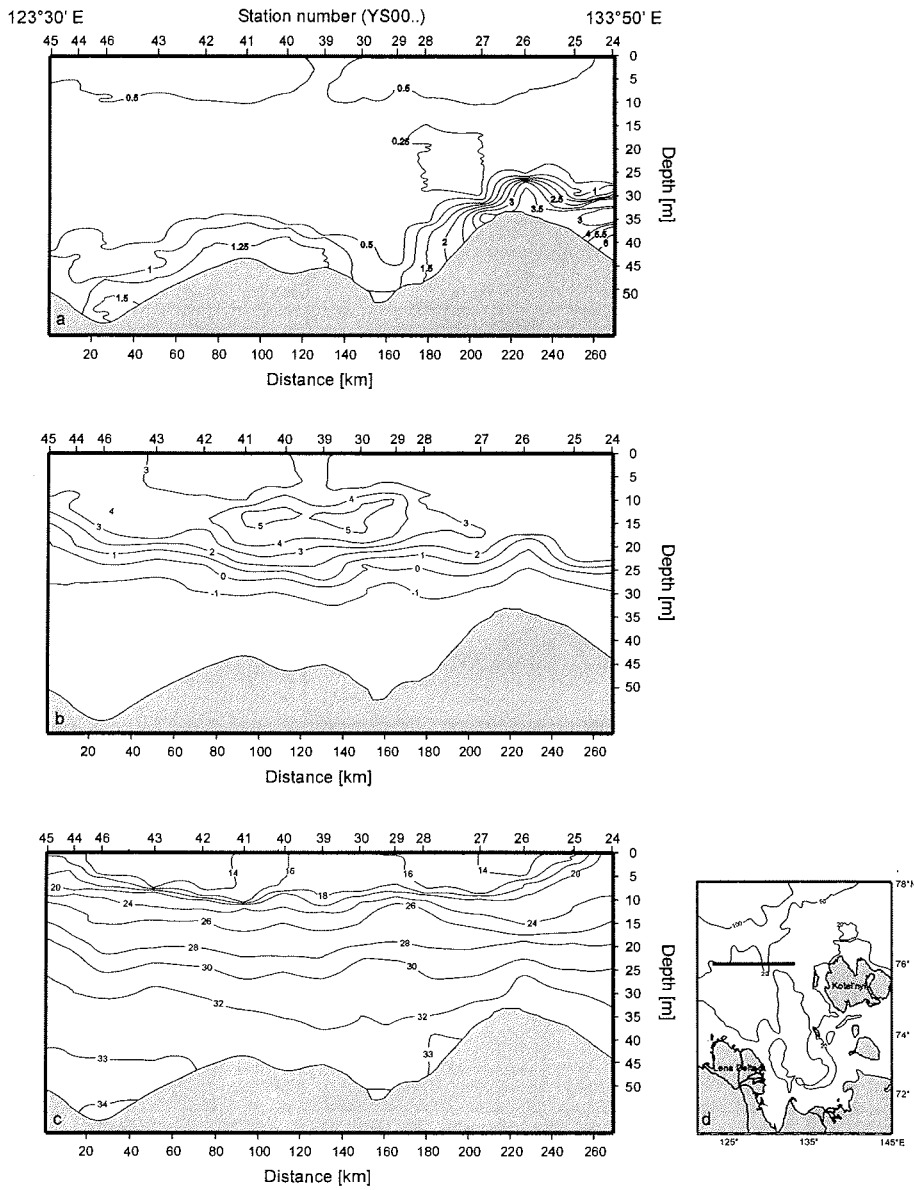


Figure 4-5: (a) SPM_{optic} concentration [mg l⁻¹], (b) temperature [°C] and (c) the salinity distribution on a EW-transect at 76°N (d).

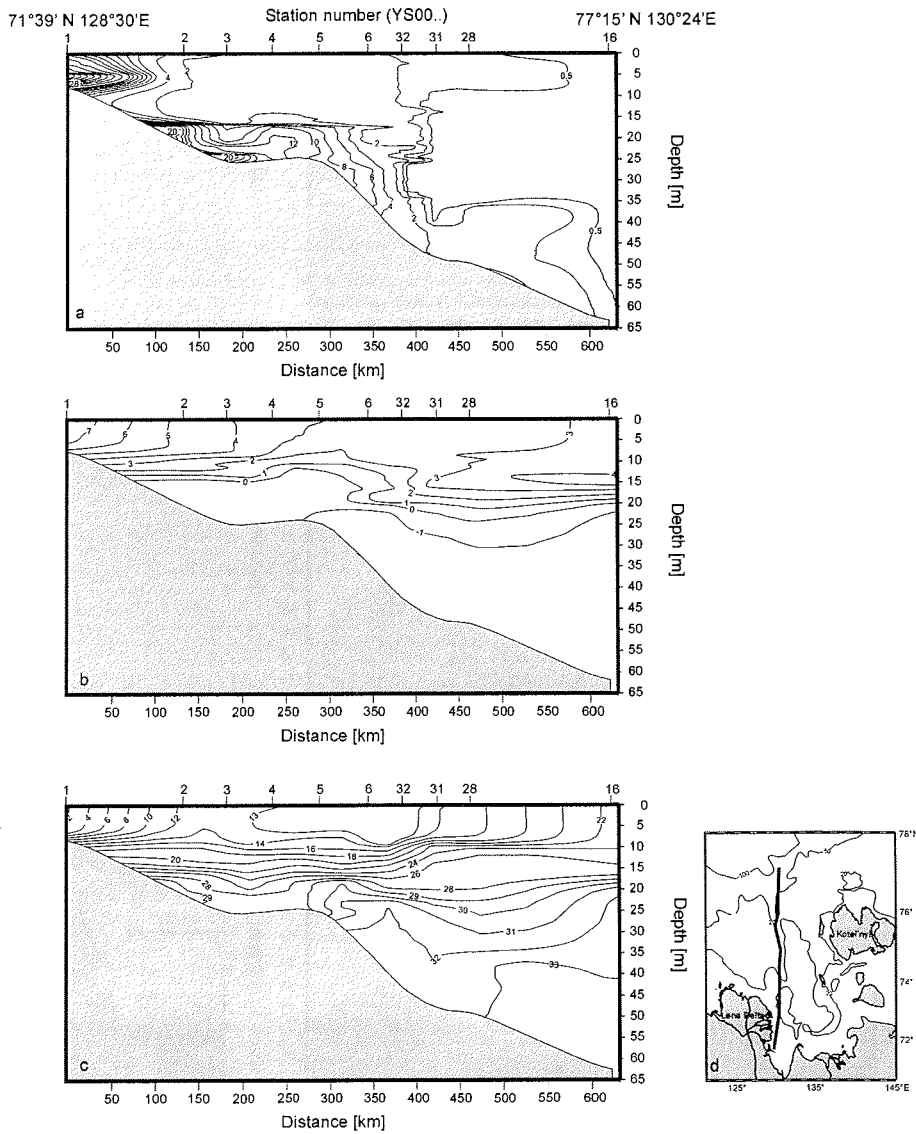


Figure 4-6: (a) SPM_{optic} concentration [mg l⁻¹], (b) temperature [°C] and (c) salinity on a NS-transect along the Eastern Lena Valley (d).

As the riverine sediment supply by the Lena River is an important sediment source, a NS-orientated transect along the Eastern Lena Valley was investigated. Along this NS-profile the SPM_{optic} concentration in the bottom nepheloid layer decreased from south to north (Figure 4-6a). Near the Lena Delta the surface and bottom layer tended to merge. Almost the entire water column seemed to be turbid. However, highest SPM_{optic} concentrations (up to 28 mg l^{-1}) were reached near the bottom at station YS0001. A second maximum in SPM_{optic} with concentrations of about 20 mg l^{-1} was found in the bottom nepheloid layer between stations YS0003 and YS0004. Towards the north the SPM_{optic} concentration decreased remarkably (0.7 mg l^{-1} at station 16). With increasing distance from the Lena Delta the salinity increased (Figure 4-6c), but temperature decreased (Figure 4-6b).

4.4.3 Bottom currents

Current velocities and directions were studied in the Eastern Lena Valley, Yana Valley and the central shelf region to investigate transport dynamics in the bottom nepheloid layer (Figure 4-7). A significant north-south orientation of the bottom currents was noted at one-year bottom-mooring station YANA (Figure 4-7). For a monitoring period of 4 days in September 2000, current data were obtained in the Yana Valley at station YS0024 (Figure 4-7). The bottom currents were directed towards the east-southeast (Figure 4-7). The current velocities were smaller compared to velocities measured in the Eastern Lena Valley. At station YS0011 in the central Laptev Sea bottom currents were directed towards the northeast during the monitoring period of 8 days in 2000 (Figure 4-7). The average bottom current velocity was lower than the estimated critical threshold velocity of incipient motion and significantly lower than in the east (Figure 3-7).

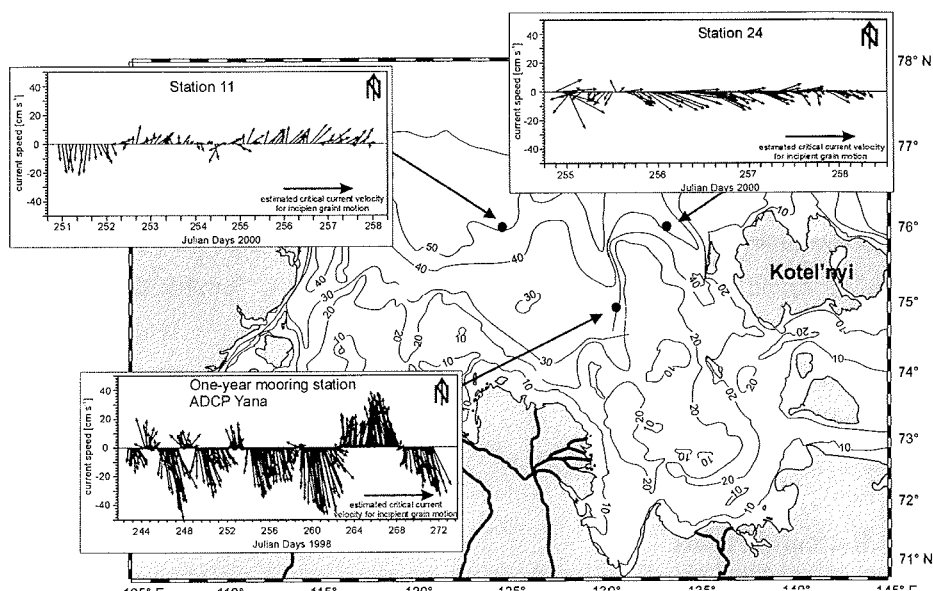


Figure 4-7: Current speed and directions 3 m above the seafloor determined from bottom-moored ADCPs.

4.5 Discussion

4.5.1 The formation and spatial distribution of the nepheloid layers

The vertical turbidity profiles showed two nepheloid layers during the ice-free period: a surface layer of about 5 m thickness and a bottom layer. An intermediate nepheloid layer was distinguished only in the vicinity of Stolbovoy Bank.

The surface nepheloid layer on the central and outer Laptev Sea shelf showed an SPM_{optic} concentration between 0.5 and 0.8 mg l⁻¹. Pigment analysis during the TRANSDRIFT V expedition (August 1998) along a similar NS-transect showed high Chl *a* but low Phaeo *a* concentrations in the central and outer shelf region (Tuschling, 2000). High zooplankton abundance and biomass were observed in the surface layer during TRANSDRIFT VIII (Abramova et al., 2001). Changes in concentration can

therefore be related to changes in phytoplankton biomass and probably in zooplankton. In the vicinity of the Lena Delta, on the other hand, highest $SPM_{filter/optic}$ and highest Chl *a* concentrations (Tuschling, 2000) have been determined suggesting that the surface layer is composed of both algal and riverine material during the ice-free period. The SPM concentration decreased rapidly with increasing distance from the Lena Delta (Figure 4-6a). $SPM_{filter/optic}$ concentration in the surface layer was up to 18 mg l^{-1} near the Lena Delta and thus about 20 times higher than on the central and outer shelf. This decrease in concentration is in the same order of magnitude as found by Burenkov et al. (1997). Therefore, it can be assumed that during the ice-free period the material discharged by the Lena River settles quickly and forms the bottom nepheloid layer. The situation is different during the river-ice breakup when most of the riverine material is transported far out onto the shelf in the surface layer (Pivovarov et al., 1999).

In the intermediate layer at the slopes of Stolbovoy Bank the algal portion is negligible as the Chl *a* concentration was close to zero (Figure 4-3b). Burenkov et al. (1997) observed these intermediate layers as well. They suggested an intrusive origin as the layers corresponded in depth with temperature inversions. Nepheloid layers are not supplied principally by particle settling but through lateral spread from topographic highs as well (Drake et al., 1972). During our monitoring period the height of layers of comparably higher temperatures did not correspond to the height of the intermediate SPM maximum. Therefore, the intermediate layer is assumed to be the result of the lateral displacement of the bottom nepheloid layer of the topographically elevated Stolbovoy Bank towards the valleys and the northeasterly current flow measured at station YS0024 rather than to be of intrusive origin.

The concentration in the bottom nepheloid layer decreased from east to west (Figure 4-5a) and from south to north (Figure 4-6a). A similar NS-distribution has been recognized by Hölemann et al. (1995). A decrease in bottom current velocities in the eastern outer shelf region (station YS0024 and station YANA; Figure 4-7) was not observed in contrast to Burenkov et al. (1997). As a first approach this decrease in SPM concentration can therefore mainly be explained by progressive dispersion of SPM across the shelf and only to some extent by sedimentation. The development of the bottom nepheloid layer is generally related to local resuspension of particles by waves

and currents (Cacchione & Drake, 1986; Gardner, 1989) as well as by internal waves (Gardner, 1989). Storm events may cause sediment resuspension and may subsequently lead to particle transfer on continental shelves as well (Hill & Nadeau, 1989). In the Laptev Sea bottom current velocities strong enough to cause resuspension are often wind-induced (Dmitrenko et al., 2001b). Hence, the concentration of the bottom nepheloid layer increased due to resuspension during and after periods of higher wind speed (Burenkov et al., 1997; Kuptsov et al., 1999). But horizontal supply of SPM from riverine input governs the SPM concentration within the bottom nepheloid layer as well (Ruch et al., 1993). Due to the high seasonality of the riverine input onto the Laptev Sea shelf, the substantial load of SPM discharged during and briefly after the river-ice breakup is likely to spread over the shelf in the bottom nepheloid layer and is kept in suspension at least during the ice-free period. Thus, the bottom nepheloid layer is not only composed of resuspended material as suggested by Burenkov et al. (1997) and Kuptsov et al. (1999) but also of residual material from the suspended load discharged during and briefly after the river-ice breakup, which did not settle in the meanwhile. The bottom nepheloid layer varies in concentration and thickness as stated already by Burenkov et al. (1997) and Kuptsov et al. (1999). Changes in concentration are mostly due to an irregular load of SPM derived from seafloor erosion after resuspension events. The thickness of the bottom nepheloid layer showed the highest variability in the vicinity of Stolbovoy Bank where additional material is displaced (Figure 4-3a). The thickness of the bottom nepheloid layer and of the bottom mixed layer corresponded only at some stations (Figure 4-3a – 4-6a). Therefore it may be assumed that bottom-stirring processes are mostly insufficient to spread SPM throughout the bottom mixed layer, as also described by Johnson et al. (2000) for the Kara Sea.

4.5.2 The significance of the bottom nepheloid layer for sediment transport

Generally the permanent presence of the bottom nepheloid layer suggests that repeated resuspension of surface sediments takes place before they finally become settled (Bothner et al., 1981). This seems to be true at least for the ice-free period on the Laptev Sea shelf as well. Sedimentation rates derived from sediment cores from the Laptev Sea shelf are lowest on the mid-shelf (Bauch et al., 2001). Average sedimentation rates for

the mid-shelf range from 2 to 11 cm x 10⁻³ yr⁻¹ during the past 5000 years (Bauch et al., 2001). These comparatively low sedimentation rates may be explained by repeated resuspension as well as by the fact that part of the material is only transported through the Pleistocene river valleys.

Sediment transport on shelves is mostly a function of wave-current interactions (Cacchione & Drake, 1990). Resuspension due to wave-current interaction as well as lateral transport take place on the eastern Laptev Sea shelf. Wide parts of the Pleistocene river valleys are probably only transport conduits for fine material during the ice-free period, where the material is only shifted and no sedimentation takes place. In the Pleistocene river valleys bottom current directions are strongly affected by bottom topography (Figure 4-7). Hence, the material is mostly moved within the eastern shelf area. In the central shelf area (station YS0011) material is mainly carried towards and over the continental margin. These current records apparently reflect a general current pattern. Geochemical data can be used additionally to investigate sediment transport directions in the Laptev Sea (Rachold, 1999). The Laptev Sea shelf can be divided into three provinces in terms of distribution of heavy minerals and trace elements with the eastern and western shelf showing clearly different compositions (Hölemann et al., 1999; Peregovich, 1999). They are mainly related to the different geochemical compositions of the rivers (Hölemann et al., 1999; Rachold, 1999). Therefore, material discharged by the Lena River seems to be transported mostly within the eastern shelf area, whereas in the central shelf region SPM is transported mostly over the continental margin, which corresponds to the current measurements.

4.6 Conclusions

Combined turbidity and current measurements enabled us to investigate the dynamics of SPM on the shelf and to gain new insights in sediment transport processes on Siberian shelves during the ice-free period. Based on these measurements it can be assumed that most of the sediment transport on the Laptev Sea shelf takes place within in the bottom nepheloid layer. The bottom layer supposedly develops during and briefly after the river-ice breakup when an immense load of SPM is discharged onto the shelf. The material spreads over the shelf and is kept in suspension within the bottom nepheloid

layer. SPM concentrations in the bottom nepheloid layer decreased from south to north and from east to west respectively. This decrease is mainly due to dispersion of SPM and only partly due to sedimentation. During the ice-free period almost no sedimentation takes place and this may explain the relatively low sedimentation rates on the mid-shelf. During and after periods of high wind speeds bottom material is partly resuspended, in particular in Pleistocene river valleys and on the shoals of the eastern Laptev Sea. The valleys act as transport conduits during the ice-free period. SPM is shifted within the valleys, even transported to the inner shelf region and not towards the continental margin. On the central Laptev Sea shelf, however, resuspension seems to be less common due to generally smaller bottom current velocities. SPM is mostly transported over the continental margin into the deep Arctic Ocean.

In general two nepheloid layers were observed in the eastern and central Laptev Sea during the ice-free period, a surface and a bottom layer. In the vicinity of the Lena Delta the surface layer is comprised of riverine and biogenic material. Therefore, only here the SPM concentration is strongly dependent on riverine discharge. The formation and dynamics of the surface layer on the remaining shelf are mainly related to changes in phytoplankton biomass and zooplankton migration. Close to Stolbovoy Bank an intermediate nepheloid layer was discerned. This intermediate layer was caused by the displacement of the bottom nepheloid layer of Stolbovoy Bank from the topographic high into the valleys causing a variation of the bottom nepheloid layer thickness in the valleys.

As most of the sediment transport takes place in the bottom nepheloid layer and as this layer seems to be a general phenomenon in the adjacent shelf seas as well, the dynamics of this layer should be studied in more detail, especially during the time of ice coverage to quantify the sediment budget.

5 CHAPTER 5

Seasonal Variations in Sediment Dynamics on the Laptev Sea Shelf (Siberian Arctic)

5.1 Abstract

The knowledge on sediment dynamics on Arctic shelves is limited, especially during the time of ice coverage and beneath the polynya as the shelves are exceedingly difficult to reach during this period. Hence, sediment budget calculations have so far been problematic. The Laptev Sea (Siberian Arctic) is one of the largest Siberian shelf seas and ice-covered for about nine months a year. To investigate sediment dynamics for a one-year period, two oceanographic bottom-mooring stations were deployed on the eastern Laptev Sea shelf between August 1998 and September 1999. Both mooring stations were equipped with an Acoustic Doppler Current Profiler (ADCP) and a Conductivity Temperature Depth meter (CTD). Thus, for the first time information on current, suspended particulate matter (SPM), and bottom temperature variations were provided throughout one seasonal cycle for a Siberian shelf sea.

The unique data set indicated that during and shortly after the river-ice breakup (June/early July) sediment transport is dominated by riverine input and transport onto the eastern Laptev Sea shelf within the surface layer. When ice-free conditions prevail (mid-July to September), SPM is suggested to be mainly trapped within a circulation system, which retards the escape of the sediment into the deep Arctic Ocean. During this period SPM discharged by the Lena River is transported within the surface layer onto the mid-shelf area where it sinks through the water column into the bottom nepheloid layer only to be carried back onto the inner shelf again additionally with resuspended material. On the inner shelf the material is partly transported back into the surface layer by turbid mixing and carried out onto the mid-shelf again. On the inner shelf during freeze-up (October), however, the SPM in the surface layer is rather

incorporated into newly formed ice. Beneath the ice cover (November to June/July) SPM slowly sinks and sediment transport is of minor importance on the inner shelf. However, beneath the polynya bottom material is still resuspended after storm events and transported onto the inner shelf where it temporarily settles.

5.2 Introduction

During the past decades, studies of sediment dynamics on continental shelves have focused on the need to identify the actual processes that control the sediment transport and the final fate of most suspended particulate matter (SPM) derived from the continents. Several studies focused on sediment dynamics on the Arctic shelves (e.g., Harper & Penland, 1982; Hill & Nadeau, 1989; Hill et al., 1991; Hequette & Hill, 1993; Macdonald et al., 1998; Johnson et al., 2000; McClimans et al., 2000; Sternberg et al., 2001) and on the variability of SPM flux under a permanent ice cover (e.g., Hargrave et al., 1994). However, direct current and SPM measurements throughout one seasonal cycle are still rare and insights into the sediment dynamics on Arctic shelves are limited, especially during the time of ice coverage (Macdonald et al., 1998).

The Laptev Sea is located between the Kara and the East Siberian seas and has a gentle relief truncated only by low-relief cross-shelf valleys, which represent Pleistocene river valleys (Holmes & Creager, 1974; Kleiber & Niessen, 1999; Figure 5-1). In general, the hydrography of the Laptev Sea is characterized by a high seasonality of freshwater discharge from several Siberian rivers, especially the Lena River (Pivovarov et al., 1999), ice coverage for about nine months a year and water exchange with the adjacent seas and the deep Arctic Ocean (Pavlov et al., 1996; Pavlov, 1998). For the investigation of sediment-transport dynamics bottom-current measurements are significant, but direct measurements are sparse. Wind-induced sea-level deformations cause strong bottom currents in the Pleistocene river valleys on the eastern Laptev Sea shelf with highest current speeds during the ice-free period (Dmitrenko et al., 2001b). The bottom currents are much weaker or even absent during the time of ice coverage, but increase significantly as soon as the polynya opens. The tidal range with 20 cm on

the open shelf is only low (Dmitrenko et al., 2001b). Studies on SPM distribution on the Laptev Sea shelf focus mainly on the ice-free period (Anoshkin et al., 1995; Antonow et al., 1997; Burenkov et al., 1997; Hölemann et al., 1995; Lisitsin et al., 2000; Wegner et al., in press) and on the time of the river-ice breakup off the Lena Delta (Pivovarov et al., 1999). Combined SPM and current measurements have only been carried out during the ice-free period (Wegner et al., in press). Most sediment transport on the eastern Laptev Sea shelf during this period is assumed to take place in the Pleistocene river valleys within a bottom nepheloid layer, a layer of increased SPM concentration with up to 12 m thickness (Wegner et al., in press). However, sediment-transport dynamics during the period of ice coverage and beneath the polynya on the Laptev Sea shelf are unknown.

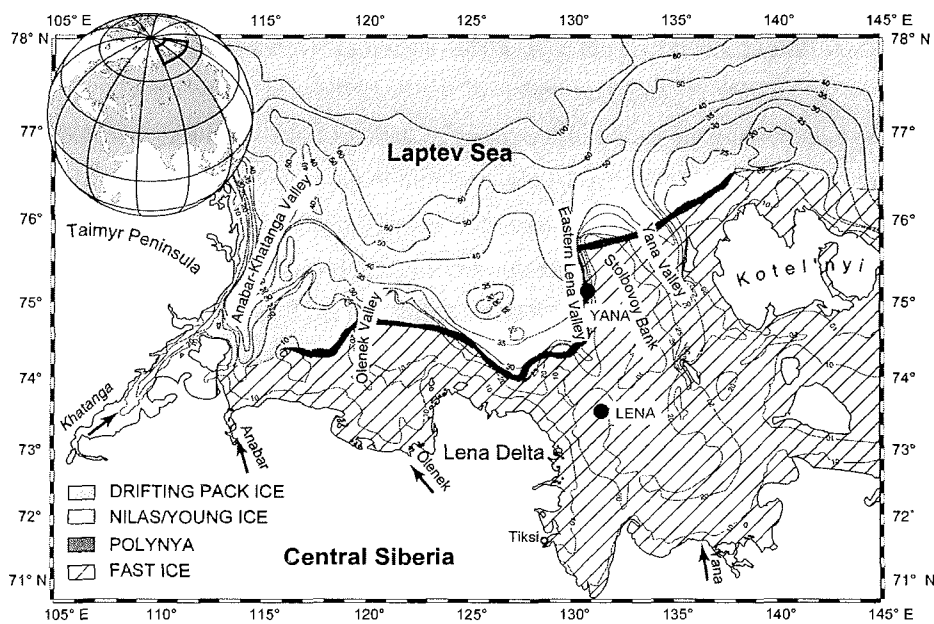


Figure 5-1: Bathymetry of the Laptev Sea shelf with Pleistocene river valleys. The locations of the bottom-mooring stations LENA ($73^{\circ}27.37'N$ $131^{\circ}41.98'E$) and YANA ($75^{\circ}09.01'N$ $130^{\circ}49.94'E$) are marked with circles. The distribution of fast-ice, pack ice and the average position of the polynya were reconstructed from RADARSAT ScanSAR images of the end of April 1999.

To investigate sediment dynamics beneath the ice cover and the polynya, two oceanographic bottom-mooring stations were deployed on the Laptev Sea shelf for a one-year period (August 1998-September 1999) within the German-Russian project "Laptev Sea System 2000". The mooring stations were equipped with an Acoustic Doppler Current Profiler (ADCP) and a Conductivity Temperature Depth meter (CTD). These combined measurements enabled us to describe the variations in current speed and direction, SPM dynamics and in bottom temperature for one seasonal cycle and the implications of changes in these parameters for sediment transport.

5.3 Methods

For a one-year period two oceanographic bottom-mooring stations, stations LENA and YANA, were deployed at key positions for sediment transport on the eastern Laptev Sea shelf (Figure 5-1). As riverine input is an important sediment source (Ivanov & Piskun, 1999; Rachold et al., 2000), station LENA was deployed on the inner shelf in the vicinity of important outlets of the Lena River at a water depth of 22 m (Figure 5-1). During the period of ice coverage station LENA was located beneath the fast ice (Figure 5-1). Station YANA was deployed in the mid-shelf area on the slope of the Eastern Lena Valley in the region of the average position of the fast-ice edge at a water depth of 44 m (Figure 5-1). An upwards-looking broadband ADCP (WH Sentinel 307.2 kHz, RD-Instruments) and a CTD (OTS, ME Marine Electronics, Germany) were installed within the mooring stations to provide data on current speed and direction, SPM concentrations, and bottom temperature.

ADCPs are used for the investigation of current speed and direction (e.g., Griffiths & Roe, 1993; Gordon, 1996) as well as for the estimation of SPM concentrations (e.g., Thorne et al., 1991; Hay & Sheng, 1992; Crawford & Hay, 1993; Griffiths & Roe, 1993; Seibt-Winckler, 1996; Deines, 1999; Holdaway et al., 1999). Due to calibration procedures the echo intensity data of the bottom-mooring stations were converted into SPM concentration ($SPM_{acoustic}$; see CHAPTER 2.3.2 and 3). ADCP measurements at both stations were carried out at intervals of 1 minute and averaged over 30 minutes in different depth cells (bins). Bottom-mooring station LENA

had a bin size of 1.5 m with the first bin measuring at 3.5 m above bottom (mab). Bin size of bottom-mooring station YANA was 2 m with the first bin measuring at 4 mab. Since most of the sediment transport on the Laptev Sea shelf is assumed to take place within the bottom nepheloid layer (Wegner et al., in press), mainly data of the first bin were taken into account. The recorded time-series of the bottom-mooring stations have been divided into different seasonal periods, depending on the ice conditions, because a sea-ice cover checks across-shelf sediment transport by limiting the fetch of winds in Arctic settings (Nittrouer & Wright, 1994). The extent of sea-ice coverage during winter 1998/99 was estimated from weekly sea-ice charts of the Arctic and Antarctic Research Institute (AARI), St. Petersburg, Russia (http://www.aari.nw.ru/clgmi/sea_charts/sea_charts_en.html).

The threshold velocities for incipient grain motion were estimated following Soulsby & Whitehouse (1997) using grain-size parameters of Lindemann (1994), because directly measured threshold velocities are lacking. At bottom-mooring station LENA the estimated threshold velocity is about 27 cm s^{-1} , at station YANA about 30 cm s^{-1} (see CHAPTER 2.4). With SPM grain-size parameters of Dethleff (1995), Burenkov et al. (1997), and Binder (2001) settling velocities were estimated. They ascertained an average SPM grain size of smaller than 6 Phi ($15.6 \mu\text{m}$). Therefore the settling velocity is mostly below 0.002 cm s^{-1} (e.g., McCave, 1975; Puls et al., 1995; see CHAPTER 2.4). The instantaneous horizontal SPM fluxes were estimated by multiplying the instantaneous current speeds and SPM concentrations for each current component. The resultant vector of the flux components describes the estimated magnitude of the net horizontal SPM flux and its direction at the mooring sites (Wright, 1995; Puig et al., 2001; Palanques et al., 2002; see CHAPTER 2.5).

5.4 Results

5.4.1 Currents and hydrography

Inner shelf – bottom-mooring station LENA

Current speeds recorded in the first bin (3.5 mab) at bottom-mooring station LENA ranged from 0 to 48.6 cm s⁻¹ during the entire monitoring period (Figure 5-2a). The eastward current component varied between -48.60 and 33.60 cm s⁻¹, the northward component between -35.60 and 34.50 cm s⁻¹ (Figure 5-2b-c). The general bottom-current direction was towards the north. The time-series of bottom currents reveal significant seasonal variations: highest current speeds were recorded during the ice-free period with a mean current speed of 11.40 cm s⁻¹ and a maximum of 48.60 cm s⁻¹ (Table 5-1). Mean current speeds during freeze-up were still high with 9.98 cm s⁻¹ even though the recorded maximum was only 32.30 cm s⁻¹. During the time of ice coverage currents were considerably reduced as seen in both the maximum and mean speeds. At that time, the mean speed was reduced by the factor 2 compared with the ice-free period (Table 5-1).

Table 5-1: Summary of current speed, eastward (u) and northward (v) current component, and temperature (T) measurements at the bottom-mooring stations for the first bins (LENA: 3.5 mab; YANA: 4 mab).

Sea-ice conditions	Time mm/dd/yy	Current speed _{max} [cm s ⁻¹]	Current speed _{mean} [cm s ⁻¹]	u _{mean} [cm s ⁻¹]	v _{mean} [cm s ⁻¹]	T _{mean} [°C]
Bottom-mooring station LENA¹						
Ice-free (summer)	08/02/ – 10/03/98 06/28/ – 08/29/99	48.60	11.40	0.21	2.47	-0.96
Freeze-up (fall)	10/04/ – 10/31/98	32.30	9.98	0.14	0.82	-1.07
Ice coverage (winter)	11/01/98 – 06/27/99	31.90	5.46	0.10	0.46	-1.35
Bottom-mooring station YANA¹						
Ice-free (summer)	08/13/ – 10/03/98 06/24/ – 08/30/99	47.00	13.72	1.92	-6.74	-1.67
Freeze-up (fall)	10/04/ – 10/23/98	33.60	15.38	2.53	-7.75	-1.82
Ice coverage (winter)	10/24/98 – 01/29/99 02/14/ – 04/09/99 05/31/ – 06/23/99	35.90	8.41	0.10	-1.39	-1.76
Polynya (winter)	01/30/ – 02/13/99 04/10/ – 05/30/99	39.70	10.53	1.97	-5.44	-1.67

¹ Kassens & Dmitrenko (in press a)

The same seasonality is indicated in the time-series of the bottom temperature (3.5 mab): the temperature varied from -0.96 °C during the ice-free period to -1.35 °C during the time of ice coverage (Table 5-1). The bottom temperature increased much faster at the beginning of the ice-free period than it decreased during the freeze-up and at the beginning of ice coverage (Figure 5-2d).

Mid-shelf area – bottom-mooring station YANA

Current speeds in the first bin (4 mab) at bottom-mooring station YANA varied between 0 and 47 cm s^{-1} over the entire monitoring period (Figure 5-3a). The eastward current component ranged from -13.30 to 16.10 cm s^{-1} , whereas the northward component was significantly stronger with a range between -46.40 and 31.50 cm s^{-1} (Figure 5-3b and c). The general mean current direction was towards the south. The seasonal variability in bottom currents is not as pronounced as at bottom-mooring station LENA. The maximum bottom current speed was recorded during the ice-free period, the highest mean current speed of 15.38 cm s^{-1} during the freeze-up (Table 5-1). During the time of ice coverage the bottom currents decreased, but they increased as soon as the polynya opened (Table 5-1).

The temperature at 4 mab varied between -1.46 and -1.86 °C. The lowest mean temperature was recorded during the cooling period, the highest during the ice-free period in 1999 (Table 5-1).

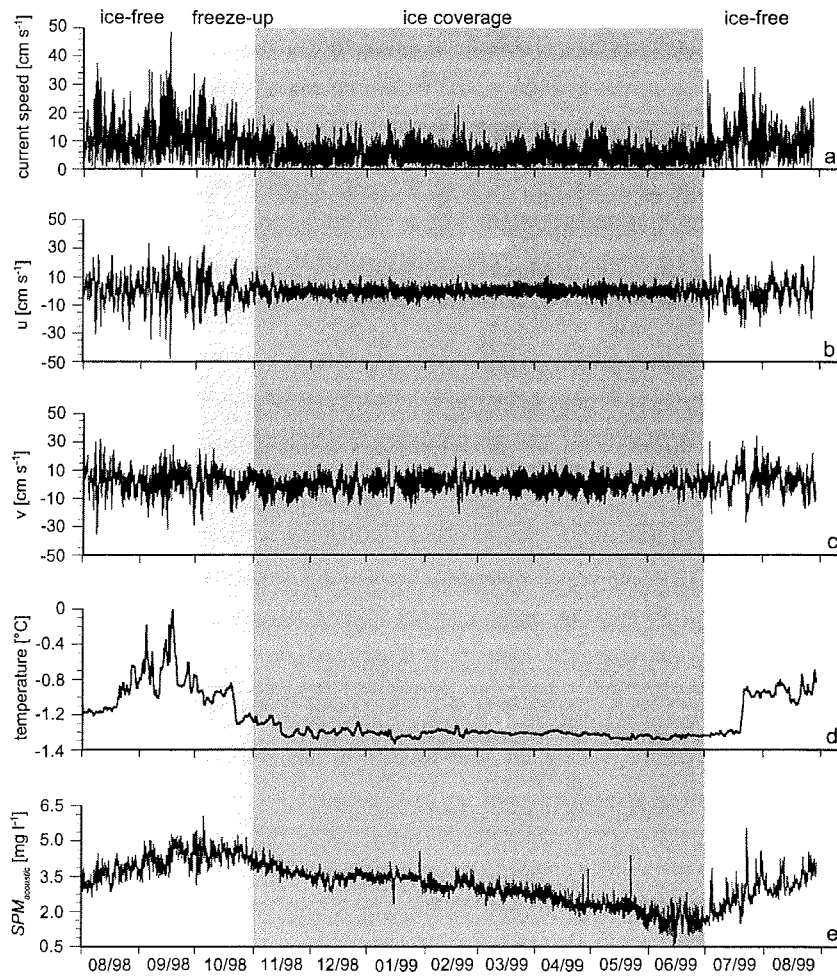


Figure 5-2: One-year time-series observations (August 1998-September 1999) from bottom-mooring station LENA on the inner shelf at 3.5 mab with current speed [cm s⁻¹] (a), eastward u [cm s⁻¹] (b) and northward current component v [cm s⁻¹] (c), temperature [°C] (d), and SPM_{acoustic} concentration [mg l⁻¹] (e).

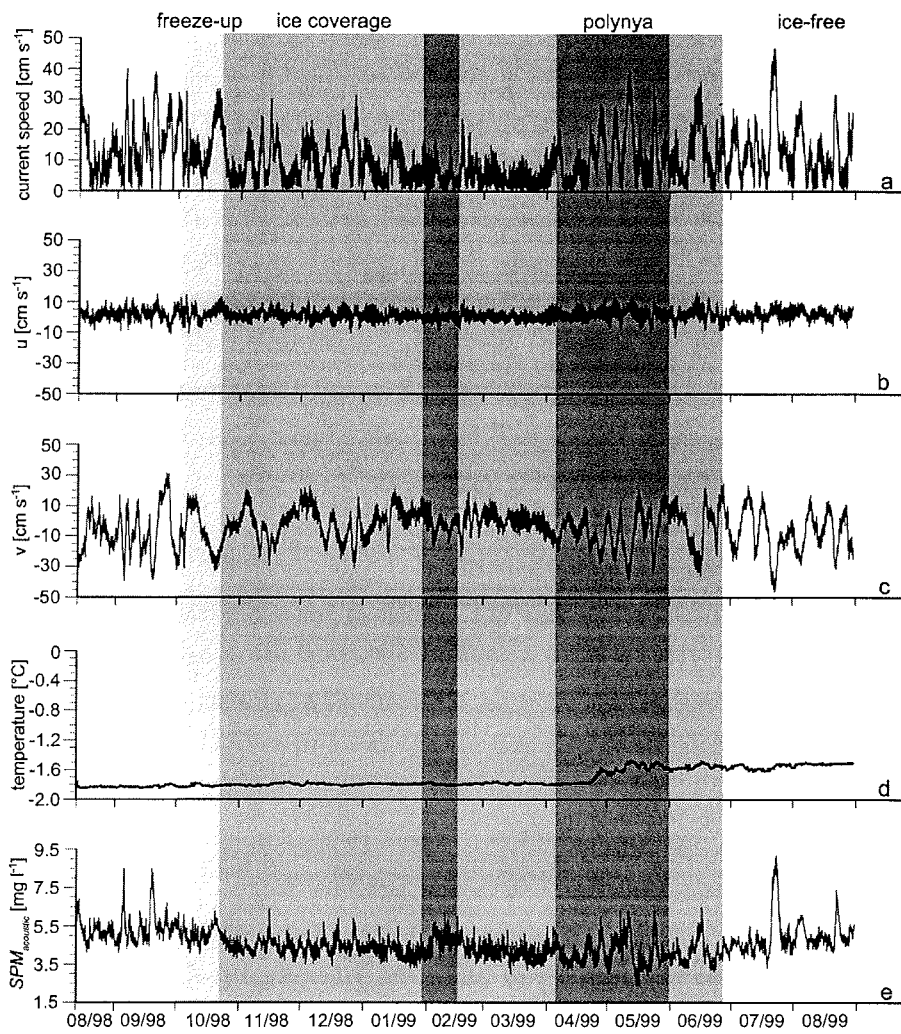


Figure 5-3: One-year time-series observations (August 1998-September 1999) from bottom-mooring station YANA on the inner shelf at 4 mab with current speed [cm s⁻¹] (a), eastward u [cm s⁻¹] (b) and northward current component v [cm s⁻¹] (c), temperature [°C] (d), and SPM_{acoustic} concentration [mg l⁻¹] (e).

5.4.2 SPM concentration

Inner shelf – bottom-mooring station LENA

The estimated $SPM_{acoustic}$ concentration at 3.5 mab at bottom-mooring station LENA was between 0.5 and 6 mg l⁻¹ during the entire monitoring period (Figure 5-2e). These $SPM_{acoustic}$ concentrations were lower than expected considering the close vicinity to the Lena Delta. This can be explained by the fact that only the upper part of the bottom nepheloid layer was detected since the ADCP started to measure only at 3.5 mab. Highest $SPM_{acoustic}$ concentrations were estimated during the freeze-up. In contrast to the time-series of bottom currents, $SPM_{acoustic}$ concentrations revealed no strong seasonal variability. The concentration remained rather constant for a long time even beneath the fast ice and decreased only very slowly (Figure 5-2e). The concentration increased after ice breakup in July 1999 (Figure 5-2e).

Mid-shelf area – bottom-mooring station YANA

At bottom-mooring station YANA $SPM_{acoustic}$ concentration at 4 mab varied between 2.25 and 9.1 mg l⁻¹ (Figure 5-3e). A seasonal variability was recognized in terms of periods with remarkably high $SPM_{acoustic}$ concentrations. Events with the highest $SPM_{acoustic}$ concentration were recorded during the ice-free period and the freeze-up (Figure 5-3e).

5.5 Discussion

5.5.1 SPM dynamics during and after the river-ice breakup (June/early July)

River-ice breakup of the Lena River usually takes place at the beginning of June. For the Lena River 40% of the mean annual freshwater and 60% of the mean annual sediment discharge takes place during the river-ice breakup (Ivanov & Piskun, 1999). The near-shore area is still covered with fast-ice and the enormous amount of river water discharged during the breakup flows either beneath the fast ice or overflows it (Macdonald, 2000). Figure 5-4a shows a time-series of $SPM_{acoustic}$ concentration within

the water column at bottom-mooring station LENA from early June to late July 1999. At the beginning of June, just before the breakup, $SPM_{acoustic}$ concentrations were below 2 mg l^{-1} in the entire water column, in line with estimations from off the Lena Delta in 1996 (Pivovarov et al., 1999). Bottom currents at 3.5 mab were low with a mean speed of 5.5 cm s^{-1} and mainly directed towards the north (Figure 5-4b). During the course of the river-ice breakup a strong pycnocline between the SPM-rich freshwater plume and the brackish shelf water established (Pivovarov et al., 1999). They observed highest SPM concentrations shortly after the breakup with concentrations of about 20 mg l^{-1} above the pycnocline (max $> 70 \text{ mg l}^{-1}$). However, the concentration below the pycnocline changed only slightly. The northern extension of the freshwater plume is normally found within the polynya (Dmitrenko et al., 1998). Hence, it can be assumed that after the breakup most of the material is transported onto the mid-shelf within the SPM-rich freshwater layer (Figure 5-7a). Part of the discharged material is transported on top of the fast ice (Lindemann, 1998). However, increased $SPM_{acoustic}$ concentrations in the upper water column at bottom-mooring station LENA were only recorded at the end of June and early July 1999 (Figure 5-4a). Pivovarov et al. (1999) suggested that the SPM-rich freshwater plume spreads into the southeastern Laptev Sea. This might explain the temporal offset of SPM increase at station LENA because of its position north of the Lena Delta. Within two weeks, in the middle of July, the material started to settle, the whole water column was turbid (Figure 5-4a) and a bottom nepheloid layer developed. Bottom currents increased in July when ice-free conditions prevailed (Figure 5-4c). Even though they exceeded only occasionally the critical threshold velocity for initial grain motion, bottom currents were apparently high enough for turbulent mixing of the water column. Therefore, it can be assumed that the bottom nepheloid layer on the inner shelf in the vicinity of the Lena Delta starts to develop after the river-ice breakup. This is mostly due to riverine input and to a much smaller extent caused by resuspension processes.

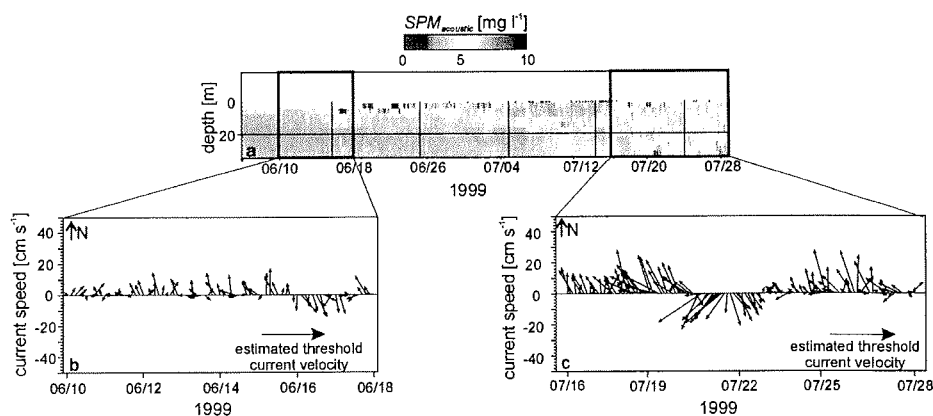


Figure 5-4: Time series of $SPM_{acoustic}$ concentration [$mg\ l^{-1}$] (a) at bottom-mooring station LENA from beginning of June to the end of July 1999. Time-series of current speed [$cm\ s^{-1}$] at 3.5 mab during the river-ice breakup (b) and at the end of July 1999 (c).

5.5.2 Ice-free period (mid-July to September)

Terrigenous sediment is supplied to the Laptev Sea shelf by riverine input ($24 \times 10^6\ t\ yr^{-1}$; Ivanov & Piskun, 1999) and coastal erosion (Rachold et al., 2000). Rachold et al. (2000) calculated a mean annual sediment input by coastal erosion of $58.4 \times 10^6\ t\ yr^{-1}$. Up to now it is not yet known how much of the material is kept within the nearshore area and only transported parallelly to the coast and how much is actually transported onto the shelf. In general it is assumed that most of the material derived from coastal erosion is kept within the nearshore area above 10 m depth (e.g., Macdonald et al., 1998; Are, 1999; Macdonald, 2000). As both bottom-mooring stations were deployed in greater depths, coastal erosion in the following discussion will not be taken into account. During the ice-free period sediment transport processes more closely resemble processes observed on lower-latitude shelves (Macdonald, 2000). Variations in the extent of summer-ice cover strongly influence transport processes from year to year and consequently seem to be a limiting factor in transport processes (Hill et al., 1991). Three principal factors are assumed to mainly control sediment transport on the Laptev Sea shelf during this period: riverine input, bottom currents, and

waves. Wave parameters in the Laptev Sea are dependent on the extent of open water (Pavlov et al., 1996). Waves with more than 3 m height are observed mainly during September, but waves of up to 1.5 m height are more common (Timokhov, 1994; Pavlov et al., 1996). Assuming the same maximum wave heights as on the Canadian Beaufort shelf (5 m; Harper & Penland, 1982), the maximum depth of wave influence is about 10 m. Between 10 and 20 m water depth the shelf bottom is occasionally disturbed by wave action but at depths below 35 m it is unaffected (Harper & Penland, 1982). Both bottom-mooring stations were deployed below 20 m water depth. Thus, the influence of waves for sediment transport processes is rather low at the mooring stations.

In general, the SPM concentration decreases from south to north and from east to west, respectively, with highest concentrations in the vicinity of the Lena Delta (Burenkov et al., 1997; Lisitsin et al., 2000; Wegner et al., in press). SPM concentration measurements near the Lena Delta show that the riverine material seems to settle relatively quickly through the water column to feed the bottom nepheloid layer (Burenkov et al., 1997; Lisitsin et al., 2000; Wegner et al., in press). Bottom currents at bottom-mooring station LENA and bottom currents recorded in 2000 (Wegner et al., in press) sporadically exceeded the threshold velocity for incipient grain motion but were high enough for turbulent mixing (Figure 5-2 and 5-7a). Hence, it can be assumed that the bottom nepheloid layer on the inner shelf is mainly fed by riverine input, resuspension seems to be of minor importance. The net horizontal flux estimated from station LENA was directed towards the north.

At station YANA, which should monitor sediment dynamics in Pleistocene river valleys on the eastern Laptev Sea shelf, increased $SPM_{acoustic}$ concentrations coincided mostly with high southerly bottom currents (Figure 5-6). These bottom currents are probably reversal currents caused by wind-induced sea-level deformations (Dmitrenko et al., 2001b). The wind-induced high bottom currents resuspended bottom material and transported it onto the inner shelf with a horizontal flux rate of more than $3 \text{ g m}^{-2} \text{ s}^{-1}$ (Figure 5-6b and 5-7b). The horizontal flux mainly seems to be dependent on the strength and duration of the increased bottom currents (Figure 5-6). $SPM_{acoustic}$ concentrations declined rapidly after the passage of storms (Figure 5-6c), indicating that

resuspended sediment rapidly settles, comparable to SPM dynamics described on the Canadian Beaufort shelf (Hill et al., 1991). In the Pleistocene river valleys on the mid-shelf the bottom nepheloid layer is therefore mostly fed by resuspension as previously suggested by Wegner et al. (in press).

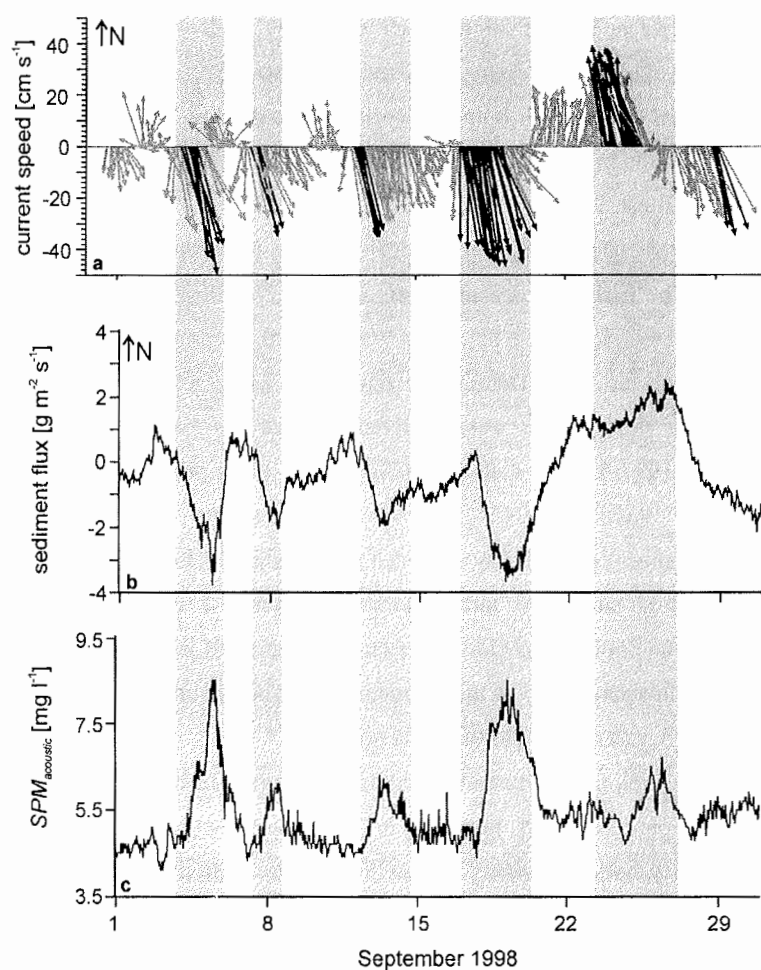


Figure 5-5: Bottom current speed [cm s^{-1}] (a), with the black vectors indicating current speeds exceeding the threshold velocity for incipient grain motion, sediment flux [$\text{g m}^{-2} \text{s}^{-1}$] (b), and SPM_{acoustic} concentration [mg l^{-1}] (c) at 4 mab at bottom-mooring station YANA during September 1998. The grey bars indicate periods of wind-induced bottom currents.

5.5.3 Sediment transport during the freeze-up period (October)

Freeze-up starts in early to mid-October after air temperature has dropped below the freezing point, the surface water has cooled to its freezing temperature, and the number of freezing-degree-days has started to accumulate (Macdonald, 2000). River runoff nearly decreases to its low winter values (Pavlov, 1998) even though substantial quantities of runoff may continue to enter the nearshore area (Macdonald, 2000). During fall the water temperature in the freshwater layer decreases rapidly down to the freezing point (Dmitrenko et al., 1998).

At bottom-mooring station YANA in October 1998 mean bottom currents were still relatively high and resuspension took place (Table 5-1; Figure 5-3). The main estimated horizontal bottom flux was directed towards the south, onto the inner shelf. At bottom-mooring station LENA bottom currents were apparently high enough for turbulent mixing (Figure 5-2) and the entire water column was still turbid. The resuspended material transported back onto the inner shelf is probably incorporated into frazil ice (Kempema et al., 1993; Reimnitz et al., 1993; Dethleff, 1995; Eicken et al., 1997; Figure 5-7a). Therefore, not only is riverine material, transported in the surface layer, incorporated into the new ice during the freeze-up period (Lindemann, 1998), but also resuspended material (Dethleff, 1995; Eicken et al., 1997). The ice either melts on the shelf during the ice-free period and transfers the SPM into the sediment cycle again (Dethleff, 1995; Kolatschek, 1998) or exports it over the continental margin into the deep Arctic Ocean (Eicken et al., 1997; Lindemann, 1998; Kolatschek, 1998; Dethleff et al., 2000). Hence, it seems that the ice acts as a sediment trap during the freeze-up period and is an important factor for sediment export on the eastern Laptev Sea shelf as previously suggested by Eicken et al. (1997).

5.5.4 Period of ice coverage (November to June/July)

There are only a few observations dealing with sediment transport beneath the ice cover, although ice cover probably has a major effect on sediment processes during the winter months (e.g., Hill et al., 1991; Macdonald et al., 1998; Macdonald, 2000). During the winter months the river discharge wanes down to only 10% of the entire annual

discharge (Gordeev et al., 1996; Pavlov, 1998). The ice cover reduces the wind stress and, therefore, also wave heights and wind-induced bottom currents. Beneath the ice cover significant sediment transport is expected to be almost completely interrupted due to both reduced riverine discharge and atmospheric forcing (Hill et al., 1991).

At bottom-mooring station LENA, which was situated beneath the fast ice for about 8 months, the influence of the ice cover on the current regime is evident: the current speed slowed down and the temperature decreased to an almost constant value of -1.35°C (Figure 5-2d). The $SPM_{acoustic}$ concentration decreased slowly. Studies on seasonal variability under a permanent ice cover in the Arctic Ocean have shown that the SPM fluxes did not differ significantly over the year (Hargrave et al., 1994). Thus, the decrease in $SPM_{acoustic}$ concentration during the period of ice coverage at station LENA is presumably caused by the settling of particles related to low currents and by almost absent riverine input. Probably, $SPM_{acoustic}$ concentrations stayed almost constant for so long because of small settling velocities and turbulent mixing. The mean current speeds at station LENA were in the same range as bottom currents that have been recorded beneath the ice cover in the Kara Sea (McClimans et al., 2000).

5.5.5 Sediment dynamics beneath the polynya

SPM dynamics at bottom-mooring stations YANA are different due to its position close to the fast ice edge and the polynya. The flaw polynyas in the Russian Arctic are caused by continuous southerly winds, which keep open large areas off the fast-ice edge (Zakharov, 1997). The polynya in the Laptev Sea is an important factor for the hydrography during winter (Dmitrenko et al., 2001a). It causes the formation of a cellular circulation with stable under-ice surface currents directed to the open water and counter currents below the pycnocline in the bottom layer because of brine rejection during ice formation (Dmitrenko et al., 2001a). During winter 1998/99 the polynya developed partly above the bottom-mooring station YANA (Table 5-1). Recorded bottom currents were only slightly lower than during the ice-free period and still exceeded the threshold velocity for incipient grain motion (Figure 5-6b). The net flux was directed towards the south, onto the inner shelf (Figure 5-6b). Thus, sediment transport onto the inner shelf occurs even during winter when most transport

mechanisms are thought to be interrupted (Hill et al., 1991). Compared to the ice-free period, when the material is transported within a circulation back and out onto the shelf, the material resuspended beneath the polynya is most likely only transported onto the inner shelf where it temporarily settles. This may explain the relatively higher sedimentation rates on the inner shelf when compared with the mid-shelf area (Bauch et al., 2001). It has often been suggested that SPM is incorporated into new ice in the polynya as well (e.g., Dethleff, 1995; Pfirman et al., 1995). Bottom currents recorded during 1998/99 beneath the polynya were not high enough for a turbid mixing of the entire water column. Therefore, incorporation into new ice beneath the polynya seems to be unlikely, at least in the eastern Laptev Sea.

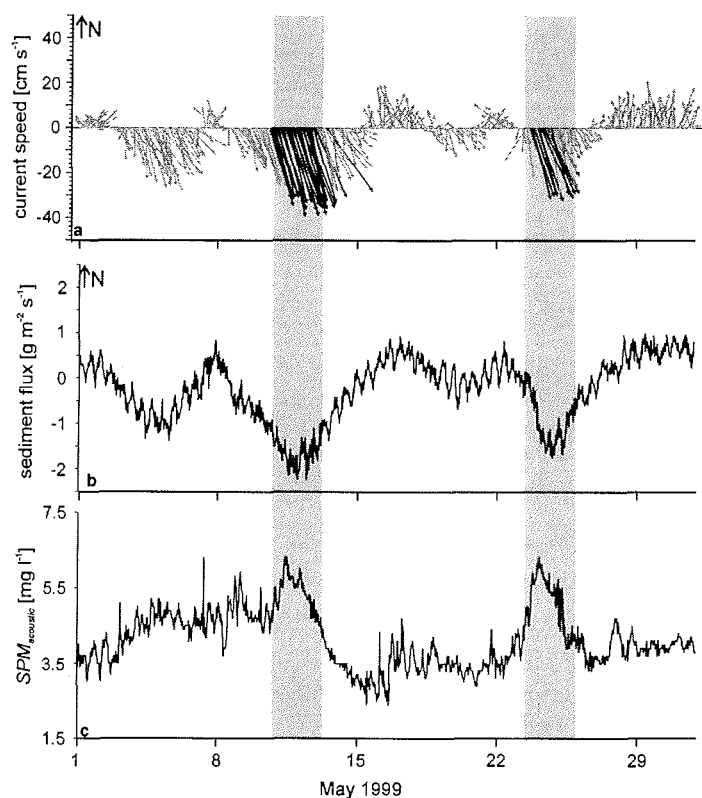


Figure 5-6: Bottom current speed [cm s^{-1}] (a), with the black vectors indicating current speeds exceeding the threshold velocity for incipient grain motion, sediment flux [$\text{g m}^{-2} \text{s}^{-1}$] (b), and SPM_{acoustic} concentration [mg l^{-1}] (c) at 4 mab at bottom-mooring station YANA beneath the polynya in May 1999. The grey bars indicate periods of wind-induced bottom currents.

5.6 Summary

The ADCP data of two one-year bottom-mooring stations allowed for some new insights into current and SPM dynamics during the period of ice coverage and beneath the polynya with the unique opportunity to describe sediment dynamics on the eastern Laptev Sea shelf throughout one seasonal cycle.

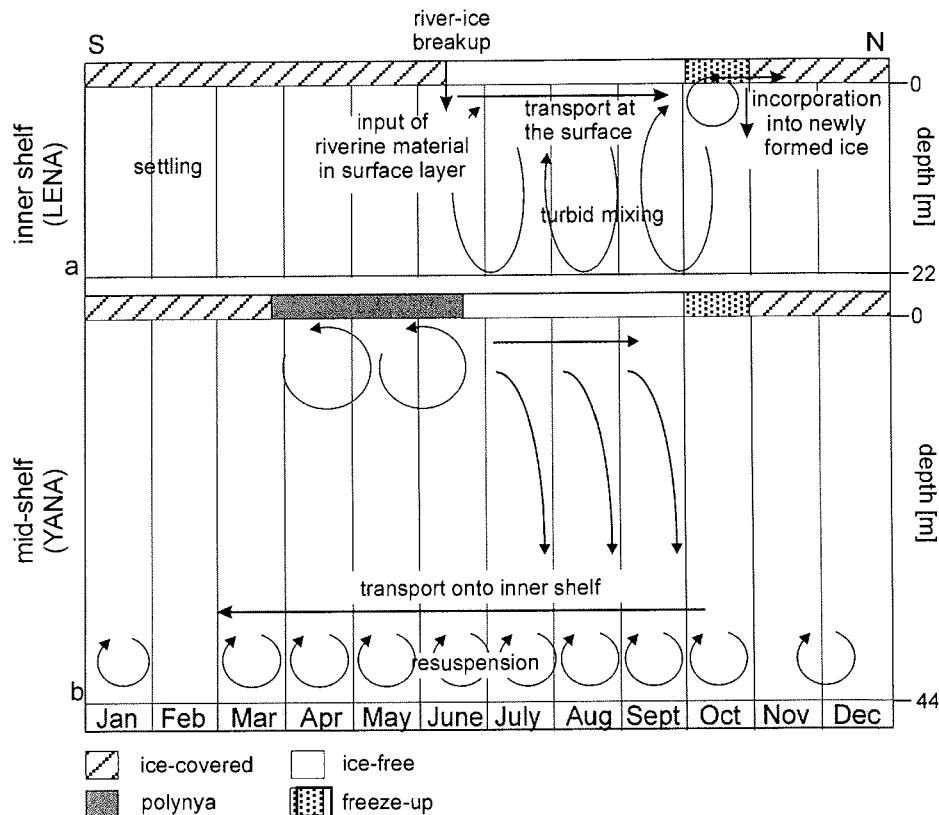


Figure 5-7: A schematic overview of the sediment dynamics throughout one year at bottom-mooring station LENA on the inner (a) and at station YANA on the mid-shelf (b).

It is indicated that during and shortly after the river-ice breakup (June/early July) less dense river water with significantly increased SPM concentrations flows over the shelf water with a marked density interface between the two water masses. The SPM transport is then dominated by riverine input and transport onto the mid-shelf in the

surface layer (Figure 5-7a). Bottom flow onto the inner shelf is only rather low. When ice-free conditions prevail (mid-July to September), SPM discharged by the Lena River is evenly distributed throughout the water column due to turbid mixing. On the inner shelf turbid mixing transfers SPM between the surface and the bottom nepheloid layer (Figure 5-7a). Within the surface layer SPM is transported to the mid-shelf. Probably due to reduced surface currents on the mid-shelf, SPM settles into the bottom nepheloid layer, only to be carried back onto the inner shelf again additionally with resuspended material (Figure 5-7b). This forms an SPM circulation acting as a sediment trap, which retards the escape of the sediment into the deep Arctic Ocean.

During the freeze-up (October) the SPM in the surface layer of the inner shelf is not only transported out onto the shelf but rather incorporated into the ice (Figure 5-7a). The incorporated material is partly transported by the ice into the deep Arctic Ocean. Beneath the ice cover (November to June/July) nearly no significant sediment transport takes place (Figure 5-7a). Suspended material settles slowly during this period. However, beneath the polynya bottom material is still resuspended after storm events and transported onto the inner shelf where it temporarily settles.

With respect to the sediment export from the eastern Laptev Sea shelf into the deep Arctic Ocean it can be assumed that during the ice-free period most of the material derived from riverine input is trapped within the quasi-estuarine circulation system described above. During the freeze-up large quantities of sediments are thought to be incorporated into the newly formed ice and partly transported into the deep Arctic Ocean. Hence, most of the sediment export on the eastern Laptev Sea shelf apparently takes place via ice export rather than bottom transport.

6 SUMMARY AND CONCLUSIONS

The aim of this study was to give insights into sediment dynamics on a seasonal time scale for the Laptev Sea, a Siberian shelf sea characterized by seasonal ice coverage and a strong seasonality in terrestrial sediment input. The implications of the sediment dynamics for sediment budget calculations and their significance for the paleo-sediment record could be studied. Some aspects of the quantification of SPM and of the variability of SPM dynamics were discussed in the three manuscripts that make up the body of this thesis. The conclusions obtained from these manuscripts are summarized below.

For the quantification of SPM concentrations optical (turbidity meter) and acoustic (ADCP) backscatter sensors were compared and their potential for the investigation of SPM dynamics on the Laptev Sea shelf was assessed. Thus, as a first step it was necessary to convert the backscattered signals of both sensors into SPM concentrations (CHAPTER 3):

- Using the linear relation between the optical backscatter signals and the SPM concentrations derived from filtered water samples turbidity meter signals were converted into SPM concentration. The ADCP signals were transformed adapting a previously established approach on the theoretical interaction of sound in water and SPM.
- The converted optical and acoustic backscatter signals showed a close similarity to SPM concentrations derived from filtered water samples, even though one sensor might miss one event recorded by the other depending on the SPM grain-size. The ADCPs and the turbidity meters provided generally good estimations, with ADCPs underestimating and turbidity meters slightly overestimating SPM concentrations.
- Both, the optical and the acoustic backscatter sensor can be used for the determination of SPM dynamics on the Laptev Sea shelf but ADCPs are more convenient for investigations on sediment transport dynamics as they provide

reasonable SPM concentrations and current records for the entire water column simultaneously.

To describe the composition, transport dynamics, and short-term variability of SPM in the nepheloid layers on the Laptev Sea shelf during the ice-free period and to characterize the significance of the nepheloid layers for sediment transport, optical backscatter profiles combined with pigment, plankton, and current records were analyzed (CHAPTER 3):

- On the inner shelf in the vicinity of the Lena Delta the SPM concentration in the surface nepheloid layer is strongly dependent on riverine discharge, whereas on the mid-shelf the formation and dynamics are mainly related to changes in phytoplankton biomass and zooplankton migration.
- The bottom nepheloid layer is composed of riverine material, resuspended bottom material, and decaying organic matter from the upper water column. The SPM concentration within the bottom nepheloid layer decreases from south to north and from east to west respectively mainly due to dispersion.

The study implicates that most of the sediment transport takes place in the bottom nepheloid layer. On the eastern Laptev Sea shelf paleo-river valleys act as transport conduits, where bottom material is resuspended and transported onto the inner shelf again. On the central Laptev Sea shelf resuspension events seem to be less common and SPM is mainly transported over the continental margin into the deep Arctic Ocean.

In order to investigate seasonal variations in currents and SPM and their implications for sediment transport and for sediment budget calculations, one-year ADCP records were examined in a paleo-river valley on the eastern Laptev Sea shelf (CHAPTER 5):

- During and shortly after the river-ice breakup (June to early July) sediment transport on the inner shelf is dominated by riverine input and transport within the surface nepheloid layer onto the mid- shelf (Figure 6-1a).

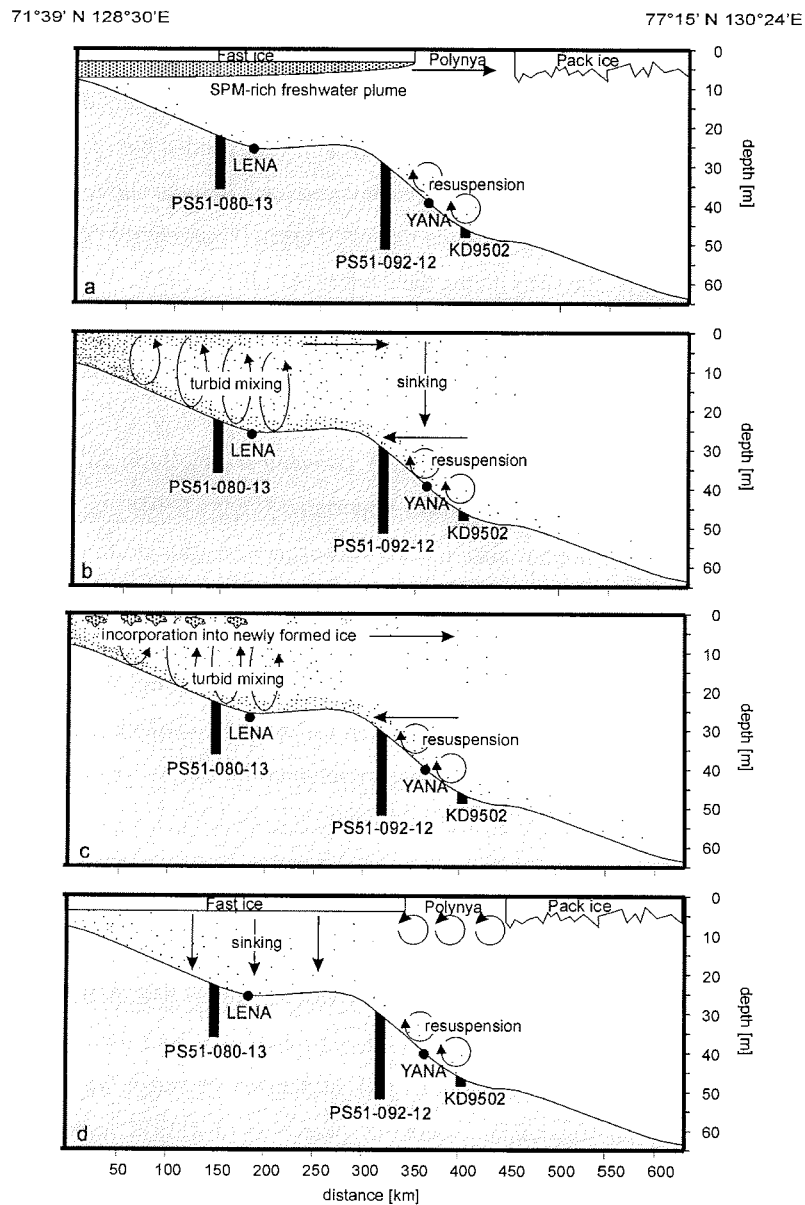


Figure 6-1: Schematic overview of sediment transport dynamics on a NS-transect along the Eastern Lena Valley during the river-ice breakup (a), the ice-free period (b), during the freeze-up (c) and beneath the fast ice (d) with the arrows indicating the general transport direction of SPM and the length of the black boxes indicating the modern sedimentation rates (PS51-080-13: $28 \text{ cm } 10^{-3} \text{ yr}^{-1}$; PS51-092-12: $41 \text{ cm } 10^{-3} \text{ yr}^{-1}$; KD9502: $3 \text{ cm } 10^{-3} \text{ yr}^{-1}$; Bauch et al., 2001).

- When ice-free conditions prevail (mid-July to September), SPM discharged by the Lena River is transported within the surface layer onto the mid-shelf where it sinks through the water column into the bottom nepheloid layer, only to be carried back onto the inner shelf additionally with resuspended bottom material. On the inner shelf the material is partly conveyed back into the surface layer by turbid mixing and carried out onto the mid-shelf again (Figure 6-1b). Thus, SPM is mainly trapped on the shelf during the ice-free period.
- During freeze-up (October) SPM in the surface layer on the inner shelf is rather incorporated into newly formed ice and partly transported within the ice over the continental margin into the deep Arctic Ocean (Figure 6-1c).
- Beneath the ice cover on the inner shelf (November-June/July) SPM slowly sinks and sediment transport is of minor importance (Figure 6-1d).
- Beneath the polynya bottom material is still resuspended after storm events and transported onto the inner shelf where it temporarily settles (Figure 6-1d).

The study suggests a quasi-estuarine sediment circulation on the eastern Laptev Sea shelf and a sediment export dominated by ice export rather than bottom transport. The seasonal sediment circulation pattern is reflected in the *modern* sedimentation rates of the last 5000 years since the Holocene sea level maximum on the eastern Laptev Sea shelf (Figure 6-1).

The unique data-sets delivered new insights into seasonal sediment dynamics on the Laptev Sea shelf and its complex land-shelf-ocean interactions. They provided the basis for a conceptual model of sediment transport on the eastern Laptev Sea shelf (Figure 6-1), which presumably can be extended to other Siberian shelf seas. This might enable us to forecast changes in transport, deposition, and suspension of sediments on Arctic shelves with changing environmental conditions, which is of critical importance to understand the overall condition of these complex systems.

7 REFERENCES

- Aagaard, K. & Carmack, E. C. 1989 The role of sea ice and other fresh water in the Arctic circulation. *Journal of Geophysical Research* **94**, C10, 414,485-414,498.
- Abramova, E., Ivanova, D. & Akhmetshina, I. 2001 Diel vertical migrations of zooplankton in the Laptev Sea shelf waters. Otto Schmidt Laboratory Fellowship Meeting December 2001, St. Petersburg (unpubl. internal report).
- Abramova, E., Ivanova, D., Tuschling, K., Dmitrenko, I., Hölemann, J. A., Akhmetshina, I. & Wegner, C. 2002 Diel vertical migrations of mesozooplankton in the Laptev Sea inferred from acoustic backscatter signal: Long- and short-term variations. *Terra Nostra* **2002**, 3, 19.
- Anoshkin, A. F., Popov, I. K., Ushakov, I. E. & TRANSDRIFT II Shipboard Scientific Party 1995 Hydrooptical measurements in the Laptev Sea: Spatial distributions of light attenuation and chlorophyll fluorescence. *Berichte zur Polarforschung* **176**, 178-186.
- Antonow, M., Fürst, B., Haase, V., Strobl, C. & Thiede, R. 1997 Multiprobe suspension and current speed measurements: Aspects of sediment dynamics during freeze-up studies in the Laptev Sea. *Berichte zur Polarforschung* **248**, 75-79.
- Arar, E. J. & Collins, G. B. 1992 Method 445.0. In vitro determination of Chlorophyll *a* and Phaeophytin *a* in marine and freshwater phytoplankton by fluorescence. Methods for the determination of chemical substances in marine and estuarine samples. U.S. Environmental Protection Agency Cincinnati OH, 1-14.
- Are, F. E. 1999 The role of coastal retreat for sedimentation in the Laptev Sea. In: Kassens, H., Bauch, H. A., Dmitrenko, I. A., Eicken, H., Hubberten, H.-W., Melles, M., Thiede, J. & Timokhov, L. A. (eds.) *Land-Ocean Systems in the Siberian Arctic: Dynamics and history*. Springer-Verlag, Berlin, 287-295.
- Bareiss, J., Eicken, H., Helbig, A. & Martin, T. 1999 Impact of river discharge and regional climatology on the decay of sea ice in the Laptev Sea during spring and early summer. *Arctic, Antarctic, and Alpine Research* **31**, 3, 214-229.
- Barnett, D. 1991 Sea ice distribution in Soviet Arctic. In: Brigham, L. A. (ed.) *The Soviet Maritime Arctic*. Belhaven Press, London, 47-62.
- Bauch, H. A., Mueller-Lupp, T., Taldenkova, E., Spielhagen, R. F., Kassens, H., Grootes, P. M., Thiede, J., Heinemeier, J. & Pertyashov, V. V. 2001 Chronology of the Holocene transgression at the north Siberian margin. *Global and Planetary Change* **31**, 1-4, 125-140.

- Binder, B. 2001 Suspensionsdynamik auf dem Schelf der Laptevsee (russische Arktis) - Erste Ergebnisse anhand von Filtrationsanalysen (1998-2000). Diploma Thesis, Technical University of Freiberg, 87 pp. (unpublished).
- Bischof, J., Koch, J., Kubisch, M., Spielhagen, R. F. & Thiede, J. 1990 Nordic seas surface ice drift reconstructions: evidence from ice rafted coal fragments during oxygen isotope stage 6. In: Dowdeswell, J. A. & Scourse, J. D. (eds.) *Glaciomarine Environments: Processes and Sediments*, Geological Society Special Publication **53**, 235-251.
- Bothner, M. H., Parmenter, C. M. & Milliman, J. D. 1981 Temporal and spatial variations in suspended matter in continental shelf and slope waters off the north-eastern United States. *Estuarine, Coastal and Shelf Science* **13**, 213-234.
- Bunt, J. A. C., Larcombe, P. & Jago, C. 1999 Quantifying the response of optical backscatter devices and transmissometers to variations in suspended particulate matter. *Continental Shelf Research* **19**, 9, 1199-1220.
- Burenkov, V. I., Kuptzov, V. M., Sivkov, V. V. & Shevchenko, V. P. 1997 Spatial distribution and size composition of suspended matter in the Laptev Sea in August-September 1991. *Oceanology* **37**, 6, 831-837.
- Byrne, J. B. & Patino, E. 2001 Feasibility of using acoustic and optical backscatter instruments for estimating total suspended solid concentrations in estuarine environments. Fed. Interagency Sed. Conf., Reno, III-135-III-138.
- Cacchione, D. A. & Drake, D. E. 1986 Nepheloid layers and internal waves over continental shelves and slopes. *Geo-Marine Letters* **6**, 147-152.
- Cacchione, D. A. & Drake, D. E. 1990 Shelf sediment transport: An overview with applications to the northern California continental shelves. In: Mehaute, B. L. & Hanes, D. M. (eds.) *The Sea* **7b**. John Wiley and Sons, New York, 729-773.
- Crawford, A. M. & Hay, A. E. 1993 Determining suspended sand size and concentration from multifrequency acoustic backscatter. *Journal of the Acoustical Society of America* **94**, 6, 3312-3324.
- Deines, K. L. 1999 Backscatter estimation using broadband Acoustic Doppler Current Profiler. IEEE 6th Working Conference on Current Measurement, San Diego, 249,253.
- Dethleff, D. 1995 Die Laptevsee - eine Schlüsselregion für den Fremdstoffeintrag in das arktische Meereis. PhD Thesis, Christian Albrechts University, Kiel, 111 pp.
- Dethleff, D., Nuernberg, D., Reimnitz, E., Saarso, M. & Savchenko, Y. P. 1993 East Siberian Arctic Region Expedition '92: The Laptev Sea - its significance for arctic sea-ice formation and transpolar sediment flux. *Berichte zur Polarforschung* **120**, 1-44.

- Dethleff, D., Rachold, V., Tintelnot, M. & Antonow, M. 2000 Sea-ice transport of riverine particles from the Laptev Sea to Fram Strait based on clay mineral studies. *International Journal of Earth Sciences* **89**, 496-502.
- Dmitrenko, I., Golovin, P., Gribanov, V. A., Kassens, H. & Hölemann, J. 1998 Influence of summer river runoff on ice formation in the Kara and Laptev seas. In: Shen, H. T. (ed.) *Ice in Surface Waters*. Balkema, Rotterdam, 251-257.
- Dmitrenko, I., Golovin, P., Gribanov, V. A. & Kassens, H. 1999 Oceanographic causes for transarctic ice transport of river discharge. In: Kassens, H., Bauch, H. A., Dmitrenko, I., Eicken, H., Hubberten, H.-W., Melles, M., Thiede, J. & Timokhov, L. (eds.) *Land-Ocean Systems in the Siberian Arctic: Dynamics and History*. Springer-Verlag, Berlin, 73-92.
- Dmitrenko, I., Hölemann, J., Tyshko, K., Churun, V., Kirillov, S. A. & Kassens, H. 2001a The Laptev Sea flaw polynya, Russian Arctic: Effects on the mesoscale hydrography. *Annals of Glaciology* **33**, 373-376.
- Dmitrenko, I. A., Hölemann, J., Kirillov, S. A., Berezovskaya, S. L., Eicken, H. & Kassens, H. 2001b Wind-forced currents as a linkage between the Laptev Sea (Siberia) and the Arctic Ocean [in Russian]. *Doklady Earth Science, MAIK Nauka* **377**, 1, 1-8.
- Drachev, S. S., Johnson, G. I., Laxon, S. W., McAdoo, D. C. & Kassens, H. 1999 Main structural elements of eastern Russian Arctic continental margin derived from satellite gravity and multichannel seismic reflection data. In: Kassens, H., Bauch, H. A., Dmitrenko, I., Eicken, H., Hubberten, H.-W., Melles, M., Thiede, J. & Timokhov, L. A. (eds.) *Land-Ocean Systems in the Siberian Arctic: Dynamics and History*. Springer-Verlag, Berlin, 667-682.
- Drake, D. E., Kolpak, R. L. & Fisher, P. J. 1972 Sediment transport on the Santa Barbara - Oxnard shelf, Santa Barbara Channel, California. In: Swift, D. J. P., Duane, D. B. & Pilkey, O. H. (eds.) *Shelf Sediment Transport*. Dowden, Hutchinson and Ross, Stroudsburg, 307-331.
- Dyer, K. R. 1994 Estuarine sediment transport and deposition. In: Pye, K. (ed.) *Sediment Transport and Depositional Processes*. Blackwell Scientific Publications, Oxford, 193-218.
- Eicken, H., Reimnitz, E., Alexandrov, V., Martin, T., Kassens, H. & Viehoff, T. 1997 Sea-ice processes in the Laptev Sea and their importance for sediment export. *Continental Shelf Research* **17**, 2, 205-233.
- Eicken, H., Kolatschek, J., Freitag, J., Lindemann, F., Kassens, H. & Dmitrenko, I. 2000 A key source area and constraints on entrainment for basin scale sediment transport by Arctic sea ice. *Geophysical Research Letter*, **27**, 13, 1919-1922.

- Fisher, F. H. & Simmonis, V. P. 1977 Sound absorption in sea water. *Journal of the Acoustical Society of America* **62**, 3, 558-564.
- Fugate, D. C. & Friedrichs, C. T. 2002 Determining concentration and fall velocity of estuarine particle populations using ADV, OBS and LISST. *Continental Shelf Research* **22**, 1867-1886.
- Gardner, W. D. 1989 Periodic resuspension in Baltimore Canyon by focusing of internal waves. *Journal of Geophysical Research* **94**, C 12, 118185-118194.
- Gartner, J. W. 2002 Estimation of suspended solid concentrations based on acoustic backscatter intensity: Theoretical background. Turbidity and other sediment surrogates workshop, Reno, NV.
- Gartner, J. W. & Cheng, R. T. 2001 The promises and pitfalls of estimating total suspended solids based on backscatter intensity from Acoustic Doppler Profilers. Fed. Interagency Sed. Conf., Reno, III-119-III-126.
- Gordeev, V. V. 2000 River input of water, sediment, major ions, nutrients and trace metals from Russian territory to the Arctic Ocean. In: Lewis, E. L., Jones, E. P., Lemke, P., Prowse, T. D. & Wadhams, P. (eds.) *The Freshwater Budget of the Arctic Ocean*. Kluwer Academic Publisher, Dordrecht, 297-322.
- Gordeev, V. V., Martin, J. M., Sidorov, I. S. & Sidorova, M. V. 1996 A reassessment of the Eurasian river input of water, sediment, major elements, and nutrients to the Arctic Ocean. *American Journal of Sciences* **229**, 664-691.
- Gordon, R. L. 1996 *Acoustic Doppler Current Profiler - Principles of Operation - a Practical Primer*. RD Instruments, San Diego, 54 pp.
- Graf, G. & Rosenberg, R. 1997 Bioresuspension and biodeposition: A review. *Journal of Marine Systems* **11**, 269-278.
- Grebmeier, J. M. & Whitley, T. E. 1996 *Arctic System Science Ocean-Atmosphere-Ice Interactions Biological Initiative in the Arctic: Shelf-Basin Interactions Workshop*. University of Washington, Seattle, 63 pp.
- Griffiths, G. & Flatt, D. 1987 A self-contained Acoustic Doppler Current Profiler: Design and operation. International Conference on Electronics for Ocean Technology, Edinburgh, 41-47.
- Griffiths, G. & Roe, H. S. J. 1993 Acoustic Doppler Current Profilers - a tool for both physical and biological oceanographers. *Acoustic Sensing and Imaging*, London, 178-182.
- Hanes, D. M., Vincent, C. E., Huntley, D. A. & Clarke, T. L. 1988 Acoustic measurements of suspended sand concentration in the C²S² experiment at Stanhope Lane, Prince Edward Island. *Marine Geology* **81**, 185-196.

- Harder, M. 1996 Dynamik, Rauigkeit und Alter des Meereises in der Arktis - Numerische Untersuchungen mit einem großskaligen Modell. *Berichte zur Polarforschung* **203**, 126 pp.
- Hargrave, B. T., von Bodungen, B., Stoffyn-Egli, P. & Mudie, P. J. 1994 Seasonal variability in particle sedimentation under permanent ice cover in the Arctic Ocean. *Continental Shelf Research* **14**, 2/3, 279-293.
- Harper, J. R. & Penland, S. 1982 *Beaufort Sea Sediment Dynamics*. Contract Report to Atlantic Geosciences Center for Geological Survey of Canada, Dartmouth, Nova Scotia, 125 pp.
- Hatcher, A., Hill, P. & Macpherson, P. 2000 Spectral optical backscatter of sand in suspension: Effects of particle size, composition and color. *Marine Geology* **168**, 115-128.
- Hatje, V., Birch, G. F. & Hill, D. M. 2001 Spatial and temporal variability of particulate trace metals in Port Jackson Estuary, Australia. *Estuarine, Coastal and Shelf Science* **53**, 63-77.
- Hay, A. E. & Sheng, J. 1992 Vertical profiles of suspended sand concentration and size from multifrequency acoustic backscatter. *Journal of Geophysical Research* **97**, C10, 15,661-15,677.
- Hequette, A. & Hill, P. R. 1993 Storm-generated currents and offshore sediment transport on a sandy shoreface, Tibjak Beach, Canadian Beaufort Sea. *Marine Geology* **113**, 283-304.
- Hill, P. R. & Nadeau, O. C. 1989 Storm-dominated sedimentation on the inner shelf of the Canadian Beaufort Sea. *Journal of Sedimentary Petrology* **59**, 3, 455-468.
- Hill, P. R., Blasco, S. M., Harper, J. R. & Fissel, D. B. 1991 Sedimentation on the Canadian Beaufort Sea. *Continental Shelf Research* **11**, 8-10, 821-842.
- Holdaway, G. P., Thorne, P. D., Flatt, D., Jones, S. E. & Prandle, D. 1999 Comparison between ADCP and transmissometer measurements of suspended sediment concentration. *Continental Shelf Research* **19**, 421-441.
- Hölemann, J. A., Schirmacher, M. & Prange, A. 1995 Transport and distribution of trace elements in the Laptev Sea: First results of the TRANSDRIFT expeditions. *Berichte zur Polarforschung* **176**, 297-302.
- Hölemann, J. A., Schirmacher, M., Kassens, H. & Prange, A. 1999 Geochemistry of surficial and ice-rafted sediments from the Laptev Sea (Siberia). *Estuarine, Coastal and Shelf Science* **49**, 45-59.
- Holmes, M. L. 1967 Late Pleistocene and Holocene history of the Laptev Sea. MSc. Thesis, University of Seattle, 176 pp.
- Holmes, M. L. & Creager, J. 1974 Holocene history of the Laptev Sea continental shelf. In: Herman, Y. (ed.) *Marine Geology and Oceanography of the Arctic Sea*. Springer, New York, 211-229.

- Ishimaru, A. 1978 *Wave Propagation in Random Media*. Academic Press, New York, 12-14.
- Ivanov, V. V. & Piskun, A. A. 1999 Distribution of river water and suspended sediment loads in the deltas of rivers in the basins of the Laptev and East Siberian seas. In: Kassens, H., Bauch, H. A., Dmitrenko, I. A., Eicken, H., Hubberten, H.-W., Melles, M., Thiede, J. & Timokhov, L. A. (eds.) *Land-Ocean Systems in the Siberian Arctic: Dynamics and History*. Springer-Verlag, Berlin, 239-250.
- Johnson, D. R., Asper, V., McClimans, T. & Weidemann, A. 2000 Optical properties of the Kara Sea. *Journal of Geophysical Research* **105**, C4, 8805-8811.
- Kassens, H. & Karpuy, V. 1994 Russian-German Cooperation: The TRANSDRIFT I expedition to the Laptev Sea. *Berichte zur Polarforschung*, **151**, 168 pp.
- Kassens, H., Dmitrenko, I., Timokhov, L. & Thiede, J. 1997 The TRANSDRIFT III expedition: freeze-up studies in the Laptev Sea. *Berichte zur Polarforschung*, **248**, 190 pp.
- Kassens, H. & Dmitrenko, I. in press a The TRANSDRIFT V expedition to the Laptev Sea (RV Polarstern, ARK XIV/1b). *Berichte zur Polarforschung*.
- Kassens, H. & Dmitrenko, I. in press b The TRANSDRIFT VI expedition to the Laptev Sea Polynya. *Berichte zur Polarforschung*.
- Kempema, E. W., Reimnitz, E., Clayton, J. R. & Payne, J. R. 1993 Interactions of frazil and anchor ice with sedimentary particles in a flume. *Cold Region Science Technology* **21**, 137-149.
- Kleiber, H. P. & Niessen, F. 1999 Late Pleistocene paleo-river channels on the Laptev Sea shelf - implications from sub-bottom profiling. In: Kassens, H., Bauch, H. A., Dmitrenko, I., Eicken, H., Hubberten, H.-W., Melles, M., Thiede, J. & Timokhov, L. A. (eds.) *Land-Ocean Systems in the Siberian Arctic: Dynamics and History*. Springer-Verlag, Berlin, 657-665.
- Kolatschek, J. S. 1998 Meereisdynamik und Sedimenttransport in der Arktis - Ergebnisse aus Feldstudien, Fernerkundung und Modellierung. PhD Thesis, University of Bremen, 114 pp.
- Kolatschek, J., Eicken, H., Alexandrov, V. & Kreyscher, M. 1996 The sea-ice cover of the Arctic Ocean and the Eurasian marginal seas: A brief overview of present day patterns and variability. *Berichte zur Polarforschung* **212**, 2-18.
- Kuptsov, V. M. & Lisitsin, A. P. 1996 Radiocarbon of Quaternary along shore and bottom deposits of the Lena and the Laptev sediments. *Marine Chemistry* **53**, 301-311.
- Kuptsov, V. M., Lisitsin, A. P., Shevchenko, V. P. & Burenkov, V. I. 1999 Suspended matter fluxes in the bottom sediments of the Laptev Sea. *Oceanology* **39**, 4, 597-604.

- Libicki, C., Bedford, K. W. & Lynch, J. F. 1989 The interpretation and evaluation of a 3-MHz acoustic backscatter device for measuring benthic boundary layer sediment dynamics. *Journal of the Acoustical Society of America* **85**, 4, 1501-1511.
- Lindemann, F. 1994 Sonographische und sedimentologische Untersuchungen in der Laptev-See, sibirische Arktis. Diploma Thesis, Christian Albrechts University of Kiel, 75 pp. (unpublished).
- Lindemann, F. 1998 Sedimente im arktischen Meereis - Eintrag, Charakterisierung und Quantifizierung. *Berichte zur Polarforschung* **283**, 124 pp.
- Lisitsin, A. P., Shevchenko, V. P. & Burenkov, V. I. 2000 Hydrooptics and suspended matter of arctic seas. *Atmospheric Oceanic Optics* **13**, 1, 61-71.
- Ludwig, K. A. & Hanes, D. M. 1990 A laboratory evaluation of optical backscatterance suspended solids sensors exposed to sand-mud mixtures. *Marine Geology* **94**, 173-179.
- Lynch, J. F. 1985 Theoretical analysis of ABSS data for HEBBLE. *Marine Geology* **66**, 277-298.
- Lynch, J. F. & Agrawal, Y. C. 1991 A model-dependent method for inverting vertical profiles of scattering to obtain particle size spectra in boundary layers. *Marine Geology* **99**, 387-401.
- Lynch, J. F., Irish, J. D., Sherwood, C. R. & Agrawal, Y. C. 1994 Determining suspended sediment particle size information from acoustical and optical backscatter measurements. *Continental Shelf Research* **14**, 10/11, 1139-1165.
- Lynch, J. F., Gross, T. F., Sherwood, C. R., Irish, J. D. & Brumley, B. H. 1997 Acoustical and optical backscatter measurements of sediment transport in the 1988-1989 STRESS experiment. *Continental Shelf Research* **17**, 337-366.
- Maa, J. P.-Y., Xu, J. & Victor, M. 1992 Notes on the performance of an optical backscatter sensor for cohesive sediments. *Marine Geology* **104**, 215-218.
- Macdonald, R. W. 2000 Arctic estuaries and ice: A positive-negative estuarine couple. In: Lewis, E. L., Jones, E. P., Lemke, P., Prowse, T. D. & Wadhams, P. (eds.) *The Freshwater Budget of the Arctic Ocean*. Kluwer Academic Publishers, Dordrecht, 383-407.
- Macdonald, R. W., Solomon, S. M., Cranston, R. E., Welch, H. E., Yunker, M. B. & Gobeil, C. 1998 A sediment and organic carbon budget for the Canadian Beaufort shelf. *Marine Geology* **144**, 255-273.
- Marsh, A. G. & Tenore, K. R. 1990 The role of nutrition in regulating the population dynamics of opportunistic, surface deposit feeders in a mesohaline community. *Limnology and Oceanography* **35**, 710-724.
- McCave, I. N. 1975 Vertical flux of particles in the ocean. *Deep-Sea Research* **22**, 491-502.

- McClimans, T., Johnson, D. R., Krosshavn, D. R., King, S. E., Carroll, J. & Grenness, O. 2000 Transport processes in the Kara Sea. *Journal of Geophysical Research* **105**, C6, 14,121-14,139.
- Müller-Lupp, T. 2002 Short- and long-term environmental changes in the Laptev Sea (Siberian Arctic) during the Holocene. *Berichte zur Polarforschung* **424**, 85 pp.
- Mysak, L. A. & Manak, D. K. 1989 Arctic sea ice content and anomalies 1953-1984. *Atmosphere Ocean* **27**, 2, 376-405.
- Nittrouer, C. A. & Wright, L. D. 1994 Transport of particles across continental shelves. *Review of Geophysics* **32**, 1, 85-113.
- Osborne, P. D., Vincent, C. E. & Greenwood, B. 1994 Measurement of suspended sand concentrations in the nearshore: Field intercomparison of optical and acoustic backscatter sensors. *Continental Shelf Research* **14**, 2/3, 159-174.
- Palanques, A., Puig, P., Guillen, J., Jimenez, J., Gracia, V., Sanchez-Arcilla, A. & Madsen, O. 2002 Near-bottom suspended sediment fluxes on the microtidal low-energy Ebro continental shelf (NW Mediterranean). *Continental Shelf Research* **22**, 285-303.
- Pavlov, V. K. 1998 Features of the structure and variability of the oceanographic processes in the shelf zone of the Laptev and East Siberian seas. In: Robinson, I. S. & Brink, K. H. (eds.) *The Sea*. John Wiley and Sons, New York, 759-787.
- Pavlov, V. K., Timokhov, L. A., Baskakov, G. A., Kulakov, M. Y., Kurazhov, V. K., Pavlov, P.V., Pivovarov, S. V. & Stanovoy, V.V. 1996 Hydrometeorological regime of the Kara, Laptev, and East Siberian seas. Technical Memorandum APL-UW TM1-96, University of Washington, 179 pp.
- Peregovich, B. 1999 Die postglaziale Sedimentationsgeschichte der Laptev-See: schwermineralogische und sedimentpetrographische Untersuchungen. *Berichte zur Polarforschung* **316**, 85 pp.
- Pfirman, S. L., Kögeler, J. & Anselme, B. 1995 Coastal environments of the western Kara and eastern Barents seas. *Deep-Sea Research* **42**, 6, 1391-1412.
- Pivovarov, S., Hölemann, J. A., Kassens, H., Antonow, M. & Dmitrenko, I. 1999 Dissolved oxygen, silicon, phosphorus and suspended matter concentrations during the spring breakup of the Lena River. In: Kassens, H., Bauch, H. A., Dmitrenko, I., Eicken, H., Hubberten, H.-W., Melles, M., Thiede, J. & Timokhov, L. (eds.) *Land-Ocean Systems in the Siberian Arctic: Dynamics and History*. Springer-Verlag, Berlin, 251-264.

- Puig, P., Palanques, A. & Guillen, J. 2001 Near-bottom suspended sediment variability caused by storms and near-inertial internal waves on the Ebro mid-continental shelf (NW Mediterranean). *Marine Geology* **178**, 81-93.
- Puls, W., Kühl, H., Frohse, A. & König, P. 1995 Measurements of the suspended matter settling velocity in the German Bight (North Sea). *German Journal of Hydrography* **47**, 4, 259-276.
- Rachold, V. 1999 Major, trace and rare earth element geochemistry of suspended particulate material of East Siberian rivers draining to the Arctic Ocean. In: Kassens, H., Bauch, H. A., Dmitrenko, I., Eicken, H., Hubberten, H.-W., Melles, M., Thiede, J. & Timokhov, L. (eds.) *Land-Ocean Systems in the Siberian Arctic: Dynamics and History*. Springer-Verlag, Berlin, 199-222.
- Rachold, V., Grigoriev, M. N., Are, F. E., Solomon, S., Reimnitz, E., Kassens, H. & Antonow, M. 2000 Coastal erosion vs riverine sediment discharge in the arctic shelf seas. *International Journal of Earth Sciences* **89**, 450-460.
- Rachold, V., Grigoriev, M. N. & Bauch, H. A. 2002 An estimation of the sediment budget in the Laptev Sea during the last 5,000 years. *Polarforschung*, **70**, 151-157.
- Reid, P. C., Lancelot, C., Gieskes, W. C., Hagmeier, E. & Weichart, G. 1990 Phytoplankton in the North Sea and its dynamics: A review. *Netherlands Journal of Sea Research* **26**, 2-4, 295-331.
- Reimnitz, E., Marincovich, L. J., McCormick, M. & Briggs, W. M. 1992 Suspension freezing of bottom sediment and biota in the Northwest Passage and implications for Arctic Ocean sedimentations. *Canadian Journal of Earth Science*, **29**, 693-703.
- Reimnitz, E., Clayton, J. R., Kempema, E. W., Payne, J. R. & Weber, W. S. 1993 Interaction of rising frazil ice with suspended particles: Tank experiments with application to nature. *Cold Region Science Technology* **21**, 117-135.
- Reimnitz, E., Dethleff, D. & Nürnberg, D. 1994 Contrasts in arctic shelf sea-ice regimes and some implications: Beaufort Sea versus Laptev Sea. *Marine Geology* **119**, 215-255.
- Rigor, I. & Colony, R. 1997 Sea-ice production and transport of pollutants in the Laptev Sea. *The Science of the Total Environment* **202**, 89-110.
- Rose, C. P. & Thorne, P. D. 2001 Measurements of suspended sediment transport parameters in a tidal estuary. *Continental Shelf Research* **21**, 1551-1575.
- Ruch, P., Mirmand, M., Jouanneau, J.-M. & Latouche, C. 1993 Sediment budget and transfer of suspended sediment from the Gironde Estuary to Cap Ferret Canyon. *Marine Geology* **111**, 109-119.

- Santamarina Cuneo, P. & Flemming, B. W. 2000 Quantifying concentration and flux of suspended particulate matter through a tidal inlet of the east Frisian Wadden Sea by Acoustic Doppler Current Profiling. In: Flemming, B. W., Delafontaine, M. T. & Liebezeit, G. (eds.) *Muddy Coast Dynamics and Resource Management*. Elsevier-Science, Amsterdam, 39-52.
- Seibt-Winckler, A. 1996 Physikalische Aspekte der akustischen, quantitativen Detektierbarkeit von Schwebstoff am Beispiel zweier Messungen in der Brackwasserzone der Elbe mit einem 3-Frequenz-Echolot. PhD Thesis, University of Hamburg, 137 pp.
- Sheng, J. & Hay, A. E. 1988 An examination of the spherical scatterer approximation in aqueous suspension of sand. *Journal of the Acoustical Society of America* **83**, 2, 598-609.
- Smith, S. D., Muench, R. D. & Pease, C. H. 1990 Polynyas and leads: An overview of physical processes and environment. *Journal of Geophysical Research* **95**, C6, 9461-9479.
- Soulsby, R. L. 1983 The bottom boundary layer of shelf seas. In: Johns, B. (ed.) *Physical Oceanography of Coastal and Shelf Seas*. Elsevier, Amsterdam, 189-266.
- Soulsby, R. L. & Whitehouse, R. J. W. 1997 Threshold of sediment motion in coastal environments. *Pacific Coasts and Ports '97*, Christchurch, 149-154.
- Stein, R. 2000 Circum-arctic river discharge and its geological record: An introduction. *International Journal of Earth Sciences* **89**, 447-449.
- Stein, R. Fahl, K., Niessen, F. & Seibold, M. 1999 Late Quaternary carbon and biomarker records from the Laptev Sea continental margin (Arctic Ocean): implications for organic flux and composition. In: Kassens, H., Bauch, H. A., Dmitrenko, I., Eicken, H., Hubberten, H.-W., Melles, M., Thiede, J. & Timokhov, L. A. (eds.) *Land-Ocean Systems in the Siberian Arctic: Dynamics and History*. Springer-Verlag, Berlin, 635-655.
- Sternberg, R. W., Aagaard, K., Cacchione, D. A., Wheatcroft, R. A., Beach, R. A., Roach, A. T. & Marsden, M. A. H. 2001 Long-term near-bed observations of velocity and hydrographic properties in the northwest Barents Sea with implications for sediment transport. *Continental Shelf Research* **21**, 509-529.
- Sutherland, T. F., Lane, P. M., Amos, C. L. & Dowing, J. 2000 The calibration of optical backscatter sensors for suspended sediment of varying darkness levels. *Marine Geology* **162**, 587-597.
- Thevenot, M. M. & Kraus, N. C. 1993 Comparison of acoustical and optical measurements of suspended material in the Chesapeake Estuary. *Journal of Marine Environmental Engineering* **1**, 65-79.

- Thorne, P. D., Vincent, C. E., Hardcastle, P. J., Rehmann, S. & Pearson, N. 1991 Measuring suspended sediment concentrations using acoustic backscatter devices. *Marine Geology* **98**, 7-16.
- Thorne, P. D. & Hardcastle, P. J. 1997 Acoustic measurements of suspended sediments in turbulent currents and comparison with *in-situ* samples. *Journal of the Acoustical Society of America* **101**, 5, 2603-2614.
- Thosteson, E. D. & Hanes, D. M. 1998 A simplified method for determining sediment size and concentration from multiple frequency acoustic backscatter measurements. *Journal of the Acoustical Society of America* **104**, 2, 820-830.
- Timokhov, L. A. 1994 Regional characteristics of the Laptev and East Siberian seas: Climate, topography, ice phases, thermohaline regime, circulation. *Berichte zur Polarforschung* **144**, 15-31.
- Treshnikov, A. F. 1985 *Atlas of the Arctic*. Main Department of Geodesy and Cartography of the Council of Ministers of the USSR, 204 pp.
- Tuschling, K. 2000 Zur Ökologie des Phytoplanktons im arktischen Laptevmeer - ein jahreszeitlicher Vergleich. *Berichte zur Polarforschung* **347**, 1-144.
- Urick, R. J. 1948 The absorption of sound in suspensions of irregular particles. *Journal of the Acoustical Society of America* **20**, 3, 283-289.
- Wegner, C., Hölemann, J. A., Dmitrenko, I., Kirillov, S. A., Tuschling, K., Abramova, E. & Kassens, H. in press Suspended particulate matter on the Laptev Sea shelf (Siberian Arctic) during ice-free conditions. *Estuarine, Coastal and Shelf Science*.
- Wheatcroft, R. A. & Butman, C. A. 1997 Spatial and temporal variability in aggregated grain-size distributions, with implications for sediment dynamics. *Continental Shelf Research* **17**, 4, 367-390.
- Wright, L. D. 1995 *Morphodynamics of Inner Continental Shelves*. CRC Press, Boca Raton, 241 pp.
- Zakharov, V. F. 1997 *Sea Ice in the Climate System*. World Meteorological Organization, WMO/TD 782, Geneva, 80 pp.

DANKSAGUNG

Herrn Prof. Dr. Jörn Thiede (AWI, Bremerhaven und GEOMAR, Kiel) danke ich recht herzlich für die Vergabe und Betreuung dieser Arbeit. Herrn Prof. Dr. Burghard Flemming (Senckenberg-Institut, Wilhelmshaven) danke ich für die Übernahme des Korreferats.

Ein großes Dankeschön gebührt dem Laptev-Dreier-Team: Jens Hölemann für die zahlreichen Diskussionen und Anregungen „ganz nah dran“ darüber, wo das ganze „Zeug“ denn auf dem Schelf bleibt; Heidemarie Kassens für ihr unermüdliches Engagement in Sachen „Laptevhausen“, durch das alles viel reibungsloser vonstatten geht; Kirsten Tuschling für die Bereitstellung der Chlorophyll-Daten und für die Einweisung in die Geheimnisse des Phytoplanktons für Nicht-Biologen.

Ohne die beiden „obersten Instanzen“ Jan Helmke und Thomas Müller-Lupp sähe diese Arbeit wohl anders aus. Für ihre unermüdliche Bereitschaft, sich immer wieder meiner Manuskripte anzunehmen, sich auch durch dröge Theorie durchzubeißen, sich mit „Chef-Designer“-Blick meinen Abbildungen zu widmen und mir dann in ihrer diplomatischen und äußerst konstruktiven Art klarzumachen, wie's besser geht, gilt mein besonders herzlicher Dank.

Ein herzliches Dankeschön geht an die starken Helfer im Hintergrund: Angelika Finke, die keine Mühen gescheut hat, die notwendige, leider oft sehr schwer zugängliche Literatur zu besorgen; Super-Hiwi Torben Klagge, der selbst noch zu später Stunde seine Programmierkünste eingesetzt und auch in brenzligen Situationen immer Humor und Nerven bewahrt hat; Karen Volkmann-Lark und Ortrud Runze, bei denen nicht ein einziger Wortverdrehen eine Chance hatte; Harold A. Thomas Sr. von RD-Instruments für die prompte, ausführliche und geduldige Beantwortung sämtlicher technischer Fragen zu „meinen“ ADCPs.

Für die konstruktiven Diskussionen, die vielen offenen Ohren und für das gute Arbeitsklima danke ich neben den schon oben genannten Freunden und Kollegen Henning Bauch, Natasja Brughmanns, Sascha Flögel, Tobias Mörz, Johannes Simstich, Manu Söding, Robert Spielhagen, Arne Sturm und Anja Wolf. Natürlich nicht zu vergessen für die Einführung in die wundersame Welt des Fußballs und des Dartspiels und in das Leben damals 1983 in England – es hat Spaß gemacht mit Euch allen.

Allen russischen und deutschen Kollegen von „Laptevhausen“ danke ich für die ausgesprochen nette und unkomplizierte Zusammenarbeit, sowohl fachlich als auch menschlich – Spasibo Bolschoje.

Dem Kapitän und der Besatzung der „Yakov Smirnitskiy“ danke ich für ihren Einsatz während der Expedition, die eine komplikationslose Probennahme und somit eine erfolgreiche Expedition ermöglichten.

Meiner Familie, die mir auf dem ganzen Weg bis hierher immer den Rücken gestärkt und alles mit großem Interesse verfolgt hat, kann ich gar nicht of genug danken. Schließlich ein ganzes Feuerwerk an Dankeschöns für Christof, der immer für mich da war und ohne den alles nur halb so schön wäre.

Die vorliegende Arbeit ist im Rahmen des deutsch-russischen Verbundvorhabens „System Laptev-See 2000“ entstanden. Für die Finanzierung möchte ich mich beim BMBF bedanken.

LIST OF ABBREVIATIONS

A_s	see equation (3.3)
ADCP	Acoustic Doppler Current Profiler
CTD	Conductivity Temperature Depth meter
EI	recorded echo intensity of the ADCP
K	see equation (3.3)
K_s	see equation (3.1)
K_t	see equation (3.1)
K_*	see equation (3.2)
OI	recorded optical backscatter intensity of the turbidity meter
$SPM_{acoustic}$	suspended particulate matter concentration derived from ADCP measurements
SPM_{filter}	suspended particulate matter concentration derived from <i>in situ</i> water samples
SPM_{optic}	suspended particulate matter concentrations derived from turbidity meter measurements
R_s	receive sensitivity of the transducer
SPM	suspended particulate matter
TD	TRANSDRIFT expeditions
$a_s(r)$	particle radius at height r
a_t	transceiver radius
c	speed of sound in water
d_{50}	median grain diameter
$f_m(r)$	describes the scattering properties of the SPM
g	acceleration due to gravity ($g=9.81 \text{ m s}^{-2}$)
k	wave number
mab	meter above seafloor
p	pressure
r	distance from the transducer
r_0	reference distance (usually 1 m)
u	eastward current component of the velocity field
u_{cr}	threshold current speed for incipient grain motion
v	northward current component of the velocity field
z	depth of flow
z_0	bed roughness length
α_s	attenuation coefficient due to scatterers in suspension
α_w	attenuation coefficient due to water
κ	von Karman's constant ($\kappa = 0.4$)
ρ_s	sediment density
τ	pulse duration
ζ	sediment attenuation constant
θ_{cr}	threshold shields parameter by Soulsby and Whitehouse (1997)

„Berichte zur Polarforschung“

Eine Titelübersicht der Hefte 1 bis 376 (1981 - 2000) erschien zuletzt im Heft 413 der nachfolgenden Reihe „Berichte zur Polar- und Meeresforschung“. Ein Verzeichnis aller Hefte beider Reihen sowie eine Zusammenstellung der Abstracts in englischer Sprache finden Sie im Internet unter der Adresse:
<http://www.awi-bremerhaven.de/Resources/publications.html>

Ab dem Heft-Nr. 377 erscheint die Reihe unter dem Namen:

„Berichte zur Polar- und Meeresforschung“

- Heft-Nr. 377/2000 – „Rekrutierungsmuster ausgewählter Wattfauna nach unterschiedlich strengen Wintern“ von Matthias Strasser
- Heft-Nr. 378/2001 – „Der Transport von Wärme, Wasser und Salz in den Arktischen Ozean“, von Boris Cisewski
- Heft-Nr. 379/2001 – „Analyse hydrographischer Schnitte mit Satellitenaltimetrie“, von Martin Losch
- Heft-Nr. 380/2001 – „Die Expeditionen ANTARKTIS XI/1-2 des Forschungsschiffes POLARSTERN 1998/1999“, herausgegeben von Eberhard Fahrbach und Saad El Naggar.
- Heft-Nr. 381/2001 – „UV-Schutz- und Reparaturmechanismen bei antarktischen Diatomeen und *Phaeocystis antarctica*“, von Lieselotte Riegger.
- Heft-Nr. 382/2001 – „Age determination in polar Crustacea using the autofluorescent pigment lipofuscin“, by Bodil Blumh.
- Heft-Nr. 383/2001 – „Zeitliche und räumliche Verteilung, Habitatspräferenzen und Populationsdynamik benthischer Copepoda Harpacticoida in der Potter Cove (King George Island, Antarktis)“, von Gritta Veit-Köhler.
- Heft-Nr. 384/2001 – „Beiträge aus geophysikalischen Messungen in Dronning Maud Land, Antarktis, zur Auffindung eines optimalen Bohrpunktes für eine Eiskerntiefbohrung“, von Daniel Steinhage.
- Heft-Nr. 385/2001 – „Actinium-227 als Tracer für Advektion und Mischung in der Tiefsee“, von Walter Geibert.
- Heft-Nr. 386/2001 – „Messung von optischen Eigenschaften troposphärischer Aerosole in der Arktis“ von Rolf Schumacher.
- Heft-Nr. 387/2001 – „Bestimmung des Ozonabbaus in der arktischen und subarktischen Stratosphäre“, von Astrid Schulz.
- Heft-Nr. 388/2001 – „Russian-German Cooperation SYSTEM LAPTEV SEA 2000: The Expedition LENA 2000“, edited by Volker Rachold and Mikhail N. Grigoriev.
- Heft-Nr. 389/2001 – „The Expeditions ARKTIS XVI/1 and ARKTIS XVI/2 of the Research Vessel 'Polarstern' in 2000“, edited by Gunther Krause and Ursula Schauer.
- Heft-Nr. 390/2001 – „Late Quaternary climate variations recorded in North Atlantic deep-sea ostracodes“, by Claudia Didié.
- Heft-Nr. 391/2001 – „The polar and subpolar North Atlantic during the last five glacial-interglacial cycles“, by Jan. P. Helmke.
- Heft-Nr. 392/2000 – „Geochemische Untersuchungen an hydrothermal beeinflussten Sedimenten der Bransfield Straße (Antarktis)“, von Anke Dählmann.
- Heft-Nr. 393/2001 – „The German-Russian Project on Siberian River Run-off (SIRRO): Scientific Cruise Report of the Kara-Sea Expedition 'SIRRO 2000' of RV 'Boris Petrov' and first results“, edited by Ruediger Stein and Oleg Stepanets.
- Heft-Nr. 394/2001 – „Untersuchung der Photooxidantien Wasserstoffperoxid, Methylhydroperoxid und Formaldehyd in der Troposphäre der Antarktis“, von Katja Riedel.
- Heft-Nr. 395/2001 – „Role of benthic cnidarians in the energy transfer processes in the Southern Ocean marine ecosystem (Antarctica)“, by Covadonga Orejas Saco del Valle.
- Heft-Nr. 396/2001 – „Biogeochemistry of Dissolved Carbohydrates in the Arctic“, by Ralph Engbrodt.
- Heft-Nr. 397/2001 – „Seasonality of marine algae and grazers of an Antarctic rocky intertidal, with emphasis on the role of the limpet *Nacilla concinna* Strebel (Gastropoda: Patellidae)“, by Dohong Kim.
- Heft-Nr. 398/2001 – „Polare Stratosphärenwolken und mesoskalige Dynamik am Polarwirbelrand“, von Marion Müller.
- Heft-Nr. 399/2001 – „North Atlantic Deep Water and Antarctic Bottom Water: Their Interaction and Influence on Modes of the Global Ocean Circulation“, by Holger Brix.
- Heft-Nr. 400/2001 – „The Expeditions ANTARKTIS XVIII/1-2 of the Research Vessel 'Polarstern' in 2000“ edited by Victor Smetacek, Ulrich Bathmann, Saad El Naggar.
- Heft-Nr. 401/2001 – „Variabilität von CH₂O (Formaldehyd) - untersucht mit Hilfe der solaren Absorptionsspektroskopie und Modellen“ von Torsten Albrecht.
- Heft-Nr. 402/2001 – „The Expedition ANTARKTIS XVII/3 (EASIZ III) of RV 'Polarstern' in 2000“, edited by Wolf E. Arntz and Thomas Brey.
- Heft-Nr. 403/2001 – „Mikrohabitatansprüche benthischer Foraminiferen in Sedimenten des Südatlantiks“, von Stefanie Schumacher.
- Heft-Nr. 404/2002 – „Die Expedition ANTARKTIS XVII/2 des Forschungsschiffes 'Polarstern' 2000“, herausgegeben von Jörn Thiede und Hans Oerter.
- Heft-Nr. 405/2002 – „Feeding Ecology of the Arctic Ice-Amphipod *Gammarus wilkitzkii*. Physiological, Morphological and Ecological Studies“, by Carolin E. Arndt.
- Heft-Nr. 406/2002 – „Radiolarienfauna im Ochotskischen Meer - eine aktuopaläontologische Charakterisierung der Biozönose und Taphozönose“, von Anja Nimmergut.
- Heft-Nr. 407/2002 – „The Expedition ANTARKTIS XVIII/5b of the Research Vessel 'Polarstern' in 2001, edited by Ulrich Bathmann.
- Heft-Nr. 408/2002 – „Siedlungsmuster und Wechselbeziehungen von Seepocken (Cirripedia) auf Muschelbänken (*Mytilus edulis* L.) im Wattenmeer“, von Christian Buschbaum.